UNIVERSITAT DE BARCELONA

Nutrigenomic approach to study the potential role of walnut polyphenols and their human metabolites in cancer prevention and treatment

Claudia Alejandra Sánchez González

Aquesta tesi doctoral està subjecta a la llicència ***Reconeixement- NoComercial – CompartirIgual 4.0. Espanya de Creative Commons***.

Esta tesis doctoral está sujeta a la licencia ***Reconocimiento - NoComercial – CompartirIgual 4.0. España de Creative Commons***.

This doctoral thesis is licensed under the ***Creative Commons Attribution-NonCommercial-ShareAlike 4.0. Spain License***.

Universitat de Barcelona

FACULTAT DE FARMÀCIA

PROGRAMA DE DOCTORAT ALIMENTACIÓ I NUTRICIÓ

NUTRIGENOMIC APPROACH TO STUDY THE POTENTIAL ROLE OF WALNUT POLYPHENOLS AND THEIR HUMAN METABOLITES IN CANCER PREVENTION AND TREATMENT.

Claudia Alejandra Sánchez González, 2015

FACULTAT DE FARMÀCIA

PROGRAMA DE DOCTORAT ALIMENTACIÓ I NUTRICIÓ

NUTRIGENOMIC APPROACH TO STUDY THE POTENTIAL ROLE OF WALNUT POLYPHENOLS AND THEIR HUMAN METABOLITES IN CANCER PREVENTION AND TREATMENT.

Memoria presentada por Claudia Alejandra Sánchez González para optar al título de doctor por la Universidad de Barcelona

Dra. Maria Izquierdo-Pulido
Directora y Tutora

Dra. Verónica Noé Mata
Directora

Claudia Alejandra Sánchez González

Barcelona, 2015

This thesis was financed by grants from the following institutions:

California Walnut Commission

Spanish Ministry
of Science and Innovation
(SAF2011-23582 and SAF2014-51825-R)

The doctoral candidate was supported with a scholarship from the Mexican Council of Science and Technology "Consejo Nacional de Ciencia y Tecnología (CONACYT)"

Difícilmente existen palabras suficientes para agradecerles a todas las personas que me han apoyado en esta etapa de mi vida, pero haré el intento…

Gracias a mis directoras de tesis, la Dra Maria Izquierdo Pulido y la Dra. Verónica Noé Mata por guiarme en este inicio de mi carrera profesional.

En especial quisiera agradecerle a la Dra. Maria por su apoyo incondicional. Gracias por haberme aceptado como su estudiante hace 5 años, le agradezco el tiempo, la paciencia y la dedicación para enseñarme tanto. Esta ha sido una aventura que no siempre fue fácil, pero usted me ha motivado para seguir adelante, **gracias por creer en mí**. Me considero muy afortunada de haber tenido el placer de tenerla como directora, pero sobre todo como mentora y amiga.

A la Dra. Verónica, gracias por ser mi guía en el mundo de la Bioquímica y Biología Molecular. Quisiera agradecerte en especial tu esfuerzo para que todas en el CCVN lab valoremos lo afortunadas que somos y por motivarnos a ser cada día mejores.

Al Dr. Carlos Ciudad, muchas gracias por el tiempo que me has dedicado. Sé que soy un poco terca pero te agradezco la paciencia que has tenido conmigo y la disposición para aconsejarme siempre que lo he necesitado. Te agradezco también por tantas buenas ideas!

A mis maestras, compañeras y amigas del CCLAB, esta tesis no hubiera sido posible sin ustedes. Nadie ha tenido más paciencia conmigo que Carlota, Nuria, Xenia, Laura y Anna, gracias por estar siempre disponibles para contestar mis preguntas, enseñarme y simplemente escucharme. Las quiero mucho!!

Carlota y Nuria ustedes han sido un gran ejemplo a seguir. Espero tener siempre ese amor a la ciencia que ustedes me han transmitido.

Xenia, GRACIAS, por todo el tiempo que me has dedicado, me has enseñado mucho en estos años y sin ti me hubiera vuelto loca en el lab!! Eres una gran persona, con una personalidad única, nunca cambies.

Lau, tu puedes lograr todo lo que te propongas, no dejes nunca que alguien te diga lo contrario! Gracias por esas conversaciones motivacionales sobre el futuro, por compartir tantas ideas conmigo, por tus consejos. Ya veras que lo mejor esta por venir.

Anneta, la meva companya de poyata. Gracies pels riures, per transmetre tanta felicitat, humor i energia. Els dies al lab no serien el mateix sense tu. Et trobare a faltar moltissim. T´estimo!!

A mis compañeras del MIP lab, mis nutris mexicanas, Ale y Tania… gracias por esas pláticas que son tan necesarias para seguir adelante. Sigan siempre con ese ánimo de lograr sus metas.

A las niñas del grupo de antioxidantes, gracias por ser tan buena compañía y por compartir tan lindos momentos conmigo. Las voy a extrañar mucho.

A mi familia, por que sin su apoyo incondicional yo no podría llegar a ningún lado. Gracias por creer en mí sin importar la loca idea con la que salga. Gracias por apoyarme en todo momento y sobre todo por ser mi más grande ejemplo a seguir.

A mis amigos, los que están lejos y a los que tengo cerca, soy tan afortunada de tenerlos en mi vida. Gracias por apoyarme, por motivarme y por empujarme a lograr mis metas. Caro, gracias por inspirarme siempre a querer ser una mejor persona. A la que se convirtió en mi familia española, Miguel, Pau, Yiyi, Alex y Anni, gracias por ser tan especiales y por hacerme sentir en casa. A Iris y Laura, porque además de ser amigas y roomies, son hermanas. Iris, gracias por estar siempre dispuesta a regalarme un poquito de tu tiempo para escucharme y aconsejarme. Laura, quien hubiera dicho que viviríamos tantas aventuras juntas, gracias por hacerme desconectar en ese momento que tanto lo necesitaba!!!

“The biggest adventure you can take is to live the life of your dreams.”

ABBREVIATIONS

ABTS	2,2'-azino-bis(3-ethylbenzothiazoline-6-sulphonic acid)
AD	Androgen dependent
AI	Androgen independent
ANOVA	Analysis of variance
APRT	Adenine phosphoribosyltransferase
AR	Androgen receptor
ARE	Androgen response element
Bak	BCL2- antagonist/killer
BAN	Biological association network
Bax	BCL2-associated X protein
Bcl	B-cell CLL/lymphoma
bp	Base pairs
BSA	Bovine serum albumin
CRPC	Castratration resistant prostate cancer
cDNA	Complementary DNA
Ci, µCi	Curie, Microcurie
CNT	Control
cpm	Counts per minute
Ct	Threshold cycle
DEPC	Diethyl pyrocarbonate
DHT	Dehydrotestosterone
DMSO	Dimethyl sulfoxide
DNA	Deoxyribonucleic acid
dNTPs	Deoxyribonucleotides triphosphate
DTT	1,4-dithiothreitol
DPPH	2,2-diphenyl-1-picrylhydrazyl
EA	Ellagic Acid
EGCG	Epigallocatechin-3-gallate
EGF, EGFR	Epidermal growth factor
ET	Ellagitannin
EMSA	Electrophoretic mobility shift assay
EPI	Epicatechin
ER	Estrogen receptor
ERE	Estrogen response element
FBS	Fetal bovine serum
GAE	Gallic acid equivalents
G0, G1	Cell cycle phase G
GEO	Gene Expression Omnibus
GS	Gel shift
GTP	Guanosine-triphosphate
HPLC	High-performance liquid chromatography
IGF-1	Insulin-like growth factor

IL-6	Interleukin 6
JAK	Janus kinase
Kb	Kilobase
KDa	Kilodalton
Keap1	Kelch-like ECH-associated protein 1
LUC	Luciferase reporter vector
M, mM, µM, nM,	Molar, Milimolar, Micromolar, Nanomolar
MAPK	Mitogen-activated protein kinase
MEK	Mitogen-activated protein kinase kinase
MDA	Malondialdehyde
mQ	MiliQ water
mRNA	Messenger ribonucleic acid
MS	Mass spectrometry
MTT	4,5-Dimethylthiazol-2-yl)-2,5-diphenyltetrazolium bromide
NAPD+, NADPH	Nicotinamide adenine dinucleotide phosphate
NE	Nuclear extract
NF-κβ	Nuclear factor kappa-light-chain-enhancer of activated B cells
Nrf2	Nuclear factor erythroid 2-related factor 2
OVN	Overnight
p21	Tumor protein p21
PBS	Phosphate buffered saline
PCR	Polymerase chain reaction
PI	Propidium iodide
PI3K	Phosphoinositide 3-kinase
PMSF	Phenylmethanesulfonylfluoride
PSA	PSA
Rho123	Rhodamine 123
RLU	Relative luminiscence units
RNA	Ribonucleic acid
RNAse	Ribonuclease
ROS	Reactive oxygen species
RT	Room Temperature
RT-PCR	Reverse transcription-polymerase chain reaction
S	Cell cycle phase S
SDS	Sodium dodecyl sulfate
SE	Standard error
SNPs	Single nucleotide polymorphisms
STAT 3	Signal transducer and activator of transcription 3
STP	Staurosporine
TBE	Tris/Borate/EDTA buffer
TBS	Tris-buffered saline
TE	Tris-EDTA buffer
TF	Transcription factor
UA, UB	Urolithin A, Urolithin B

TABLE OF CONTENTS

PRESENTATION

The relationship between diet and health is well established, but renewed interest in biologically active food compounds and the examination as to how they exert their effects is being powered by the development of nutritional genomics. Nutritional genomics is the application of high throughput functional genomic technologies to nutrition research.

There is overwhelming evidence that diet is a key environmental factor that affects the incidence of many chronic diseases. Clearly, a potential for immense benefit through successful characterization and exploitation of health-promoting factors in foods exists. The food we eat contains thousands of biologically active substances, many of which may have the potential to provide substantial health benefits.

The role of nutrition in cancer depends on how it impacts fundamental cell processes. Nutrients and bioactive compounds in food have effects that can inhibit events that lead or contribute to cancer development. Several food derived compounds are among the most promising chemo-preventive agents which are under evaluation nowadays, although our understanding of their mechanisms of action is still quite limited. Nutrigenomics is a novel research field that can aid to clarify the impact that nutrients or bioactive compounds may have on mechanisms related to cancer development and in the elucidation of our response to diet.

The following work aims to reveal molecular pathways modulated by walnut polyphenol metabolites in a prostate cancer model using a nutrigenomic approach. The main objectives were: I) to identify the polyphenol profile in walnuts, II) to analyze the effect of walnut polyphenol metabolites in key signaling pathways in prostate carcinogenesis and development, and III) to determine key genes affected by walnut polyphenol incubation in prostate cancer cells.

1. INTRODUCTION

1.1. POLYPHENOLS IN WALNUTS

Current nutritional approaches reflect a fundamental change in our understanding of health. Increasing knowledge regarding the impact of diet on regulation at the genetic and molecular levels is redefining the way we consider the role of nutrition, resulting in new dietary strategies. Diet not only provides adequate nutrients to meet metabolic requirements, but can also contribute to the improvement of human health (Biesalski et al., 2009). Consequently, the food industry has been increasingly interested in functional components in food.

Bioactive compounds are constituents that typically occur in small quantities in foods. They are intensively studied to evaluate their effects on health. Many bioactive compounds have been discovered and they vary broadly in chemical structure and function. Thus, these compounds are usually grouped accordingly to their particular characteristics (Zhang et al., 2011). Polyphenols are one of the main groups of bioactive compounds found in food and beverages (Table 1).

Table 1. Polyphenols and major dietary sources.

Phenolic Compound	Dietary Source
Phenolic Acids	
Hydroxycinnamic Acids	Blueberries, carrots, cereals, citrus fruits, spinach, tomatoes
Hydroxybenzoic Acids	Blueberries, cereals, cranberries, oilseeds
Flavonoids	
Anthocyanins	Blueberries, cherries, grapes, strawberries
Chalcones	Apples
Flavanols	Apples, blueberries, grapes, onion, lettuce
Flavanonols	Grapes
Flavanones	Citrus fruits
Flavonols	Apples, beans, blueberries, cranberries, lettuce, onion, olive, pepper, tomatoes
Flavones	Citrus fruits, celery, parsley, spinach
Isoflavones	Soybeans
Xanthones	Mango
Tannins	
Condensed	Apples, pears, grapes, peaches, plums
Hydrolysable	**Walnuts**, almonds, pomegranate, raspberries

Adapted from (Ignat, Volf, & Popa, 2011).

Polyphenols have been widely studied and have been attributed a role in the prevention of several diseases such as cancer, diabetes, obesity, in addition to neurodegenerative and cardiovascular diseases (Vauzour, Rodriguez-Mateos, Corona, Oruna-Concha, & Spencer, 2010). Hence, the elucidation of common dietary sources of polyphenols remains essential. In particular, walnuts have significantly higher total polyphenol content when compared to other nuts common in our diets, such as almonds, hazelnuts, pistachios and peanuts (Abe, Lajolo, & Genovese, 2010; Vinson & Cai, 2012). Among the polyphenols contained in walnuts, **ellagitannins** have been reported to be the main phenolic compounds found (Fukuda, 2009).

1.1.1. Ellagitannins

1.1.1.1 Chemical structure

Ellagitannins belong to the hydrolysable tannin class of polyphenols (Quideau & Feldman, 1996). They can be found mainly in fruits such as, pomegranates, black raspberries, raspberries and strawberries, and in nuts, specifically, **walnuts** and almonds (Landete, 2011). It is well documented that the most abundant ellagitannin in walnuts is **pedunculagin** ($C_{34}H_{26}O_{22}$) (Figure I.1) (Cerdá, Periago, Espín, & Tomás-Barberán, 2005; Regueiro et al., 2014). Ellagitannins constitute a complex class of polyphenols characterized by one or more hexahydroxydiphenoyl (HHDP) moieties esterified to a polyol usually, glucose or quinic acid (Regueiro et al., 2014). These polyphenols have an enormous structural variability due to the different possibilities for the linkage of HHDP residues with the sugar moiety, and particularly due to their strong tendency to form dimeric and oligomeric derivatives (Niemetz & Gross, 2005). In the hydrolysis of ellagitannins with acids or bases, ester bonds are hydrolyzed, and the HHDP group spontaneously rearranges into **ellagic acid**, which has poor water solubility (Garcia-Muñoz & Vaillant, 2014).

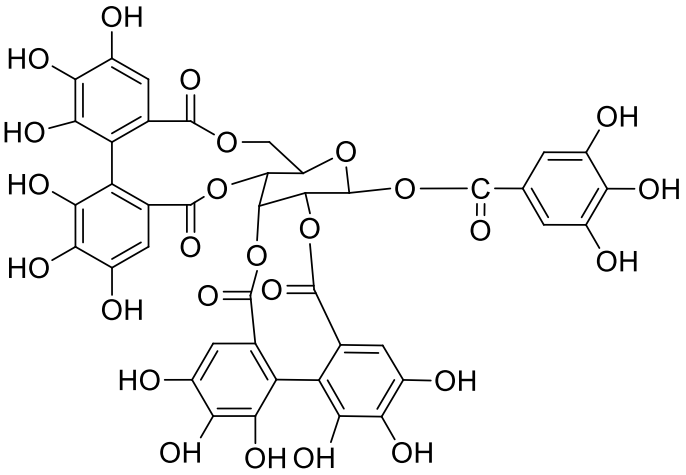

Figure I.1: Pedunculagin chemical structure.

1.1.1.2 Metabolism, absorption and excretion

The absorption and metabolism of ellagitannins in humans is still quite unknown but several animal studies have contributed to their understanding. Several authors have observed that ellagitannins are not usually absorbed and must be metabolized prior to absorption (Mertens-Talcott, Jilma-Stohlawetz, Rios, Hingorani, & Derendorf, 2006). The absorption of food polyphenols is determined primarily by their chemical structure, which depends on factors such as the degree of glycosylation, hydroxylation, acylation, conjugation with other phenolics, molecular size, degree of polymerization and solubility (Karakaya, 2004). Previous animal studies showed that ellagitannins could be hydrolyzed to ellagic acid at the pH found in the small intestine and cecum (Daniel et al., 1989; Espín et al., 2007). The presence of free ellagic acid in human plasma could be due to its release from the hydrolysis of ellagitannins, enabled by physiological pH and/or gut microbiota (Figure I.2).

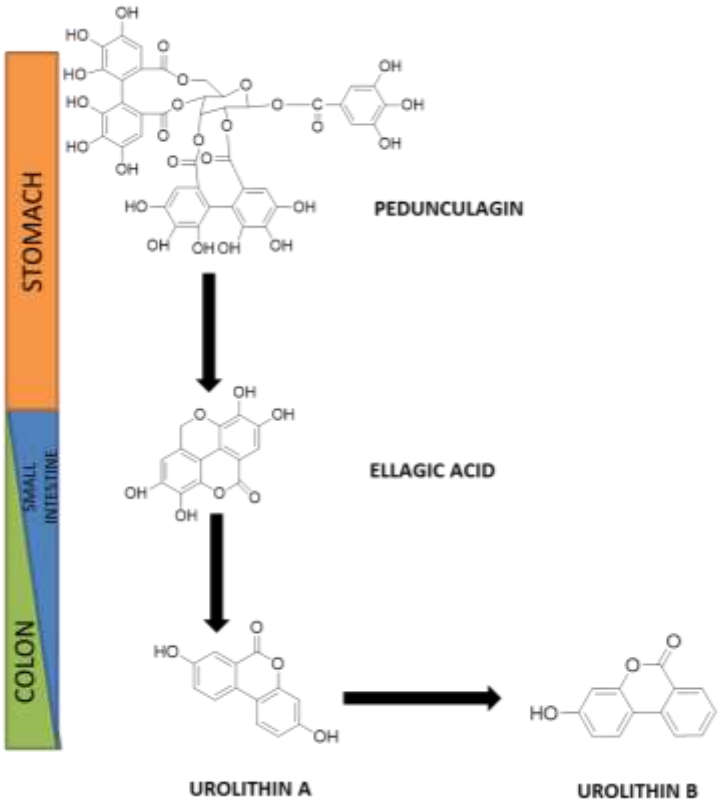

Figure I.2: Pedunculagin metabolism in gastrointestinal tract. Adapated from (Garcia-Muñoz & Vaillant, 2014)

In a study by Espin et al. (2007) performed on Iberian pigs, the authors observed that ellagitannins release ellagic acid under physiological conditions *in vivo.* Then, ellagic acid is gradually metabolized in the intestine, starting in the jejunum, to produce urolithin D, urolithin C and finally **urolithin A** and **urolithin B**. Urolithin B is mainly produced at the distal parts of the intestine. Glucuronides and methyl glucuronides of ellagic acid and particularly urolithin A, C, and D derivatives were detected in bile, confirming active enterohepatic circulation. Urolithins A and B, and dimethyl-EA glucuronide were also detected in peripheral plasma (Espín et al., 2007). Some studies have observed that urolithins appear in human systemic circulation within a few hours after ellagitannin-rich foodstuff consumption, reaching maximum concentrations between 24 h and 48 h post-intake, but they can be present in plasma and urine for up to 72 h, in free and conjugated forms (Larrosa, González-Sarrías, García-Conesa, Tomás-Barberán, & Espín, 2006; Mertens-Talcott et al., 2006; Seeram, Lee, & Heber, 2004). The presence of ellagic

acid metabolites in bile and urine and its absence in intestinal tissues suggest that its absorption takes place in the stomach.

Urolithin A is the main ellagitannin-derived metabolite detected in feces in both pigs and humans (Cerdá et al., 2005; Espín et al., 2007), whereas urolithin B is not detected in either feces or bile. The large inter-individual variability observed in the production and excretion of these metabolites, and the fact that urolithins are excreted independently of the ellagitannins consumed, would suggest microbial involvement. Consequently, urolithin production in the colon is most likely dependent of the individual's microbiota (Garcia-Muñoz & Vaillant, 2014). Moreover, regarding tissue distribution of urolithins and their conjugates, González-Sarrías *et al.* (2010) found that these molecules reach and enter the human prostate after consumption of ellagitannin-rich foods. This was confirmed in a parallel study with rats (González-Sarrías et al., 2013). Other tissue disposition studies reveal that urolithins are enriched in prostate, intestinal, and colon tissues in mice (Seeram et al., 2007). Thus, urolithins can be considered biomarkers of human exposure to dietary EA derivatives (Landete, 2011).

1.1.1.3 Biological activity

Ellagitannins, ellagic acid and their derived metabolites possess a wide range of biological activities which suggest that they could have beneficial effects on human health (Espín, Larrosa, García-Conesa, & Tomás-Barberán, 2013; Landete, 2011). Ellagitannins have well-known antioxidant and anti-inflammatory bioactivity, and several studies have assessed the potential role of ellagitannins against disease initiation and progression, including cancer, cardiovascular and neurodegenerative diseases. The health effects attributed to urolithins, based on studies carried out *in vitro* and *in vivo*, are numerous and diverse, from anti-malarial properties to powerful antioxidant activity (Landete, 2011). Authors have also attributed estrogenic and anti-estrogenic activity to urolithins based on their binding affinity to the estrogen receptor in MCF-7 cells and the androgen receptor in LNCaP cells, labeling urolithins as potential endocrine-disruptive molecules (Larrosa et al., 2006; Sánchez-González, Ciudad, Noé, & Izquierdo-Pulido, 2014).

The chemo-preventive properties of polyphenols have been widely studied. Polyphenols exert their anticancer effects by several mechanisms, such as the reduction of pro-oxidative effect of carcinogenic agents (Duthie & Dobson, 1999; Owen et al., 2000), the modulation of cancer cell signaling (Corona et al., 2007; Khan & Mukhtar, 2013), cell cycle progression (Corona et al., 2009), and promotion of apoptosis (Fabiani et al., 2002; Mantena, Baliga, & Katiyar, 2006). Polyphenols have also been shown to act on multiple targets in pathways not only related to cellular proliferation and death (Fini et al., 2008), but also in inflammation (N. J. Kang, Shin, Lee, & Lee, 2011), angiogenesis (Granci, Dupertuis, & Pichard, 2010), and drug and radiation resistance (Garg, Buchholz, & Aggarwal, 2005).

In particular, ellagitannins and ellagic acid seem to exhibit diverse anti-cancer effects, and recent research has shown that ellagitannin-rich walnut extracts have dose-dependent inhibitory effects on several cancer models (Heber, 2008), both *in vitro* and *in vivo*, including colon cancer (Qiu et al., 2013), breast cancer cells (Rocha, Wang, Penichet, & Martins-Green, 2012) and prostate cancer (Bell & Hawthorne, 2008; Naiki-Ito et al., 2015). The effects of walnut polyphenols on cancer prevention have been extensively studied showing promising results. Both *in vitro* and *in vivo* studies that assess the role of ellagitannins in several molecular pathways related to cancer initiation, development and progression have been performed.

1.2. ANALYTICAL METHODS FOR THE DETERMINATION AND QUANTIFICATION OF POLYPHENOLS IN FOOD

In order to assess the biological activity of a determined food source, it is of uttermost importance to correctly identify its particular constituents to further evaluate their potential bioactive role. To achieve this, the use of accurate and sensitive analytical methods is necessary for adequate identification. Analytical signals can be measured in many types of dimensions or domains. Typical domains are the time domain (chromatography), the wavelength domain (spectrometry), and the space domain (surface analysis) (Schoonjans, Questier, Massart, & Borosy, 2000).

Chromatography is a tool used in the identification of molecular compounds using the time domain (François, Sandra, & Sandra, 2009). It involves a sample dissolved in a mobile phase, and the mobile phase is then forced through a stationary phase. The phases are chosen so that each component of the sample has differing solubility in each phase. (François et al., 2009). Techniques such as High Performance Liquid Chromatography (HPLC) and Gas Chromatography (GC) use columns packed with stationary phase, through which the mobile phase is forced. The sample is transported through the column by continuous addition of mobile phase. This process is called elution. The average rate at which an analyte moves through the column is determined by the time it spends in the mobile phase.

Despite a great number of research, the separation and quantification of different polyphenols remain difficult (Tsao, 2010). Among the different methods available, HPLC is preferred for the separation and quantification of polyphenols in fruits. The type of column used to separate phenolics and their glycosides is generally a reverse-phase C18-bonded silica column ranging from 100 to 300 mm in length and with an internal diameter of 2–4.6 mm (Merken & Beecher, 2000), although occasionally C8 columns are used to separate phenolic acids. Columns are maintained from room temperature to 40°C during the analysis but thermostated columns give more repeatable elution times and greater resolution, and allow the backpressure of the LC column to be reduced at high flow rates (Lamuela-Raventos, 2014).The use of a binary system is essential for the separation of structurally varied phenolic compounds. Gradient elution is usually performed with a solvent A, including an aqueous acidified polar solvent or water-containing buffer, and a solvent B, which can be an organic solvent such as methanol or acetonitrile, pure or acidified (Merken & Beecher, 2000; Tsao & Deng, 2004).

Nevertheless, due to the disadvantages in detection limit and sensitivity, HPLC methods present limitations especially in complex matrix, such as crude food plant extracts and biological fluids. **Chromatography–mass spectrometry (LC–MS)** techniques are nowadays the best analytical approach to study polyphenols in a complex matrix. These techniques are the most effective tool for studying the structure of complex polyphenols such as, ellagitannins,

procyanidins, anthocyanins, and flavonoids, it also provides experimental evidence for structures that were previously only hypothesized (Flamini, 2003). The mass spectrometer ionizes the compounds to generate charged molecules and molecule fragments, measuring their mass-to-charge ratios (Ignat et al., 2011; Marston & Hostettmann, 2009; Wolfender, 2009). Different sources can be used for compound ionization: fast atom bombardment (FAB), electrospray ionization (ESI), atmospheric pressure chemical ionization (APCI), atmospheric pressure photo-ionization (APPI), and matrix-assisted laser desorption ionization (MALDI). The detection of the compounds can be performed in positive or negative ion mode, the latter being more common in polyphenol analyses (Ignat et al., 2011; Magiera, Baranowska, & Kusa, 2012; J. Wang & Sporns, 2000).

Different types of mass analyzers can be used in polyphenol analysis: single quadrupole (MS), triple-quadrupole (MS/MS), ion-trap mass spectrometers (MSn), time-of-flight (ToF), quadrupole-time-of-flight (QToF), Fourier transform mass spectrometry (FTMS), and *Orbitrap-based* hybrid mass spectrometers (LTQ-Orbitrap) (Hooft & Vos, 2012; Meda et al., 2011; Mikulic-Petkovsek, Slatnar, Stampar, & Veberic, 2012).

Quadrupoles consist of four parallel rods connected together, with voltages applied between one pair of rods and the other. Ions with a specific mass-to-charge ratio (*m/z*) will pass through the quadrupole when a particular voltage is applied. This enables quadrupoles to filter the ions en route to the detector. Triple quadrupole systems are also available, in which the first (Q1) and third quadrupole (Q3) work as filters while the second quadruple (Q2) acts as the collision cell. The generic mode for screening in MS systems is the full scan, where a mass spectrum is acquired every few seconds, thus allowing the identification of the protonated or deprotonated molecule and consequently the calculation of the molecular weight of the substance. Tandem mass spectrometry enables polyphenols to be detected and quantified in complex matrices through MS/MS techniques such as product ion scan, precursor ion scan, and neutral loss scan. A product ion scan mass spectrum contains the fragment ions generated by the collision of the molecular ion. A precursor ion mass spectrum is obtained by limiting the fragment ion to a single ion of interest. Parent ions (molecular ions) are scanned to determine

which of them give the target fragment ion. Neutral loss mass spectra show fragment ions with a particular loss of mass (Lamuela-Raventos, 2014).

An ion-trap mass spectrometer (MSn) consists of a chamber with two electrodes and two end pieces that trap ions with a series of electromagnetic fields. Once the ions are inside, another magnetic field is applied, and only selected ions remain in the chamber. This mass analyzer is useful for structural elucidation purposes, performing multiple stage MSn (Anari, Sanchez, Bakhtiar, Franklin, & Baillie, 2004; Wolfender, 2009). The LTQ-Orbitrap, which combines an ion-trap analyzer with FTMS, allows MS and MSn analysis with an error of less than 2 ppm. LTQ-Orbitrap-MS is a good tool for qualitative analysis, facilitating the structural elucidation of unknown compounds (Peterman, Duczak, Kalgutkar, Lame, & Soglia, 2006).

Efforts have been previously carried out in order to elucidate the **phenolic composition of walnuts** (Gómez-Caravaca, Verardo, Segura-Carretero, Caboni, & Fernández-Gutiérrez, 2008), although the specific identities of the major phenolic components of walnuts remains to be established. Thus, a strong necessity for the development of an accurate and sensitive analytical method to evaluate polyphenolic composition in walnuts exists. In this regard, the use of HPLC coupled to MS/MS can provide abundant information for structural elucidation of a wide range of compounds. Recently, the combination of Orbitrap technology with LTQ has been shown to enable fast, sensitive and reliable detection and identification of small molecules regardless of relative ion abundance (Vallverdú-Queralt, 2010).

1.3. NUTRITIONAL GENOMICS

The impact of food bioactive compounds on health maintenance and disease prevention can be assessed by several methods, but a particularly interesting and novel approach is the field of **nutritional genomics**. (Elliot & Ong, 2002). Nutritional genomics is a relatively recent research area in the functional genomics field, which integrates molecular biology, genetics, and nutrition. Nutritional genomics is the application of high throughput functional genomic technologies to nutrition research (DeBusk, Fogarty, Ordovas, & Kornman, 2005).

The term nutritional genomics encompasses two different research areas, nutrigenomics and nutrigenetics. It is important to note the difference between both terms because although they are closely related, they are not interchangeable due to the nature of gene-nutrient interaction they focus on, as seen on Figure I.3. Nutrigenomics focuses on the effects of nutrients on genes, proteins, and metabolic processes, whereas nutrigenetics involves determining the effect of individual genetic variation, such as polymorphisms, on the interaction between diet and disease (Afman & Müller, 2006).

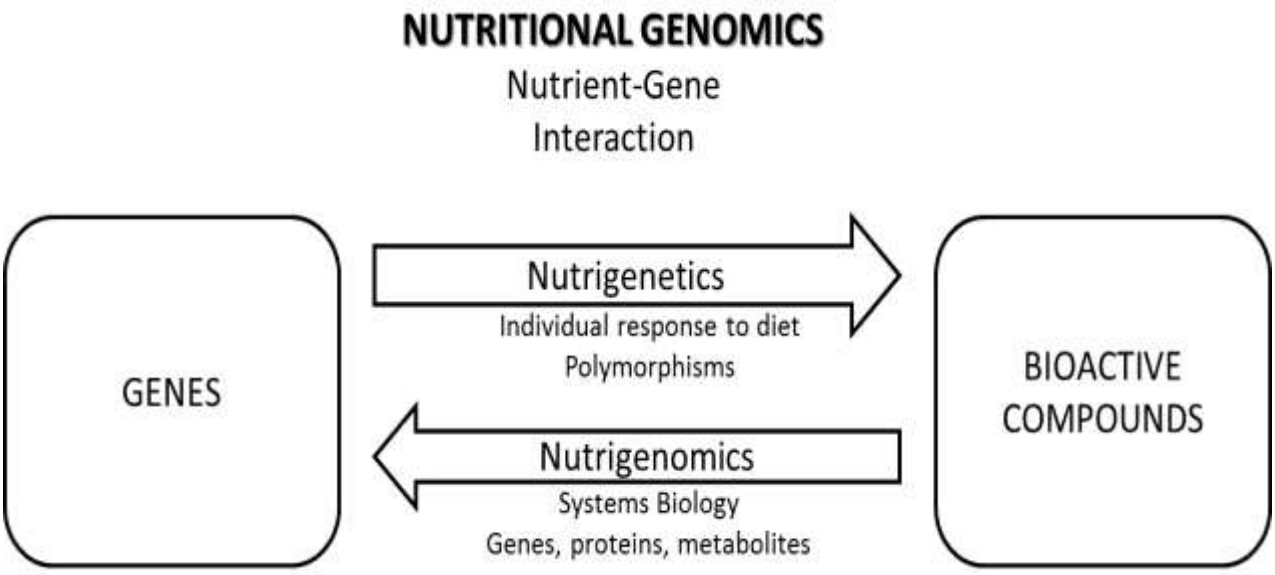

Figure I.3: Nutrient-Gene interaction in Nutritional Genomics. Adapted from (Gillies, 2003).

In the future, the integration of nutrition and genomics may lead to the use of truly personalized diets to prevent or delay the onset of disease and to optimize and maintain human health.

Nutrigenetics aims to understand how the genetic makeup of an individual defines the response to diet. If the human population was genetically identical and lived in a constant environment, then the response to diet and drugs would be equal; however, this is clearly not the case (Mutch, Wahli, & Williamson, 2005). Consequently, nutrigenetics tries to elucidate how genetic heterogeneity and nutritional components act jointly in determining an individual's response to food and/or the risk for developing a condition or disease (Mutch et al., 2005).

Currently, the majority of nutrigenetics research efforts are focused on single nucleotide polymorphisms (SNPs), which are variations with a frequency of more than 1% and they account for 90% of all human genetic variation (Wittwer et al., 2011). Nutrigenetics has the potential to provide a basis for personalized dietary recommendations based on the individual's genetic makeup to prevent common multifactorial disorders decades before their clinical manifestation.

Novel research in nutrition has focused in the description of how nutritional factors affect gene and protein function with a translational output to human health, this concept is known as **nutrigenomics** (Ferguson, 2009). The field of nutrigenomics compromises multiple disciplines and includes dietary effects on genome stability (DNA damage at the molecular and chromosome level), epigenome alterations (DNA methylation), RNA and micro-RNA expression (transcriptomics), protein expression (proteomics) and metabolite changes (metabolomics), all of which can be studied independently or in an integrated manner (Kussmann, Raymond, & Affolter, 2006). In this approach, nutrients, other food components and even whole diets are considered as "dietary signals" that are detected by "cellular sensors". These sensors, that are part of cellular signaling cascades, can affect in turn all the processes involved in cell function. Therefore, these dietary signals can influence transcription, translation and/or protein expression in one or multiple metabolic and regulatory pathways, which ultimately form the phenotype (Ommen & Stierum, 2002). The pre-requisite of nutrigenomics is the integration of genomics, transcriptomics, proteomics and metabolomics to define a "healthy" phenotype.

The long-term result of nutrigenomics research is personalized nutrition for health maintenance and disease prevention. Transcriptomics serves to put proteomic and metabolomic markers into a larger biological perspective and it is suitable for a first "round of discovery" in regulatory networks. The analysis of gene expression expands the understanding of regulatory networks, it aids in the identification of diagnostic and prognostic biomarkers as well as potential targets for medical and nutritional intervention. Moreover, transcriptomic studies have improved the understanding of the complex interaction between genetic and environmental factors, such as

lifestyle and nutrition (Hocquette, 2005) and have enabled the assessment of nutritional interventions at a global gene expression level (Kussmann et al., 2006).

Nutrigenomics offers a powerful approach to discover the effects of diet on health. The potential of such an approach for nutrition and its role in health management is substantial, however, it requires a change on the conception of nutrition. Nutrition can no longer be viewed as simply epidemiological studies whose aims are to identify relationships between nutrition and chronic disease in genetically uncharacterized populations. Instead, an approach that uses complex cell and molecular biology coupled with biochemistry and genetics are required if the goals of nutrigenomics are to be accomplished (Mutch et al., 2005).

1.4 NUTRIGENOMICS AND PROSTATE CANCER

Prostate cancer is the second most frequently diagnosed cancer and the sixth leading cause of cancer death among men. Actually, the highest rates are recorded in North America, Oceania, and Northern and Western Europe (American Cancer Society, 2011). Approximately 1 in 6 men will be diagnosed with prostate cancer during their lifetime, with over 200,000 men diagnosed annually. The conventional treatments for prostate cancer are associated with significant morbidity, however, prostate cancer is an attractive target for a preventive approach because it generally grows very slowly before symptoms arise and a diagnosis is finally established. The long latency period of the disease offers an opportunity for chemo-preventive intervention particularly with dietary and lifestyle-based strategies (Venkateswaran & Klotz, 2010).

Dietary factors are major elements accounting for the international and interethnic differences in the rate of prostate cancer. Epidemiology supports the important role of nutrition in prostate cancer prevention (Stacewicz-Sapuntzakis, Borthakur, Burns, & Bowen, 2008). In addition, a nutrigenomic approach facilitates the identification of the molecular targets of dietary compounds with chemo-preventive activity in prostate cancer. Many agents have been evaluated for their chemo-preventive capacities, including soy proteins, lycopene, vitamin E, selenium, ω-3 fatty acids, polyphenols including ellagitannins and isoflavones (Venkateswaran & Klotz, 2010).

Androgens and the androgen-receptor signaling axis are fundamental for the growth and development of both normal and cancerous cells in the prostate. Prostate cancer tumor growth is initially androgen-dependent. As shown in figure I.4, androgen-dependent signaling takes place through dihydrotestosterone stimulation of the androgen receptor.

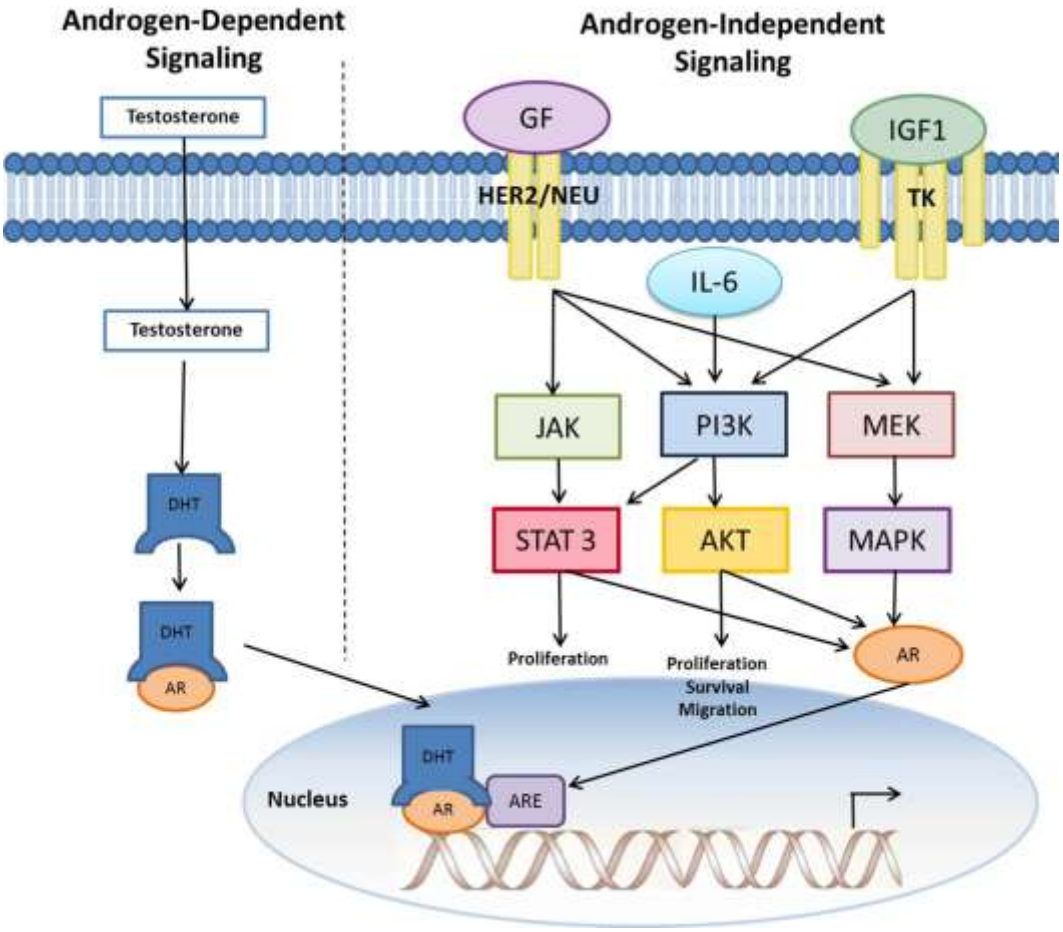

Figure I.4. Androgen receptor signaling in prostate cancer. Adapted from (Lattouf & Srinivasan, 2006).

Thus, the mainstay therapy for prostate cancer is androgen ablation, which causes the regression of androgen-dependent tumors. Prostate cancer growth depends on the ratio of cells proliferating to those dying. Androgens are the main regulator of this ratio by both stimulating proliferation and inhibiting apoptosis (Tamburrino et al., 2012). Therefore, prostate

cancer depends on a crucial level of androgenic stimulation for growth and survival (Schrijvers, 2007). However it is well documented that many men fail this therapy and perish of recurrent androgen-independent prostate cancer (Schrijvers, 2007). Androgen-independent prostate cancer usually maintains the expression of the AR protein. Some of these tumors initially adapt to low androgen environment, while others acquire mutations that allow them to evade the normal growth regulation by androgens. It seems that many cases of androgen-independent prostate cancer do not develop from a loss of androgen signaling, but rather from the acquisition of genetic changes that lead to aberrant activation of the androgen-dependent axis through stimulation of multiple signaling pathways (Figure I.4), including the PI3K and the MAPK pathways (Koochekpour, 2010). Therefore, multi-targeted therapies that modulate both androgen levels and androgen receptor activation are of crucial necessity.

Both **walnut extracts and ellagitannins** have been linked to the suppression of prostate cancer cell proliferation and the induction of apoptosis (Alshatwi et al., 2012; Naiki-Ito et al., 2015; Vicinanza, Zhang, Henning, & Heber, 2013). Walnut green husk extracts modulated the expression of apoptosis-related genes in a time and dose-dependent manner in PC-3 cells (Alshatwi et al., 2012). Furthermore, several authors have observed anti-apoptotic effects of ellagitannins in androgen-independent models using prostate cancer cells, such as PC-3 and DU-145 (Vicinanza et al., 2013)**.** Another established target in prostate cancer chemoprevention is the cytochrome P450 enzyme, CYP1B1. Compounds inhibiting CYP1B1 activity are contemplated to exert beneficial effects at three stages of prostate cancer development, that is, initiation, progression, and development of drug resistance. Urolithins and specially urolithin A, were found to decrease CYP1B1 activity and protein expression (Kasimsetty et al., 2009).

Animal and human studies on the potential link between **walnuts and prostate cancer** prevention are still limited, but the results seem promising. Reiter et al. (2013) tested whether a walnut-enriched diet influenced the growth of prostate cancer xenografts in male nude mice. They found that the walnut-enriched diet reduced the number of tumors and the growth of the LNCaP xenografts. These authors hypothesized that the walnut-enriched diet forestalled the growth of prostate cancer tumors due to an inhibitory effect consequence of the combined

actions of several phytochemicals, including the polyphenolic compounds. In addition, another study observed that prostate tumor weight and growth rate were reduced in the TRAMP (transgenic adenocarcinoma of mouse prostate) cancer model after a diet rich in walnuts (Davis et al., 2012). Like Reiter et al. (2013), the authors stated the beneficial effects of a walnut-enriched diet probably represent the effects of multiple constituents in whole walnuts and not due to specific bioactive compounds.

Regarding human studies , an intervention study done in sixty-three patients with either benign prostate hyperplasia or prostate cancer is worth mentioning. The patients were divided into three groups, controls, walnut intake (35g walnuts/day), or pomegranate intake (200mL pomegranate juice/day) for 3 days before prostate surgery. The main metabolite detected after consumption was urolithin A glucuronide. No apparent changes in the expression of CDKN1A, MKi-67 or c-Myc (all related to cancer cell proliferation) were found after consumption of walnuts or pomegranate juice. The results from this study demonstrated that conjugates of urolithins, specifically glucuronides, and dimethyl ellagic acid can reach and enter the human prostate gland upon consumption of ETs-rich sources such as pomegranate juice and walnuts. Considering their results and the lack of changes in proliferation markers, these authors expressed the need to design better *in vitro* studies that should focus on the bioactivity and exposure time of the actual *in vivo* metabolites formed upon consumption of ellagitannins. (González-Sarrías et al., 2010)**.**

It is evident that the previously mentioned studies seem to indicate the promising effects of walnut polyphenols against prostate cancer and also signal the need to further continue the exploration of the interaction between ellagitannins and molecular pathways related to cancer development and progression.

2. HYPOTHESIS AND OBJECTIVES

2.1 HYPOTHESIS

Walnut polyphenols and their derived metabolites modulate the expression of genes known to play an important role in the cancer process.

2.2 GENERAL OBJECTIVE

To determine and analyze the changes on gene expression in prostate cancer cells induced by walnut polyphenol metabolites using a nutrigenomic approach.

2.3 SPECIFIC OBJECTIVES

1. To study the **qualitative** and **quantitative** profile of the **polyphenols in walnuts**.
   1.1. To measure total polyphenol content and antioxidant activity in walnuts.
   1.2. To develop an analytical methodology for the determination of polyphenols in walnuts using HPLC-MS.
2. To identify specific molecular pathways in prostate cancer development and progression that could be modulated by walnut polyphenol metabolites (urolithins A and B).
   2.1. To identify the effect of **urolithins A** and **B** on androgen dependent signaling, including:
      2.1.1. AR expression and AR-ARE binding.
      2.1.2. PSA expression and transcriptional regulation.
   2.2. To determine the role of **urolithins** on the induction of apoptosis.
3. To study the effects of **urolithin A** on whole genome expression in a prostate cancer model using a functional genomics approach.
   3.1. To identify differentially expressed genes upon **urolithin A** incubation.
   3.2. To determine gene nodes or key genes using Biological Association Networks.
   3.3. To validate the differential expression of gene nodes and further explore the molecular pathways where the identified key gene(s) are involved.

3. MATERIALS AND METHODS

The methodology used for the development of this thesis is described in the articles enclosed in the **Results** section. A detailed description of the most relevant methods and materials used in this work is included in this section.

3.1 MATERIALS

3.1.1. Walnut polyphenol extract

A walnut polyphenol extract was used to determine the polyphenolic profile in walnuts. In summary 50 g of shelled walnut kernels were used (described below in Methods) to obtain a walnut extract. Polyphenol content was determined using the Folin-Ciocalteu method and expressed in mg/mL of gallic acid equivalents (Vallverdú-Queralt, 2010).

3.1.2. Urolithin A and B

Urolithin A (3,8-dihydroxy-6H-dibenzo[b,d]pyran-6-one) with 95% purity and Urolithin B (UB; 3-dihydroxy-6H-dibenzo[b,d]pyran-6-one) with 98% purity were both synthetized by the Department of Organic Chemistry, School of Pharmacy at the University of Barcelona (Barcelona, Spain). Urolithin A and B were dissolved in DMSO into 20 mM aliquots. For cellular incubation 40 μM of either urolithin A or urolithin B, or a combination composed of 20 μM UA and 20 μM UB were used. The final concentration of DMSO in the culture medium was always $\leq$ 0.5%.

3.1.3. Cell lines

This work focused on a prostate cancer model, two prostate adenocarcinoma cell lines were used. The main cell line used was **LNCaP** from prostate adenocarcinoma, which expresses the androgen receptor and are androgen dependent. In addition, **PC-3** prostate adenocarcinoma cells (androgen independent and AR-negative) were used as a model to assess PSA promoter activity. Both cell lines were routinely grown in Ham's F-12 medium, supplemented with 7% (V/V) fetal bovine serum (FBS, both from GIBCO, Invitrogen, Barcelona, Spain), 100U/mL sodium penicillin G and 100mg/L streptomycin, and were maintained at 37˚C in a humidified atmosphere containing 5% CO_2. Culture expansion upon confluence was

performed by trypzinization with 0.05% trypsin and 0.02% EDTA (EDTA was only used in PC3 cells) in PBS 1x (154mM NaCl, 3.88 mM H2NaPO4, 6.1 mM HNaPO4, pH 7.4) to detach adhered cells from culture dishes. The preparation of both medium and trypsin and their sterilization with a 0.2µM (pore diameter) filter was performed in our laboratory.

3.1.4. Plasmids

Expression vectors were used for the assessment of promoter activity; the following vectors were selected for this work:

- pGL3-Basic (Promega): basic vector that does not carry an enhancer or promoter sequence, but serves as a backbone to attach specific sequences. This vector is resistant to ampicillin.
- pGL3-PSA: luciferase reporter vector carrying 6-kb of the PSA promoter containing three androgen response elements. This vector is resistant to ampicillin. This construct was provided by Dr Charles Young from the Mayo Clinic, Rochester, MN.
- WWP-Luc: a p21 promoter construction in front of a luciferase reporter gene, streptomycin resistant. WWP-Luc (p21/WAF1 promoter) was obtained from Dr. Bert Vogelstein from the Johns Hopkins School of Medicine.

3.2. METHODS

3.2.1. Walnut polyphenol extract preparation

Walnut samples were treated in a darkened room with a red safety light to avoid oxidation of the polyphenols. Walnuts were manually cracked and shelled, and the seed kernels were homogenized with a blender over an ice bath. Immediately afterwards, a 0.50 g aliquot of the homogenate was vortexed for 1 min with 4 mL acetone/water (60:40, v/v) and then sonicated over an ice bath for 5 min. The extract was centrifuged at 8,000 x g for 5 minutes at 4°C. The supernatant was collected and the extraction procedure was repeated twice more. Supernatants were combined and defatted twice with 4 mL petroleum ether. The acetone-aqueous phase was then separated by centrifugation at 8,000 × g for 5 minutes at 4°C and the acetone evaporated under nitrogen flow. The aqueous extract was collected into a 5 mL

volumetric flask and filled with 0.1% formic acid in water. An aliquot of the extract was filtered by 0.20 µm (pore diameter) for further analysis.

3.2.2. Total polyphenol determination

To determine total polyphenol content in walnut polyphenol extract, 20 µL of the extract were mixed with 188 µL of Milli-Q water in a 96-well plate (nuncTM, Roskilde, Denmark). Then, 12 µl of Folin-Ciocalteu reagent and 30 µL of sodium carbonate (200 g/l) were added. The mixtures were incubated for 1 h at room temperature in the dark. After the reaction period, 50 µL of Milli-Q water were added and the absorbance was measured at 765 nm in a UV/VIS Thermo Multiskan Spectrum spectrophotometer (Vantaa, Finland). This spectrophotometer allowed the absorbance of a 96-well plate to be read in 10 s. Results were expressed as mg of gallic acid equivalents (GAE)/100 g walnut sample (dry material) (Vallverdú-Queralt, 2010).

3.2.3. Antioxidant capacity

Antioxidant activity was determined by measuring stable radicals by two methods, ABTS+ and DPPH according to the procedure described by Minoggio et al. (2003). To measure the antioxidant capacity of walnut polyphenol extract, 5 µL of the extract was mixed with 245 µL of a methanol solution containing DPPH or ABTS+. After mixing, solutions were kept in the dark for 30 minutes and 60 minutes for DPPH and ABTS+ methods respectively, and then absorbance was measured at 515 nm in case of DPPH assay and at 734 nm for ABTS+. Inhibition percentage in regards to initial absorbance obtained by the ABTS+ or DPPH methanol solution was expressed as mmol equivalents of the reference antioxidant (Trolox) per 100 g of sample.

3.2.4. Liquid chromatography coupled with electrospray ionization hybrid linear trap quadrupole-Orbitrap mass spectrometry

In order to determine the polyphenolic profile in a walnut extract, high performance liquid chromatography coupled to a LTQ Orbitrap spectrophotometer was used. These tools permit the analysis of walnut polyphenols through the determination of accurate mass measurements with errors being below 2 ppm. Liquid chromatography analyses were carried

out in an Accela HPLC system from Thermo Fisher Scientific (San Jose, CA, USA) consisting of an autosampler, a quaternary pump, a vacuum degasser, a temperature-regulated column, and a diode array detector (DAD). UV/Vis spectra were recorded from 200 to 600 nm, while acquiring at a selected wavelength of 280 nm. Chromatographic separation was performed on a reversed-phase column Atlantis T3 C18 (100 x 2.1 mm, 3 µm) from Waters (Milford, MA, USA) maintained at 25 ºC. Mobile phases A and B were 0.1% formic acid in water and 0.1% formic acid in acetonitrile, respectively. Solvent B increased in linear gradient, as follows: hold at 100% A for 1 min, decreased to 92% A over 3 min, decreased to 80% A over 20 min, decreased to 70% A over 2 min, decreased to 0% A over 2 min and hold for 6 min, then returned to initial conditions over 2 min and re-equilibrated for 5 min. The flow rate and the injection volume were set to 350 µL/min and 10 µL, respectively.

The LC system was coupled to a linear ion trap-Orbitrap mass spectrometer LTQ-Orbitrap Velos from Thermo Fisher Scientific (San Jose, CA, USA) equipped with an electrospray ionization (ESI) source. The ESI source was operated in the negative mode under the following specific conditions: source voltage, 3.5 kV; sheath gas, 40 arbitrary units; auxiliary gas, 10 arbitrary units; sweep gas, 10 arbitrary units; and capillary temperature, 320 °C. Nitrogen (> 99.98%) was employed as sheath, auxiliary and sweep gas. The scan cycle used a full scan event at resolution of 60,000 (at *m/z* 400) and three data-dependent MS/MS events acquired at a resolving power of 30,000. The most intense ions detected in full scan spectrum were selected for data-dependent scan. Parent ions were fragmented by high-energy C-trap dissociation (HCD) with normalized collision energy of 45% and an activation time of 100 ms. Instrument control and data acquisition were performed with Xcalibur 2.0.7 software (Thermo Fisher Scientific).

3.2.5. Microarray data analyses and Biological Association Networks

Microarrays were performed to obtain a high-throughput functional genomic analysis. Gene expression was analyzed by hybridization to Affymetrix Human Genome U219 array plate. This platform measures gene expression of more than 36,000 transcripts and variants that represent more than 20,000 genes.

Genomic analyses were carried out using the GeneSpring GX software v.13 (Agilent Technologies). Data was processed by computing the RMA (Robust Multichip Average) expression measure in log2 base scale, using a baseline transformation to the median of control samples. Differentially expressed genes were obtained by applying a p-value cut-off of less than 0.05 and a fold change of expression of 2 as described in Selga *et al.* (Selga, Morales, Noé, Peinado, & Ciudad, 2008). Normalized and raw data were submitted to the Gene Expression Omnibus database (GEO). The series # GSE65527 was assigned for the data set.

BANs were constructed with the aid of the Pathway Analysis within the GeneSpring v.13 (Agilent) as described by Selga *et al.* (Selga et al., 2009) starting with the list of differentially expressed genes after 24 h incubation with UA. NLP Network discovery was performed using an advanced analysis with an expanded interactions algorithm to assess relationships among entities. The software builds an association network using our differentially expressed data and the bibliographic interactions built in the databases. Relevant network associations were curated.

3.2.6. Transfection and Luciferase assay

To assess PSA promoter activity, PC-3 cells (350,000) were plated in 35 mm dishes the day before transfection. Medium (2 mL) was renewed before transfection, which was performed using FuGENE 6 (Roche, Barcelona, Spain). For each well, transfection reagent was incubated for 5 minutes in 100 µL of antibiotic and serum free medium, followed by the addition of plasmid DNA and incubated for another 20 min at a ratio of 3:1 (µL of transfection reagent : µg of plasmid DNA). One µg of plasmid DNA, either pGL3 basic vector or PSAp, a 6-kb PSA promoter construct containing three AREs in front of a luciferase reporter gene, were used for transfection.

Incubation with 40 µM of UA, UB or MIX and 1 nM of DHT was performed 6 hours after transfection, and luciferase activity was determined 24 hours after transfection. Cell extracts were prepared by lysing cells with 100 µL of Reporter Lysis Buffer (2 mM DTT, 2 mM EDTA, 10% glycerol, 1% Triton X_100, 25 mM Tris-Phosphate, pH 7.8). The lysate was centrifuged at 12,000

g for 2 min at 4˚C to pellet cell debris and supernatants were transferred to a fresh tube. Fifteen µL of the extract were added to 15 µL of the luciferase assay substrate (Promega, Madrid, Spain) at room temperature. Luminiscence was measured using the Glomax ™ 20/20 Luminometer (Promega, Madrid, Spain) and expressed as relative luminescence units (RLU). Luciferase results were normalized by total protein concentration in the cell lysates. Protein concentration was determined by the Bradford assay (Bio-Rad, Barcelona, Spain) according to the manufacturer's protocol.

To determine the effect of UA incubation on p21 promoter activity, the same experimental approach with minor modifications was performed. In this assay, LNCaP (350,000) cells were used and the chosen plasmid was WWP-Luc (previously described).

3.2.7. Nuclear extracts and Electrophoretic mobility shift assay

Nuclear extracts were prepared according to the protocol described by Andrews and Faller (Andrews & Faller, 1991). Briefly, 500,000 cells were plated and incubated the following day with urolithins A, B or MIX and 1 nM DHT. Cells were collected 24 post-treatment in cold PBS. Cells were pelleted and suspended in a cold hypotonic buffer (1.5 mM $MgCl_2$, 10 mM KCl, (AppliChem, Barcelona, Spain) 0.5 mM DTT, 0.2 mM PMSF 10 mM HEPES-KOH, pH 8.0 from Sigma-Aldrich, Madrid, Spain,). Cells were then allowed to swell for 10 minutes, vortexed and pelleted by centrifugation. The resulting pellet was then suspended in a cold high-salt buffer (25% glycerol, 420mM NaCl, 1.5 mM $MgCl_2$, 10 mM KCl, 0.5 mM DTT, 0.2 mM PMSF, 20 mM HEPES-KOH, pH 8.0) for 20 minutes. Cellular debris was removed by centrifugation and the supernatant fraction was stored at - 80˚C until further use.

EMSA assays were then performed using LNCaP nuclear extracts. AR consensus double-stranded oligonucleotide 5'-CTA GAA GTC T**GG TAC A**GG GTG TTC TTT TTG CA -3' (binding site in bold) was obtained from Santa Cruz Biotechnology, Heidelberg, Germany (sc-2551). One hundred nanograms of the AR consensus sequence was 5'-end-labeled with T4 polynucleotide kinase (New England Biolabs, Beverly, MA) and [γ-^{32}P]ATP (3000 Ci/mmol, Perkin Elmer, Madrid, Spain) as described in Rodríguez *et al*. (2013)(Rodríguez et al., 2013).

The radiolabeled probe (20,000 cpm) was incubated in a 20 µl reaction mixture also containing 1 µg of Herring Sperm DNA (Invitrogen, Barcelona, Spain) as unspecific competitor, 2 µg of nuclear extract protein, 5% glycerol, 4 mM $MgCl_2$, 60 mM KCl and 25 mM Tris–HCl, pH 8.0 (AppliChem, Barcelona, Spain). Samples were resolved by gel electrophoresis (5% polyacrylamide, 5% glycerol, 1 mM EDTA and 45 mM Tris-borate, pH 8.0; AppliChem, Barcelona, Spain). The gel was dried for 90 minutes, exposed to Europium plates overnight and analyzed using a Storm 840 Phosphorimager (Molecular Dynamics, GE Healthcare Life Sciences, Barcelona, Spain).

To determine binding specificity, the radiolabeled ARE probe was competed either with 3 ng (5-fold) of unlabeled ARE consensus or a mutant ARE oligonucleotide. The mutant AR oligonucleotide had two "GT" to "CA" substitutions in the AR binding motif 5'-CTA GAA GTC T**GC CAC A**GG **GTC ATC T**TT TTG CA -3' (binding site in bold) (sc-2552, Santa Cruz Biotechnology, Heidelberg, Germany). These experiments were performed using NE from LNCaP cells treated with 1 nM DHT.

3.2.8. Apoptosis

Apoptosis was determined by using two approaches, i) Rhodamine method and ii) Caspase 3/7 Glo assay. To measure apoptosis using Rhodamine, LNCaP cells (250,000) were plated in 35-mm 6-well dishes with 2 ml complete F-12 medium and 24h after, they were treated with either 40 µM UA, UB or MIX. Staurosporine (1µM) (Sigma-Aldrich, Madrid, Spain) was used as a positive control. Rhodamine (final concentration 5 ng/ml) (Sigma-Aldrich, Madrid, Spain) was added for 30 min and the cells were collected, centrifuged at 800 x g at 4˚C for 5 min, and washed once in PBS. The pellet was suspended in 500 ml PBS plus Propidium iodide (PI) (final concentration 5 mg/ml) (Sigma-Aldrich, Madrid, Spain). Flow cytometry data were analyzed using the Summit v4.3 software. The percentage of Rho-negative, PI negative cells, corresponded to the apoptotic population. For the Caspase-Glo 3/7 assay, 10,000 LNCaP cells were plated in a 96-well plate in 100µl F12-complete medium. After 24 h, cells were incubated with UA for 24h. The following day, 100µl of Caspase-Glo 3/7 reagent was added. After 1 h of incubation, luminiscence was measured using a ModulusTM Microplate luminometer (Turner

Biosystems, Promega, Madrid, Spain). F12-complete medium and the reagent were considered the blank control and untreated cells as background.

4. RESULTS

4.1 ARTICLE I:

Comprehensive identification of walnut polyphenols by liquid chromatography coupled to linear ion trap-Orbitrap mass spectrometry.

Jorge Regueiro*, Claudia Sánchez-González*, Anna Vallverdú-Queralt, Jesús Simal-Gándara, Rosa Lamuela-Raventós, Maria Izquierdo-Pulido.

* JR and CSG contributed equally to this work

Food Chemistry 2013; 152:340-348.

Impact Factor (JCR): 3.259.

Ranking in Food Science and Technology: 10/123 (Q1).

ABSTRACT

Introduction: Epidemiologic studies and clinical trials have demonstrated consistent benefits of walnut consumption on coronary heart disease risk and other chronic diseases. **Walnuts** (*Juglans regia* L.) have been described previously as a rich source of polyphenols with a broad array of different structures. However, an accurate screening of their complete phenolic profile is still lacking. Although efforts have been previously carried out in order to elucidate the phenolic composition of walnuts, the specific identities of the major phenolic components of walnuts remain to be established. The use of high performance liquid chromatography (HPLC) coupled to high-resolution tandem mass spectrometry (HR-MS/MS) can provide abundant information for structural elucidation of a wide range of compounds. The **aim** of the present work was to provide an accurate and comprehensive identification of the phenolic constituents found in walnuts by using LC–LTQ-Orbitrap analyses.

Materials and Methods: Extracts were prepared for the identification of phenolic compounds in walnuts by liquid chromatography coupled with electrospray ionization hybrid linear trap quadrupole-Orbitrap mass spectrometry (LC–LTQ-Orbitrap). The antioxidant activity in walnut extracts was measured using an ABTS+ radical decolorization assay and a DDPH assay. Total polyphenol content was determined using the Folin-Ciocalteu method.

Results: A total of **120 compounds**, including hydrolysable and condensed tannins, flavonoids and phenolic acids were identified or tentatively identified on the base of their retention times, accurate mass measurements and subsequent mass fragmentation data, or by comparison with reference substances and literature. The peak area of each signal in mass chromatograms was used to provide semiquantitative information for comparison purposes.

Conclusions: The most abundant ions were observed for **ellagitannins**, **ellagic acid** and its derivatives. Furthermore, the high-resolution MS analyses revealed the presence of eight polyphenols that have never been reported in walnuts: stenophyllanin C, malabathrin A, eucalbanin A, cornusiin B, heterophylliin E, pterocarinin B, reginin A and alienanin B.

Food Chemistry 152 (2014) 340–348

Contents lists available at ScienceDirect

Food Chemistry

journal homepage: www.elsevier.com/locate/foodchem

Comprehensive identification of walnut polyphenols by liquid chromatography coupled to linear ion trap–Orbitrap mass spectrometry

Jorge Regueiro [a,1], Claudia Sánchez-González [b,1], Anna Vallverdú-Queralt [b,c], Jesús Simal-Gándara [a], Rosa Lamuela-Raventós [b,c], Maria Izquierdo-Pulido [b,c,*]

[a] Nutrition and Bromatology Group, Department of Analytical and Food Chemistry, Faculty of Food Science and Technology, Ourense Campus, University of Vigo, Ourense 32004, Spain
[b] Department of Nutrition and Food Science, School of Pharmacy, University of Barcelona, Av. Joan XXIII s/n, Barcelona 08028, Spain
[c] Centro de Investigación Biomédica en Red de Fisiopatología de la Obesidad y Nutrición (CIBEROBN, CB06/03), Instituto de Salud Carlos III, Spain

ARTICLE INFO

Article history:
Received 28 April 2013
Received in revised form 19 November 2013
Accepted 26 November 2013
Available online 3 December 2013

Keywords:
Juglans regia L.
Walnuts
Phenolic compounds
Ellagitannins
Orbitrap
High-resolution mass spectrometry

ABSTRACT

Epidemiologic studies and clinical trials have demonstrated consistent benefits of walnut consumption on coronary heart disease risk and other chronic diseases. Walnuts (*Juglans regia* L.) have been described previously as a rich source of polyphenols with a broad array of different structures. However, an accurate screening of its complete phenolic profile is still lacking. In the present work, liquid chromatography coupled with electrospray ionization hybrid linear trap quadrupole-Orbitrap mass spectrometry (LC–LTQ-Orbitrap) was applied for a comprehensive identification of phenolic compounds in walnuts. A total of 120 compounds, including hydrolysable and condensed tannins, flavonoids and phenolic acids were identified or tentatively identified on the base of their retention times, accurate mass measurements and subsequent mass fragmentation data, or by comparing with reference substances and literature. The peak area of each signal in mass chromatograms was used to provide semiquantitative information for comparison purposes. The most abundant ions were observed for ellagitannins, ellagic acid and its derivatives. Furthermore, the high-resolution MS analysis revealed the presence of eight polyphenols that have never been reported in walnuts: stenophyllanin C, malabathrin A, eucalbanin A, cornusiin B, heterophylliin E, pterocarinin B, reginin A and alienanin B.

© 2013 Elsevier Ltd. All rights reserved.

1. Introduction

Walnuts (*Juglans regia* L.) have been long consumed as a highly nutritious food in many parts of the world and they are an important component of the Mediterranean diet (Bulló, Lamuela-Raventós, & Salas-Salvadó, 2011). Recently, walnuts are gathering increasing attention for their health-promoting properties, which have been reported to improve lifestyle-related diseases such as arteriosclerosis, hypercholesterolemia, hypertriglyceridemia cardiovascular disease and diabetes mellitus (Estruch et al., 2013; Pan, Sun, Manson, Willett, & Hu, 2013; Ros et al., 2004). Although the health benefits of walnuts are usually attributed to ω-3 fatty acids (Ros et al., 2004) and, to a lesser degree, to the content of vitamin E (Maguire, O'Sullivan, Galvin, O'Connor, & O'Brien, 2004), walnuts also contain significant amounts of other bioactive compounds such as plant sterols, dietary fiber and polyphenols, that may exert favorable effects on health (Vinson & Cai, 2012). It has been established that a handful of walnuts (about 50 g) has significantly more total polyphenols than a glass of apple juice (240 mL), a milk chocolate bar (43 g) or even a glass of red-wine (150 mL) (Anderson et al., 2001). Moreover, walnut's total polyphenols were significantly higher compared to other nuts common in our diets (almonds, hazelnuts, pistachios, peanuts, among others) (Abe, Lajolo, & Genovese, 2010; Vinson & Cai, 2012).

Among the polyphenols found in walnuts, ellagitannins (ETs) have been reported to be the main phenolic compounds found in the seed of *J. regia* L. (Fukuda, Ito, & Yoshida, 2003; Ito, Okuda, Fukuda, Hatano, & Yoshida, 2007). These compounds, belonging to the hydrolysable tannin class of polyphenols, are esters of hexahydroxydiphenic acid (HHDP) and a polyol, usually glucose or quinic acid (Okuda, Yoshida, Hatano, & Ito, 2009). ETs can occur as complex polymers reaching high molecular weights, which makes accurate identification difficult.

Although efforts have been previously carried out in order to elucidate the phenolic composition of walnuts (Fukuda et al., 2003; Gómez-Caravaca, Verardo, Segura-Carretero, Caboni, & Fernández-Gutiérrez, 2008; Ito et al., 2007), the specific identities of the major phenolic components of walnuts remain to be established. This is especially noteworthy if we consider the increasing number of studies dealing with the health benefits of

* Corresponding author at: Department of Nutrition and Food Science, School of Pharmacy, University of Barcelona, Av. Joan XXIII s/n, Barcelona 08028, Spain. Tel.: +34 934034839; fax: +34 934035931.
E-mail address: maria_izquierdo@ub.edu (M. Izquierdo-Pulido).
[1] These authors contributed equally to this work.

0308-8146/$ - see front matter © 2013 Elsevier Ltd. All rights reserved.
http://dx.doi.org/10.1016/j.foodchem.2013.11.158

walnut polyphenols. In this regard, the use of high performance liquid chromatography (HPLC) coupled to high-resolution tandem mass spectrometry (HR-MS/MS) can provide abundant information for structural elucidation of a wide range of compounds. Recently, the combination of Orbitrap technology with a linear ion trap (LTQ) has been shown to enable fast, sensitive and reliable detection and identification of small molecules regardless of relative ion abundance (Vallverdú-Queralt, Jáuregui, Medina-Remón, Andrés-Lacueva, & Lamuela-Raventós, 2010). This hybrid LTQ-Orbitrap analysis platform can easily perform multi-stage mass analyses (MSn) and provide high mass accuracy measurements for precursor and product ions with fast scan speeds.

The aim of the present work was to provide accurate and comprehensive identification of the phenolic constituents found in walnuts by using LC–LTQ-Orbitrap analysis. More than 100 phenolic compounds, including hydrolysable and condensed tannins, have been tentatively identified with high mass accuracy, and to the best of our knowledge, eight of them have never been reported in walnuts.

2. Materials and methods

2.1. Standards, reagents and materials

All solvents were of HPLC grade and all chemicals were of analytical reagent grade.

Formic acid (~98%) and petroleum ether were obtained from Panreac (Barcelona, Spain). Acetonitrile, acetone and methanol were purchased from Merck (Darmstadt, Germany). Ultrapure water was obtained from a Milli-Q Gradient water purification system (Millipore Bedford, MA, USA). Folin–Ciocalteau (F–C) reagent, ABTS: 2,2′-azino-bis(3-ethylbenzothiazoline-6-sulfonic acid), PBS: phosphate-buffered saline pH 7.4, Trolox: (±)-6-hydroxy-2,5,7,8-tetramethylchromane-2-carboxylic acid 97%, sodium carbonate, and manganese dioxide were purchased from Sigma–Aldrich (St. Louis, MO, USA); DPPH: 2,2-diphenyl-1-picrylhydrazyl, from Extrasynthèse (Genay, France);

Ellagic acid (EA), gallic acid, (+)-catechin, (−)-epicatechin, quercetin and chlorogenic acid were obtained from Sigma–Aldrich (St. Louis, MO, USA). Individual stock solutions of each analyte and a mixture of them were prepared in methanol. Different working standard solutions were made by appropriate dilution in 0.1% formic acid in water and then stored in amber glass vials at −20 °C.

Walnut samples (*J. regia* L.) were kindly provided by the California Walnut Commission (Folsom, CA, USA). All samples used were harvested in the state of California, USA in the year 2012.

2.2. Extraction of polyphenols

Walnut samples ($n = 5$) were treated in a darkened room with a red safety light to avoid oxidation of the polyphenols. Walnuts were manually cracked and shelled, and the seed kernels were homogenized with a blender over an ice bed. Immediately, a 0.5 g aliquot of the homogenate was vortexed for 1 min with 4 mL acetone/water (60:40, v/v) and then sonicated over an ice bed for 5 min. The extract was centrifuged at 8000*g* for 5 min at 4 °C; the supernatant was collected and the extraction procedure was repeated twice more. Supernatants were combined and defatted twice with 4 mL petroleum ether. The acetone-aqueous phase was then separated by centrifugation at 8000*g* for 5 min at 4 °C and the acetone evaporated under nitrogen flow. The aqueous extract was collected into a 5-mL volumetric flask and filled with 0.1% formic acid in water. An aliquot of the extract was filtered by 0.20 μm and analyzed by LC–LTQ-Orbitrap.

2.3. LC/MS analyses

LC analyses were carried out in an Accela HPLC system from Thermo Fisher Scientific (San Jose, CA, USA) consisting of an autosampler, a quaternary pump, a vacuum degasser, a thermostated column compartment and a diode array detector (DAD). UV/Vis spectra were recorded from 200 to 600 nm, while acquiring at a selected wavelength of 280 nm.

Chromatographic separation was performed on a reversed-phase column Atlantis T3 C18 (100 × 2.1 mm, 3 μm) from Waters (Milford, MA, USA) maintained at 25 °C. Mobile phases A and B were respectively, 0.1% formic acid in water and 0.1% formic acid in acetonitrile. The following linear gradient was used: hold at 100%A for 1 min, decreased to 92%A over 3 min, decreased to 80%A over 20 min, decreased to 70%A over 2 min, decreased to 0%A over 2 min and hold for 6 min, then returned to initial conditions over 2 min and re-equilibrated for 5 min. The flow rate and the injection volume were set to 350 μL/min and 10 μL, respectively.

The LC system was coupled to a linear ion trap–Orbitrap mass spectrometer LTQ-Orbitrap Velos from Thermo Fisher Scientific (San Jose, CA, USA) equipped with an electrospray ionization (ESI) source. The ESI source was operated in the negative mode under the following specific conditions: source voltage, 3.5 kV; sheath gas, 40 arbitrary units; auxiliary gas, 10 arbitrary units; sweep gas, 10 arbitrary units; and capillary temperature, 320 °C. Nitrogen (>99.98%) was employed as sheath, auxiliary and sweep gas. The scan cycle used a full scan event at resolution of 60,000 (at *m/z* 400) and three data-dependent MS/MS events acquired at a resolving power of 30,000. The most intense ions detected in full scan spectrum were selected for data-dependent scan. Parent ions were fragmented by high-energy C-trap dissociation (HCD) with normalized collision energy of 45% and an activation time of 100 ms.

Instrument control and data acquisition were performed with Xcalibur 2.0.7 software (Thermo Fisher Scientific). An external calibration for mass accuracy was carried out the day before the analysis according to the manufacturer's guidelines.

2.4. Total polyphenols

For the total polyphenols assay (Vallverdú-Queralt, Medina-Remón, Andres-Lacueva, & Lamuela-Raventos, 2011), 20 μL of the walnut extracts were mixed with 188 μL of Milli-Q water in a thermo microtiter 96-well plate (nuncTM, Roskilde, Denmark); afterwards, 12 μL of F–C reagent and 30 μL of sodium carbonate (200 g/L) were added. The mixtures were incubated for 1 h at room temperature in the dark. After, 50 μL of Milli-Q water were added and the absorbance was measured at 765 nm in a UV/VIS Thermo Multiskan Spectrum spectrophotometer (Vantaa, Finland). Results were expressed as mg of gallic acid equivalents (GAE)/100 g.

2.5. Antioxidant activity

The antioxidant activity in walnut extracts was measured using both an $ABTS^+$ radical decolourization assay (Minoggio et al., 2003) and an DDPH assay (Odriozola-Serrano, Soliva-Fortuny, & Martin-Belloso, 2008) with minor modifications (Vallverdú-Queralt et al., 2011). Briefly, the ABTS + assay consisted in adding 245 μL of $ABTS^+$ solution to 5 μL of Trolox or of walnut extracts. Then, the solutions were stirred for 30 s and the absorbance was recorded continuously every 30 s with a UV/VIS Thermo Multiskan Spectrum spectrophotometer for 1 h. For the DDPH assay, 250 μL of methanolic DPPH (0.025 g/L) were added to 5 μL of walnut extracts or of Trolox. Then, the solutions were mixed vigorously and then kept in darkness for 30 min. Absorption of the samples was measured on a UV/VIS Thermo Multiskan Spectrum

spectrophotometer at 515 nm. For both methods, each sample was analyzed in triplicate and the results were expressed as mmol Trolox equivalent (TE) per 100 g of sample. Methanol blanks were run in each assay.

3. Results and discussion

First of all, total phenols and the antioxidant capacity of the walnut extracts obtained were determined. The average of the total polyphenol content of the extracts was 2,464 ± 22 mg GAE/100 g. These results are in accordance to other studies done with walnuts in which values ranged from 1,576 to 2,499 mg GAE/100 g (Abe et al., 2010; Vinson & Cai, 2012). Among nuts, it is quite well established that walnuts show the highest values of total polyphenol content. On the other hand, the average values for antioxidant capacity were 21.4 ± 2.0 mmol TE/100 g and 25.7 ± 2.1 mmol TE/100 g for the $ABTS^{+}$ and DPPH assays, respectively. This is in accordance to other authors (Pellegrini et al., 2006; Vinson & Cai, 2012) who also reported that walnuts showed high scavenging activities, much higher than other nuts, such as hazelnuts, almonds or peanuts. Therefore, walnuts seem to consolidate as an important food source of polyphenols, with a significant antioxidant activity.

3.1. Identification of phenolic compounds in walnuts

Several mobile phases including methanol–water, methanol–water with 0.1% formic acid, acetonitrile–water and acetonitrile–water with 0.1% formic acid were screened in order to improve the chromatographic separation. Acetonitrile and 0.1% aqueous formic acid were the most suitable mobile phases. An aqueous-compatible reversed-phase column Atlantis T3 C18 allowed a suitable retention of the most polar compounds under highly aqueous conditions. The gradient elution was adjusted to achieve a good separation of major walnut constituents within a short analysis time. This optimized LC method was found acceptable and adequate for further MS/MS analysis.

Detection was carried out using a LTQ-Orbitrap Velos, consisting of a linear ion trap coupled with an Orbitrap FT mass analyzer, which gave highly accurate molecular weights and the fragmentation patterns acquired from multi-stage mass fragmentation for comprehensive understanding of their chemical structures. The molecular formulas were selected according to the measured accurate masses and the isotopic patterns, and then searched against the Dictionary of Natural Products, the Kyoto Encyclopedia of Genes and Genomes (KEGG) and the Plant Metabolic Network databases for tentative identification. Under these conditions, all proposed molecular formulas were estimated with mass errors below 3.5 ppm. The MS/MS spectra were compared with those of candidate compounds found in previous literature, especially when the presence of the compound was reported in walnuts.

Walnuts were found to contain a highly complex mixture of gallotannins, ellagitannins, flavonoids and phenolic acids; more than 100 individual phenolics were tentatively identified. Corresponding molecular formulas, their MS/MS fragments, mass measurement errors (Δm) and retention times are shown in Table 1. Many of these compounds had been previously detected in walnuts. However, the high-resolution MS analyses revealed the presence of other polyphenols that have never been reported in walnuts.

3.2. Hydrolysable tannins and related compounds

Major phenolic compounds found in walnut extracts belonged to the family of ellagitannins (ETs) (Table 1). These compounds are characterized by their hexahydroxydiphenoyl (HHDP) group, which is released on acid hydrolysis and spontaneously lactonizes to ellagic acid. ETs, as well as ellagic acid have attracted large attention due to their high antioxidant activity (Fukuda et al., 2003; Gil, Tomas-Barberan, Hess-Pierce, Holcroft, & Kader, 2000) and the health benefits associated with the intake of high ET-containing foods in the prevention of cardiovascular diseases (Larrosa, García-Conesa, Espín, & Tomás-Barberán, 2010) and cancer (Seeram et al., 2007).

Most of identified ETs in walnuts extracts occurred in several isomeric forms along the chromatogram (Fig. 1). ETs had two maximal UV absorptions at around 220 nm and 270–280 nm, respectively. The ratio of galloyl to HHDP groups esterified to the polyol determines the depth of the valley between these absorption maxima (Hanhineva et al., 2008).

As no standards are available for ETs, the peak area of each signal in mass chromatograms was used to provide semiquantitative information for comparison purposes. The most abundant ions were observed for three isomeric compounds with $[M–H]^{-}$ at m/z 783 (peaks 10, 14 and 23), yielding main fragment ions at m/z 301, which corresponds to ellagic acid (M–H-481, loss of HHDP-glucose) and at m/z 481, which corresponds to deprotonated HHDP-glucose (M–H-302, loss of HHDP). This fragmentation pattern corresponds to a bis-HHDP-glucose structure, presumably pedunculagin or casuariin isomers, which have been previously reported as one of the major ETs in walnuts (Cerda, Tomas-Barberan, & Espin, 2004; Fukuda, 2008, chap. 19).

On the basis of their exact mass and MS/MS data, five abundant peaks $[M–H]^{-}$ at m/z 951 (peaks 16, 24, 27, 31 and 56) were also identified as ellagitannins. All five peaks lose 44 Da from the $[M–H]^{-}$ ion, consistent with a free carboxyl group in their structure. MS/MS fragmentation also produced ions at m/z 783 (M–H-168, loss of gallic acid), m/z 481 (M–H-469, loss of a trisgalloyl group) and m/z 301, corresponding to ellagic acid. These results suggest that they consist of a HDDP-glucose and a trigalloyl group such as valoneoyl, sanguisorboyl, tergalloyl or macaranoyl groups (Okuda et al., 2009). Therefore, these ETs were tentatively identified as praecoxin A, which has already been detected in walnuts (Fukuda et al., 2003), including its isomers such as flosin A, platycariin or platycaryanin B (Tanaka, Kirihara, Nonaka, & Nishioka, 1993).

Five peaks showing significant $[M–H]^{-}$ signals at m/z 785 were found (peaks 33, 51, 67, 75 and 87), with fragment ions at m/z 633 (M–H-152, loss a galloyl unit), m/z 483 (M–H-302, loss of HHDP) and at m/z 301. This fragmentation pattern corresponded to a digalloyl-HHDP-glucose structure, probably tellimagrandin I isomers, which has been previously identified in walnuts (Fukuda et al., 2003).

Three peaks corresponding to $[M–H]^{-}$ signals at m/z 481 were also detected (peaks 1, 2 and 3). Based on their molecular weight and the presence of an intense product ion at m/z 301, they were assigned as HHDP-glucose isomers, earlier reported in walnut extracts (Fukuda, 2008, chap. 19).

Four glansrin C isomers were identified with $[M–H]^{-}$ ions at m/z 933 (peaks 72, 89, 101 and 116) and main MS/MS fragments at m/z 631 (loss of HHDP), m/z 481 (M-452, loss of trigalloyl group), m/z 451 (M-482, loss of HHDP-glucose) and m/z 301. Glansrin C was reported by Fukuda et al. (2003) in walnuts, although other isomers such as alnusnin B would fit with this fragmentation pattern.

Other monomeric ETs identified in the present study that have been previously reported to occur in walnuts are also shown in Table 1. These compounds are casuarinin/casuarictin isomers (galloyl-bis-HHDP-glucose), strictinin/isostrictinin isomers (galloyl-HHDP-glucose) and tellimagrandin II/pterocaryanin C isomers.

Another structurally related family of phenolic compounds, which could be detected in our walnut extracts, was that of flavano-ellagitannins hybrids, also referred in literature as complex tannins. The stenophyllanins A and B (Nonaka, Nishimura, & Nishioka,

Table 1
Phenolic compounds tentatively identified in walnut extracts.

Peak No.	t_R (min)	Compound identification	Formula	Measured mass	$[M–H]^-$ (*m/z*)	MS/MS fragments (*m/z*)	Δ*m* (ppm)
1	2.36	HHDP-glucose isomer	$C_{20}H_{18}O_{14}$	482.0690	481.0620	421.04, 300.99, 275.02	−1.36
2	2.74	HHDP-glucose isomer	$C_{20}H_{18}O_{14}$	482.0690	481.0620	421.04, 300.99, 275.02	−1.36
3	3.75	HHDP-glucose isomer	$C_{20}H_{18}O_{14}$	482.0690	481.0620	421.04, 300.99, 275.02	−1.36
4	4.95	Gallic acid	$C_7H_6O_5$	170.0213	169.0143	125.02	−1.31
5	5.00	Pedunculagin/casuariin isomer (bis-HHDP-glucose)	$C_{34}H_{24}O_{22}$	784.0751	783.0681	481.06, 300.99, 275.02	−1.05
6	5.10	Pterocarinin B	$C_{39}H_{32}O_{26}$	916.1171	915.1101	871.12, 781.09, 733.07, 569.11, 300.99, 275.02	−1.18
7	5.23	Strictinin/isostrictinin isomers (galloyl-HHDP-glucose)	$C_{27}H_{22}O_{18}$	634.0790	633.0720	463.05, 421.04, 300.99, 275.02	−2.54
8	5.75	Digalloyl-glucose isomer	$C_{20}H_{20}O_{14}$	484.0847	483.0777	331.07, 313.06, 169.01	−1.25
9	6.57	Strictinin/isostrictinin isomers (galloyl-HHDP-glucose)	$C_{27}H_{22}O_{18}$	634.0790	633.0720	463.05, 421.04, 300.99, 275.02	−2.54
10	6.90	Pedunculagin/casuariin isomer (bis-HHDP-glucose)	$C_{34}H_{24}O_{22}$	784.0751	783.0681	481.06, 300.99, 275.02	−1.05
11	7.10	Monogalloyl-glucose	$C_{13}H_{16}O_{10}$	332.0734	331.0664	169.01, 241.03, 271.04	−2.85
12	7.18	Procyanidin trimer	$C_{45}H_{38}O_{18}$	866.2050	865.1980	739.16, 577.13, 449.09, 299.05, 287.06, 289.07	−0.94
13	7.47	Digalloyl-glucose isomer	$C_{20}H_{20}O_{14}$	484.0847	483.0777	331.07, 313.06, 169.01	−1.25
14	7.80	Pedunculagin/casuariin isomer (bis-HHDP-glucose)	$C_{34}H_{24}O_{22}$	784.0751	783.0681	481.06, 300.99, 275.02	−1.05
15	8.24	Stenophyllanin C isomer	$C_{49}H_{36}O_{27}$	1056.1430	1055.1360	765.06, 721.07, 421.05, 289.07, 300.99	−1.32
16	8.95	Praecoxin A/platycariin isomer (trigalloyl-HHDP-glucose)	$C_{41}H_{28}O_{27}$	952.0810	951.0740	907.08, 783.07, 481.06, 300.99, 275.02	−0.84
17	9.01	Neochlorogenic acid (5-O-caffeoylquinic acid)	$C_{16}H_{18}O_9$	354.0947	353.0877	191.06, 179.034, 135.04	−1.08
18	9.11	Strictinin/isostrictinin isomers (galloyl-HHDP-glucose)	$C_{27}H_{22}O_{18}$	634.0790	633.0720	463.05, 421.04, 300.99, 275.02	−2.54
19	9.62	Flavogallonic acid dilactone isomer	$C_{21}H_{10}O_{13}$	470.0119	469.0049	425.01	−0.51
20	9.72	Stenophyllanin C isomer	$C_{49}H_{36}O_{27}$	1056.1430	1055.1360	765.06, 721.07, 421.05, 289.07, 300.99	−1.32
21	9.74	Strictinin/isostrictinin isomers (galloyl-HHDP-glucose)	$C_{27}H_{22}O_{18}$	634.0790	633.0720	463.05, 421.04, 300.99, 275.02	−2.54
22	10.33	Strictinin/isostrictinin isomers (galloyl-HHDP-glucose)	$C_{27}H_{22}O_{18}$	634.0790	633.0720	463.05, 421.04, 300.99, 275.02	−2.54
23	10.45	Pedunculagin/casuariin isomer (bis-HHDP-glucose)	$C_{34}H_{24}O_{22}$	784.0751	783.0681	481.06, 300.99, 275.02	−1.05
24	10.84	Praecoxin A/platycariin isomer (trigalloyl-HHDP-glucose)	$C_{41}H_{28}O_{27}$	952.0810	951.0740	907.08, 783.07, 481.06, 300.99, 275.02	−0.84
25	10.91	Procyanidin dimer	$C_{30}H_{26}O_{12}$	578.1421	577.1351	451.10, 425.09, 407.08, 289.07	−0.56
26	11.11	3-p-Coumaroylquinic acid	$C_{16}H_{18}O_8$	338.0993	337.0923	163.04, 119.05	−2.57
27	11.40	Praecoxin A/platycariin isomer (trigalloyl-HHDP-glucose)	$C_{41}H_{28}O_{27}$	952.0810	951.0740	907.08, 783.07, 481.06, 300.99, 275.02	−0.84
28	11.45	Procyanidin dimer	$C_{30}H_{26}O_{12}$	578.1421	577.1351	451.10, 425.09, 407.08, 289.07	−0.56
29	11.60	Digalloyl-glucose isomer	$C_{20}H_{20}O_{14}$	484.0847	483.0777	331.07, 313.06, 169.01	−1.25
30	11.61	Procyanidin tetramer	$C_{60}H_{50}O_{24}$	1154.2690	576.1275 $[M–2H]^{2-}$	865.19, 739.16, 576.12, 491.09, 289.07	−0.17
31	11.96	Praecoxin A/platycariin isomer (trigalloyl-HHDP-glucose)	$C_{41}H_{28}O_{27}$	952.0810	951.0740	907.08, 783.07, 481.06, 300.99 275.02	−0.84
32	12.16	Heterophylliin E isomer	$C_{40}H_{28}O_{25}$	908.0907	907.0837	783.07, 764.05, 481.06, 300.99, 275.02	−1.43
33	12.17	Tellimagrandin I isomer (digalloyl-HHDP-glucose)	$C_{34}H_{26}O_{22}$	786.0910	785.0840	633.07, 615.06, 483.08, 300.99, 275.02	−0.73
34	12.31	(+)-Catechin	$C_{15}H_{14}O_6$	290.0789	289.0719	245.08, 205.05, 179.03	−0.48
35	12.35	Digalloyl-glucose isomer	$C_{20}H_{20}O_{14}$	484.0847	483.0777	331.07, 313.06, 169.01	−1.25
36	12.37	Procyanidin trimer	$C4_5H_{38}O_{18}$	866.2050	865.1980	739.16, 577.13, 449.09, 299.05, 287.06, 289.07	−0.94
37	13.14	Pterocarinin A isomer	$C_{46}H_{36}O_{30}$	1068.1270	1067.1200	1023.13, 933.09, 765.11, 377.03, 300.99, 249.04	−2.00
38	13.17	Chlorogenic acid (3-O-caffeoylquinic acid)	$C_{16}H_{18}O_9$	354.0947	353.0877	191.06, 179.034, 135.04	−1.08
39	13.26	Procyanidin trimer	$C_{45}H_{38}O_{18}$	866.2050	865.1980	739.16, 577.13, 449.09, 299.05, 287.06, 289.07	−0.94
40	13.29	Coumaric acid hexoside isomer	$C_{15}H_{18}O_8$	326.0994	325.0924	265.07, 235.06, 205.049, 163.04	−2.48
41	13.48	Pterocarinin A isomer	$C_{46}H_{36}O_{30}$	1068.1270	1067.1200	1023.13, 933.09, 765.11, 377.03, 300.99, 249.04	−2.00
42	13.66	Stenophyllanin A/B isomer	$C_{56}H_{40}O_{31}$	1208.1550	1207.1480	917.07, 289.07, 300.99, 275.02	−0.29
43	13.83	Procyanidin tetramer	$C_{60}H_{50}O_{24}$	1154.2690	576.1275 $[M–2H]^{2-}$	865.19, 739.16, 576.12, 491.09, 289.07	−0.17
44	14.01	Strictinin/isostrictinin isomers (galloyl-HHDP-glucose)	$C_{27}H_{22}O_{18}$	634.0790	633.0720	463.05, 421.04, 300.99, 275.02	−2.54
45	14.29	1,2′,3′-tris-O-degalloyl rugosin F isomer	$C_{61}H_{44}O_{40}$	1416.1394	707.0627 $[M–2H]^{2-}$	933.06, 783,07, 631.05, 481.06, 300.99	−1.05
46	14.39	Glansrin B isomer	$C_{40}H_{26}O_{25}$	906.0759	905.0689	763.04, 481.06, 300.998, 275.02	−0.48
47	14.70	Casuarinin/casuarictin isomer	$C_{41}H_{28}O_{26}$	936.0856	935.0786	783.07, 633.07, 481.06, 300.99, 275.02	−1.37
48	14.72	Coumaric acid hexoside isomer	$C_{15}H_{18}O_8$	326.0994	325.0924	265.07, 235.06, 205.049, 163.04	−2.48
49	14.86	Procyanidin pentamer	$C_{75}H_{62}O_{30}$	1442.3310	720.1585 $[M–2H]^{2-}$	863.18, 577.13, 451.10, 289.07	−1.10
50	15.06	Alienanin B isomer	$C_{82}H_{54}O_{51}$	1854.1614	926.0737 $[M–2H]^{2-}$	1175.09, 633.07, 573.05, 300.99	−0.97
51	15.44	Tellimagrandin I isomer (digalloyl-HHDP-glucose)	$C_{34}H_{26}O_{22}$	786.0910	785.0840	633.07, 615.06, 483.08, 300.99, 275.02	−0.73
52	15.63	Procyanidin pentamer	$C_{75}H_{62}O_{30}$	1442.3310	720.1585 $[M–2H]^{2-}$	863.18, 577.13, 451.10, 289.07	−1.10
53	15.80	Oenothein B isomer	$C_{68}H_{48}O_{44}$	1568.1502	783.0681 $[M–2H]^{2-}$	951.07, 907.08, 615.06, 481.06, 300.99	−1.05
54	15.85	Alienanin B isomer	$C_{82}H_{54}O_{51}$	1854.1614	926.0737 $[M–2H]^{2-}$	1175.09, 633.07, 573.05, 300.99	−0.97
55	15.96	(−)-epicatechin	$C_{15}H_{14}O_6$	290.0789	289.0719	245.08, 205.05, 179.03	−0.48

(*continued on next page*)

Table 1 (*continued*)

Peak No.	t_R (min)	Compound identification	Formula	Measured mass	$[M-H]^-$ (*m/z*)	MS/MS fragments (*m/z*)	Δ*m* (ppm)
56	16.12	Praecoxin A/platycariin isomer (trigalloyl-HHDP-glucose)	$C_{41}H_{28}O_{27}$	952.0810	951.0740	907.08, 783.07, 481.06, 300.99, 275.02	−0.84
57	16.58	Valoneic acid dilactone/sanguisorbic acid dilactone isomer	$C_{21}H_{10}O_{13}$	470.0119	469.0049	450.99, 425.01, 300.99, 166.99	−0.51
58	16.61	Heterophylliin E isomer	$C_{40}H_{28}O_{25}$	908.0907	907.0837	783.07, 764.05, 481.06, 300.99, 275.02	−1.43
59	16.61	Procyanidin hexamer	$C_{90}H_{72}O_{36}$	1730.3940	864.19 $[M-2H]^{2-}$	1151.25, 788.17, 575.12, 289.07, 287.06	−1.14
60	16.70	4-p-Coumaroylquinic acid	$C_{16}H_{18}O_8$	338.0993	337.0923	173.08, 163.04	−2.57
61	16.97	Reginin A/reginin D isomer	$C_{75}H_{50}O_{48}$	1718.1440	858.0650 $[M-2H]^{2-}$	933.06, 783.07 481.06, 300.99, 275.02	−1.83
62	17.00	Trigalloyl-glucose isomer	$C_{27}H_{24}O_{18}$	636.0947	635.0877	483.08, 465.07, 423.06, 313.06, 169.01	−2.47
63	17.21	Stenophyllanin A/B isomer	$C_{56}H_{40}O_{31}$	1208.1550	1207.1480	917.07, 289.07, 300.99, 275.02	−0.29
64	17.23	Valoneic acid dilactone/sanguisorbic acid dilactone isomer	$C_{21}H_{10}O_{13}$	470.0119	469.0049	450.99, 425.01, 300.99, 166.99	−0.51
65	17.38	Procyanidin hexamer	$C_{90}H_{72}O_{36}$	1730.3940	864.19 $[M-2H]^{2-}$		−1.14
66	17.48	Glansrin B isomer	$C_{40}H_{26}O_{25}$	906.0759	905.0689	763.04, 481.06, 300.998, 275.02	−0.48
67	17.60	Tellimagrandin I isomer (digalloyl-HHDP-glucose)	$C_{34}H_{26}O_{22}$	786.0910	785.0840	633.07, 615.06, 483.08, 300.99, 275.02	−0.73
68	17.80	Oenothein B isomer	$C_{68}H_{48}O_{44}$	1568.1502	783.0681 $[M-2H]^{2-}$	951.07, 907.08, 615.06, 481.06, 300.99	−1.05
69	17.86	Procyanidin tetramer	$C_{60}H_{50}O_{24}$	1154.2690	576.1275 $[M-2H]^{2-}$	865.19, 739.16, 576.12, 491.09, 289.07	−0.17
70	17.98	Ellagic acid hexoside isomer	$C_{20}H_{16}O_{13}$	464.0587	463.0517	300.99	−0.84
71	18.00	Reginin A/reginin D isomer	$C_{75}H_{50}O_{48}$	1718.1440	858.0650 $[M-2H]^{2-}$	933.06, 783.07 481.06, 300.99, 275.02	−1.83
72	18.49	Glansrin C isomer	$C_{41}H_{26}O_{26}$	934.0700	933.0630	631.06, 481.06, 450.99, 300.99	−1.32
73	18.57	Ellagic acid hexoside isomer	$C_{20}H_{16}O_{13}$	464.0587	463.0517	300.99	−0.84
74	18.78	Reginin A/reginin D isomer	$C_{75}H_{50}O_{48}$	1718.1440	858.0650 $[M-2H]^{2-}$	933.06, 783.07 481.06, 300.99, 275.02	−1.83
75	18.94	Tellimagrandin I isomer (digalloyl-HHDP-glucose)	$C_{34}H_{26}O_{22}$	786.0910	785.0840	633.07, 615.06, 483.08, 300.99, 275.02	−0.73
76	18.97	Glansrin D/degalloyl rugosin F isomer	$C_{75}H_{52}O_{48}$	1720.1600	859.0730 $[M-2H]^{2-}$	1417.15, 1059.03, 935.07, 783.07, 633.07, 300.99	−1.63
77	19.21	Malabathrin A isomer	$C_{63}H_{44}O_{35}$	1360.1634	679.07471 $[M-2H]^{2-}$	1057.1544, 917.07, 441.08, 289.07, 300.99	−2.14
78	19.39	Alienanin B isomer	$C_{82}H_{54}O_{51}$	1854.1614	926.0737 $[M-2H]^{2-}$	1175.09, 633.07, 573.05, 300.99	−0.97
79	19.39	Procyanidin dimer	$C_{30}H_{26}O_{12}$	578.1421	577.1351	451.10, 425.09, 407.08, 289.07	−0.56
80	19.47	Procyanidin pentamer	$C_{75}H_{62}O_{30}$	1442.3310	720.1585 $[M-2H]^{2-}$	863.18, 577.13, 451.10, 289.07	−1.10
81	19.64	Euprostin A isomer	$C_{55}H_{34}O_{34}$	1238.0914	618.0387 $[M-2H]^{2-}$	935.08, 917.07, 767.07, 425.01, 300.99	−0.97
82	19.80	Reginin A/reginin D isomer	$C_{75}H_{50}O_{48}$	1718.1440	858.065 $[M-2H]^{2-}$	933.06, 783.07 481.06, 300.99, 275.02	−1.83
83	20.00	Trigalloyl-glucose isomer	$C_{27}H_{24}O_{18}$	636.0947	635.0877	483.08, 465.07, 423.06, 313.06, 169.01	−2.47
84	20.17	Casuarinin/casuarictin isomer	$C_{41}H_{28}O_{26}$	936.0856	935.0786	783.07, 633.07, 481.06, 300.99, 275.02	−1.37
85	20.17	Glansreginin B	$C_{24}H_{38}O_{15}$	566.2200	565.2130	403.16, 343.14, 283.12, 241.11, 197.12	−0.92
86	20.17	Rugosin C/platycaryanin A/glansrin A isomer	$C_{48}H_{32}O_{31}$	1104.0920	1103.0850	1059.09, 935.07, 757.09, 633.07, 300.99	−0.68
87	20.41	Tellimagrandin I isomer (digalloyl-HHDP-glucose)	$C_{34}H_{26}O_{22}$	786.0910	785.0840	633.07, 615.06, 483.08, 300.99, 275.02	−0.73
88	20.84	Rugosin C/platycaryanin A/glansrin A isomer	$C_{48}H_{32}O_{31}$	1104.0920	1103.0850	1059.09, 935.07, 757.09, 633.07, 300.99	−0.68
89	21.13	Glansrin C isomer	$C_{41}H_{26}O_{26}$	934.0700	933.0630	631.06, 481.06, 450.99, 300.99	−1.32
90	21.36	2′,3′-Bis-O-degalloyl rugosin F isomer	$C_{68}H_{48}O_{44}$	1568.1502	783.0681 $[M-2H]^{2-}$	1085.07, 935.07, 631.06, 481.06, 300.99	−1.05
91	21.40	Reginin A/reginin D isomer	$C_{75}H_{50}O_{48}$	1718.1440	858.0650 $[M-2H]^{2-}$	933.06, 783.07 481.06, 300.99, 275.02	−1.83
92	21.43	Euprostin A isomer	$C_{55}H_{34}O_{34}$	1238.0914	618.0387 $[M-2H]^{2-}$	935.08, 917.07, 767.07, 425.01, 300.99	−0.97
93	21.43	Procyanidin tetramer	$C_{60}H_{50}O_{24}$	1154.2690	576.1275 $[M-2H]^{2-}$	865.19, 739.16, 576.12, 491.09, 289.07	−0.17
94	22.12	Tellimagrandin II/pterocaryanin C isomer	$C_{41}H_{30}O_{26}$	938.1017	937.0947	785.08, 635.08, 483.07, 300.99	−0.89
95	22.20	Ellagic acid pentoside isomer	$C_{19}H1_4O_{12}$	434.0475	433.0405	300.99	−2.36
96	22.27	2′,3′-Bis-O-degalloyl rugosin F isomer	$C_{68}H_{48}O_{44}$	1568.1502	783.0681 $[M-2H]^{2-}$	1085.07, 935.07, 631.06, 481.06, 300.99	−1.05
97	22.58	Glansrin D/degalloyl rugosin F isomer	$C_{75}H_{52}O_{48}$	1720.1600	859.073 $[M-2H]^{2-}$	1417.15, 1059.03, 935.07, 783.07, 633.07, 300.99	−1.63
98	22.70	Quercetin galloylhexoside isomer	$C_{28}H_{24}O_{16}$	616.1056	615.0986	463.08, 301.03	−1.31
99	23.03	(−)-Epicatechin 3-O-gallate	$C_{22}H_{18}O_{10}$	442.0900	441.0821	331.04, 289.07, 271.06, 169.01	−2.13
100	23.20	Tetragalloyl-glucose	$C_{34}H_{28}O_{22}$	788.1066	787.0996	635.08, 617.07, 465.07, 169.01	−0.79
101	23.44	Glansrin C isomer	$C_{41}H_{26}O_{26}$	934.0700	933.0630	631.06, 481.06, 450.99, 300.99	−1.32
102	23.44	Rugosin C/platycaryanin A/glansrin A isomer	$C_{48}H_{32}O_{31}$	1104.0920	1103.0850	1059.09, 935.07, 757.09, 633.07, 300.99	−0.68
103	23.55	Ellagic acid	$C_{14}H_6O_8$	302.0059	300.9989	283.99, 257.01, 229.01, 185.02	−1.38
104	23.72	Quercetin hexoside isomer	$C_{21}H_{20}O_{12}$	464.0940	463.0870	300.03, 301.03	−3.18
105	24.26	Tetragalloyl-glucose	$C_{34}H_{28}O_{22}$	788.1066	787.0996	635.08, 617.07, 465.07, 169.01	−0.79
106	24.32	Quercetin hexoside isomer	$C_{21}H_{20}O_{12}$	464.0940	463.0870	300.03, 301.03	−3.18
107	24.70	Rugosin F	$C_{82}H_{56}O_{52}$	1872.1710	935.0785 $[M-2H]^{2-}$	1059.09, 935.07, 917.07, 767.07, 300.99	−1.47
108	24.80	Glansrin D/degalloyl rugosin F isomer	$C_{75}H_{52}O_{48}$	1720.1600	859.073 $[M-2H]^{2-}$	1417.15, 1059.03, 935.07, 783.07, 633.07, 300.99	−1.63
109	25.21	Heterophylliin D	$C_{82}H_{54}O_{52}$	1870.1560	934.071 $[M-2H]^{2-}$	1085.07, 783.07, 633.07, 450.99, 300.99	−1.13
110	25.42	Quercetin pentoside isomer	$C_{20}H_{18}O_{11}$	434.0842	433.0772	300.03, 301.03	−1.62
111	25.96	Tellimagrandin II/pterocaryanin C isomer	$C_{41}H_{30}O_{26}$	938.1017	937.0947	785.08, 635.08, 483.07, 300.99	−0.89

112	26.04	Quercetin pentoside isomer	$C_{20}H_{18}O_{11}$	434.0842	433.0772	300.03, 301.03	−1.62
113	26.26	Eucalbanin A/cornusiin B isomer	$C_{48}H_{30}O_{30}$	1086.0810	1085.0740	783.07, 633.07, 450.99, 300.99	−1.09
114	26.69	1,2,3,4,6-Pentagalloyl-glucose	$C_{41}H_{32}O_{26}$	940.1170	939.1100	787.09, 769.09, 617.08, 431.06	−1.26
115	26.77	Glansrin B isomer	$C_{40}H_{26}O_{25}$	906.0759	905.0689	763.04, 481.06, 300.998, 275.02	−0.48
116	26.81	Glansrin C isomer	$C_{41}H_{26}O_{26}$	934.0700	933.0630	631.06, 481.06, 450.99, 300.99	−1.32
117	26.97	Glansreginin A	$C_{28}H_{35}NO_{13}$	593.2100	592.2030	403.16, 343.14, 283.12, 241.11, 197.12	−0.49
118	27.09	Eucalbanin A/cornusiin B isomer	$C_{48}H_{30}O_{30}$	1086.0810	1085.0740	783.07, 633.07, 450.99, 300.99	−1.09
119	28.00	Eucalbanin A/cornusiin B isomer	$C_{48}H_{30}O_{30}$	1086.0810	1085.0740	783.07, 633.07, 450.99, 300.99	−1.09
120	28.31	Quercetin	$C_{15}H_{10}O_7$	302.0417	301.0347	151.04	−3.15

Δm = mass measurement error.

1985), in which an ET (casuarinin or casuariin) is attached via C–C linkage to the A ring of a (+)-catechin unit, were found with $[M–H]^-$ ions at *m*/*z* 1207 (peaks 42 and 63). MS/MS spectra of stenophyllanins A and B yielded ions at *m*/*z* 917 (M–H-289, loss of catechin), *m*/*z* 289 (deprotonated catechin) and *m*/*z* 301 (deprotonated ellagic acid). Stenophyllanins A and B were accompanied by the structurally related tannin, stenophyllanin C, showing a $[M–H]^-$ ion at *m*/*z* 1055 (peaks 15 and 20), which corresponded to the loss of one galloyl group from the molecular mass of stenophyllanin A or B. Fragment ions at *m*/*z* 765 (M–H-289, loss of catechin), *m*/*z* 289 and *m*/*z* 301 allowed to assign its identity. Other flavano-ellagitannin was tentatively identified as the epicatechin-based malabathrin A (Okuda et al., 2009) showing a $[M–2H]^{2-}$ ion at 679 (peak 77), corresponding to a monoisotopic mass of 1360.1634 Da, and fragment ions at *m*/*z* 917 (M–H-441, loss of epicatechin gallate), *m*/*z* 441 (epicatechin gallate), *m*/*z* 289 and m/301 (Fig. 2). To our knowledge, this is the first time that the complex tannins stenophyllanin C and malabathrin A have been identified in walnuts. Compounds belonging to the same flavano-ellagitannin family, such as accutisim A, have been reported to exert potential anticancer properties, through DNA topoisomerase II inhibition (Quideau et al., 2003).

Compounds detected at *m*/*z* 1085 (peaks 113, 118 and 119) with fragment ion at *m*/*z* 633 corresponding to the HHDP galloyl-glucose (M-452, loss of trigalloyl group) were assigned to eucalbanin A or its isomer cornusiin B. They have been previously found in leaves and fruits of Eucalyptus species (Hou, Liu, Yang, Lin, & Sun, 2000), but they have never been reported in walnuts. Heterophylliin E and pterocarinin B with $[M–H]^-$ ions at *m*/*z* 907 (peak 32) and 915 (peak 6), respectively, have been also tentatively identified here for the first time in walnut extracts.

Several dimeric ETs were detected through their $[M–2H]^{2-}$ ions that were confirmed by the 0.5 Da mass differences between the isotopic peaks. The selected resolution of 60,000 (at *m*/*z* 400) allowed the determination of the charge state with high accuracy. Among the identified ETs dimers, reginin A (dimer of casuarinin and pendunculagin) and alienanin B (dimer of casuarinin and stachyurin) isomers showed doubly-charged ions at *m*/*z* 858 (peaks 61, 71, 74, 82 and 91) and *m*/*z* 926 (peaks 50, 54 and 78), corresponding to monoisotopic masses of 1718.1440 and 1854.1614 Da, respectively (Fig. 3). Fragmentation of double-charged ions gave product ions at *m*/*z* 933, 783, 481 and 301 for reginin A isomers, and at *m*/*z* 633 and 301 for alienalin B isomers. As far as we know, this is the first report of reginin A and alienalin B in walnuts.

Although major hydrolysable tannins found in walnuts were identified as ellagitannins, important amounts of other gallotannins were also present in the extracts. As known, ellagitannins are metabolically derived from gallotannins, mainly from pentagalloyl-glucose, through C–C oxidative coupling of galloyl groups (Okuda et al., 2009). The $[M–H]^-$ ions at *m*/*z* 331, 483, 635, 787 and 939 indicated the presence of mono-, di-, tri-, tetra- and pentagalloyl-glucose, respectively. Several isomeric forms of these galloylated esters of glucose with different retention times were found in our samples (peaks 8, 11, 13, 29, 35, 62, 83, 100, 105 and 114). Fragmentation patterns of polygalloyl-glucoses were characterized by successive losses of gallic acid (170 Da) and galloyl groups (152 Da). For monogalloyl-glucose (peak 11), MS/MS fragmentation yielded a predominant ion at *m*/*z* 169 after the loss of the glucosyl moiety (162 Da) and at *m*/*z* 271 after cross-ring fragmentation of glucose (M–H-60) (Meyers, Swiecki, & Mitchell, 2006).

Ellagic acid (EA) and its derivatives were also identified. The presence of free EA was confirmed at 23.5 min by a $[M–H]^-$ ion at *m*/*z* 301 (peak 103), which yielded characteristic MS/MS fragments at *m*/*z* 257, 229 and 185 (Mullen, Yokota, Lean, & Crozier,

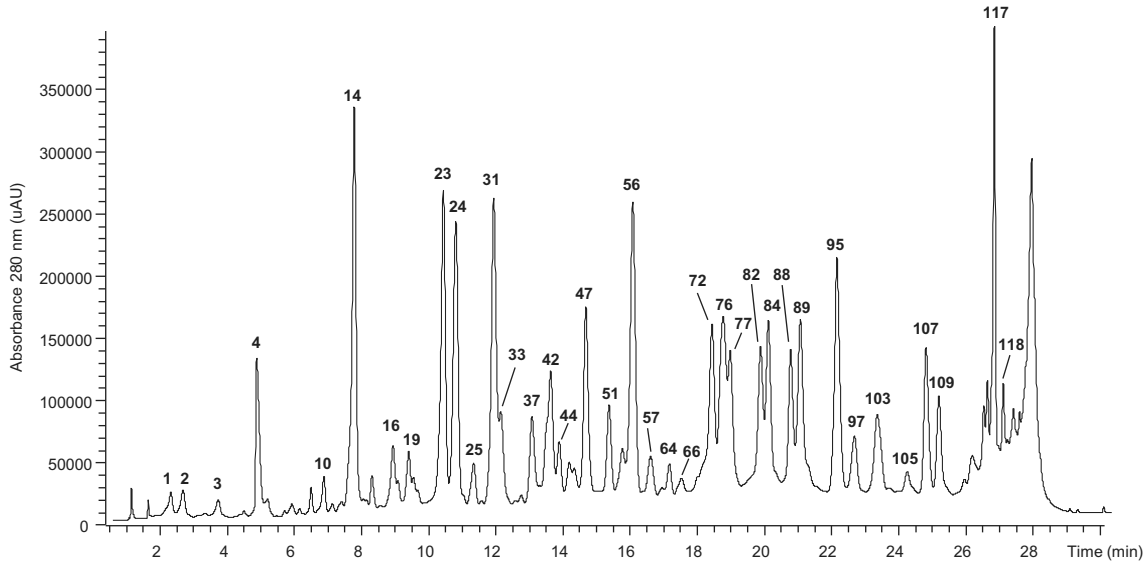

Fig. 1. Chromatographic profile obtained at 280 nm for a walnut extract. Peak number identities are displayed in Table 1.

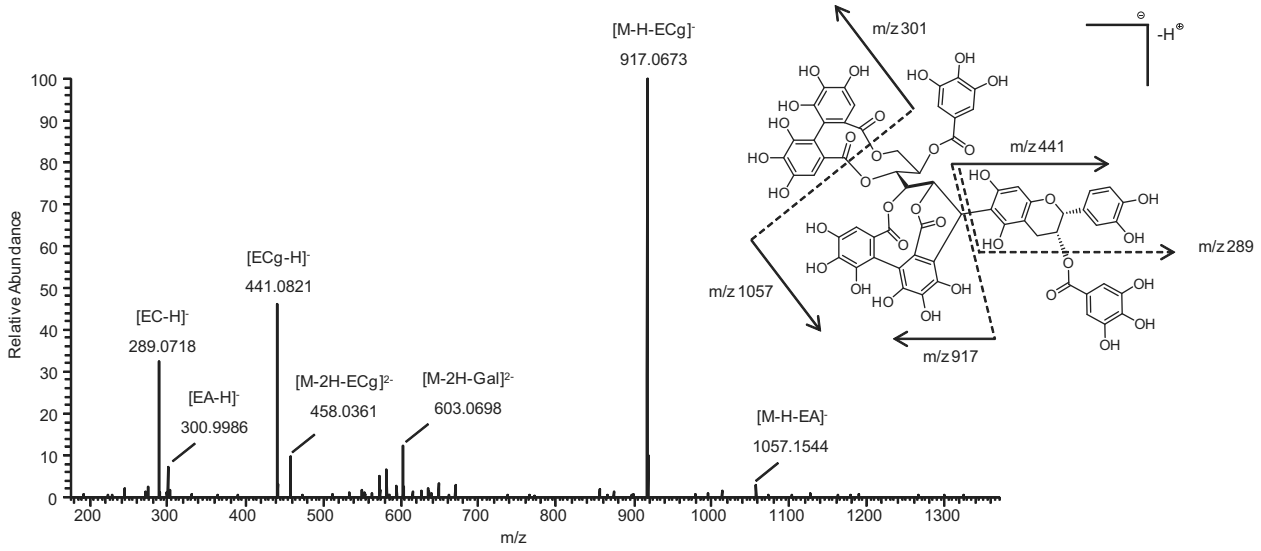

Fig. 2. MS/MS fragmentation spectrum of a malabathrin A isomer.

2003). In addition to EA, several monoglycosylated EA derivatives were observed in walnut, such as EA pentoside (*m*/*z* 433; peak 95) and EA hexoside (*m*/*z* 463; peaks 70 and 73), showing the typical fragment of EA at *m*/*z* 301 in the MS/MS analysis. The antioxidant effect of EA, in spite of its rather small size, is quite high in accordance with the high stability of its free radical. EA exhibits important health promoting effects via its antioxidant, antiproliferative, chemopreventive, and antiatherogenic activities (Larrosa et al., 2010).

Valoneic acid dilactone was also identified, providing a $[M–H]^-$ ion at *m*/*z* 469 and two main fragments at *m*/*z* 425 and 301 due to the loss of CO_2 from the deprotonated molecule and to the ellagic acid fragment, respectively. Furthermore, two isomers were also detected with a similar fragmentation pattern, which were tentatively identified as sanguisorbic acid dilactone and flavogallonic acid dilactone (Boulekbache-Makhlouf, Meudec, Mazauric, Madani, & Cheynier, 2013). The latter showed a much lower relative intensity for the ellagic acid fragment, which might be explained by the higher stability of the C–C linkage between the ellagic acid and the gallic acid moiety in this compound.

3.3. Flavonoids

(+)-Catechin was identified as the predominant flavan-3-ol with a $[M–H]^-$ ion at *m*/*z* 289 and MS/MS fragments at *m*/*z* 245, *m*/*z* 205 and *m*/*z* 179. It was in agreement with the results reported by Gómez-Caravaca et al. (2008) who found catechin in walnuts at levels from 4.0 to 6.6 mg/kg dry weight.

It was also possible to identify (−)-epicatechin (peak 55) that shares the same $[M–H]^-$ ion as catechin (peak 34), and (−)-epicatechin 3-*O*-gallate (peak 99), with an $[M–H]^-$ ion at *m*/*z* 441. Oligomeric B-type procyanidins, from dimers up (peaks 25, 28 and 79) to hexamers (peaks 59 and 65), were identified by their $[M–H]^-$ or $[M–2H]^{2-}$ ions and their characteristic MS/MS fragments (Table 1). Previous studies have reported the presence of

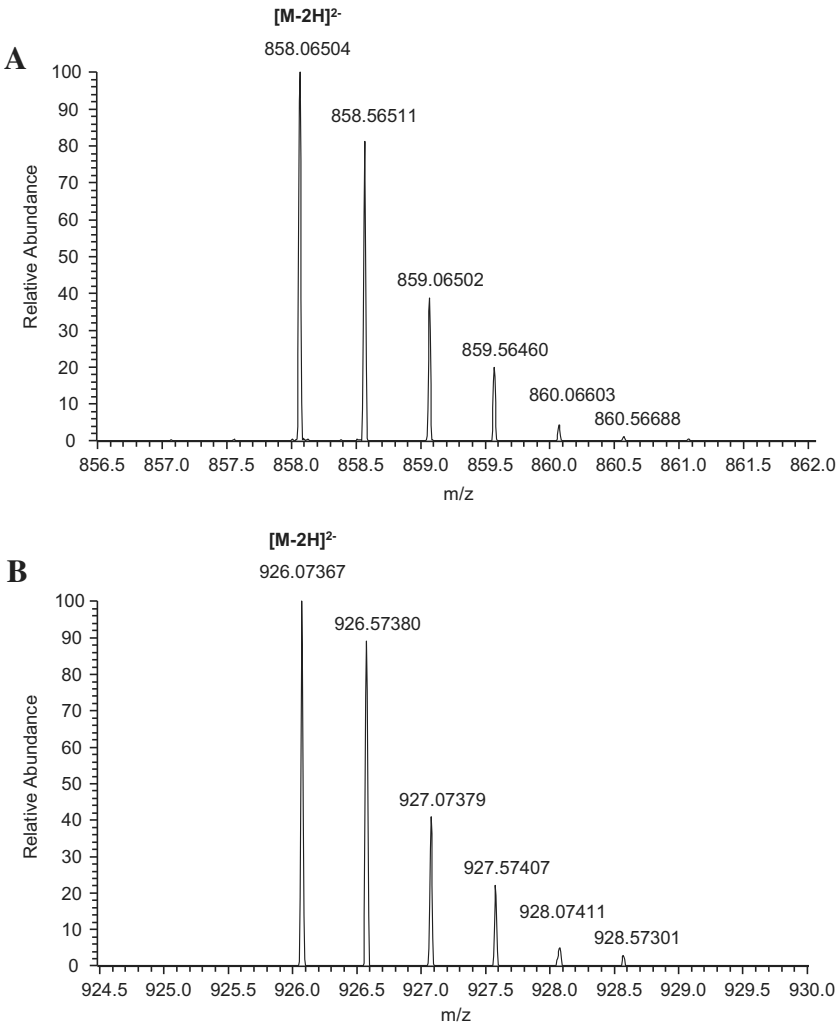

Fig. 3. Mass spectra showing the doubly-charged ions of reginin A isomer (A) and alienanin B isomer (B).

monomeric flavan-3-ols and B-type procyanidins in walnuts, although at low concentration levels (Prior & Gu, 2005).

Examination of the chromatograms also revealed the presence of some quercetin derivatives. The peak detected at *m*/*z* 615 with its fragments at *m*/*z* 463 (M–H-152, loss of galloyl group) and *m*/*z* 301.034 (M–H-162, loss of hexosyl group), was tentatively assigned to quercetin galloyl-hexoside. Peak at *m*/*z* 463 giving the 301.034 fragment, i.e. quercetin after losing a hexose unit (162 Da) was identified as a quercetin hexoside, whereas ion $[M–H]^-$ at *m*/*z* 433 was assigned to quercetin pentoside, also with MS/MS fragment at *m*/*z* 301.034. Trace amounts of quercetin aglycone were also detected at *m*/*z* 301.034. These flavonols derivatives have been previously reported in walnuts (Amaral et al., 2004). Flavonol derivatives are valuable phytochemicals consistently associated with antioxidant and anticarcinogenic activities, and a relatively longer circulation time in vivo (Nagasawa et al., 2003).

3.4. Phenolic acids and related compounds

Phenolic acids are shown to impart antimutagenic, antiglycemic, and antioxidative properties (Scalbert, Manach, Morand, Rémésy, & Jiménez, 2005). Two peaks were identified as caffeoylquinic acids (chlorogenic and neochlorogenic acids) based on their prominent $[M–H]^-$ ions at *m*/*z* 353 and characteristic fragment ions at *m*/*z* 191 (M–H-162, loss of cafeoyl moiety) and 179 (M–H-174, loss of quinoyl moiety). Only chlorogenic acid (3-caffeoylquinic acid) could be confirmed by comparing its spectrum and retention time with those of a standard. Preliminary structure-activity relationship studies on cinnamic acids and derivatives have pointed out the importance of the catechol group to their antiradical efficacy (Silva et al., 2000).

Two more phenolic acids were also identified since a quasimolecular ion $[M–H]^-$ at *m*/*z* 337 was found for two peaks. Fragmentation of the first one yielded a base peak at *m*/*z* 163, corresponding to the loss of quinic acid radical, which is in accordance with literature data found for 3-*p*-coumaroylquinic acid (Clifford, Johnston, Knight, & Kuhnert, 2003). The latter gave a base peak at *m*/*z* 173, so it was identified as 4-*p*-coumaroylquinic acid. These kind of phenolic compounds have been previously reported in walnut kernels (Gómez-Caravaca et al., 2008; Pereira et al., 2007).

4. Conclusions

The use of LC coupled with a linear trap quadrupole (LTQ) and a high-resolution Orbitrap mass analyzer (LC–LTQ-Orbitrap) allowed us to carry out a comprehensive identification of phenolic compounds present in walnuts from *J. regia* L.

A total of 120 phenolic compounds, including hydrolysable and condensed tannins, flavonoids and phenolic acids, were identified or tentatively characterized based mainly on their accurate mass

measurement from LTQ-Orbitrap (within 3.5 ppm error), the fragment ions information obtained by MS/MS experiments, as well as the mass data provided by reference standards and by literature. Ellagitannins, ellagic acid and its derivatives, coexisted as major constituent of walnuts, yielding a complex phenolic profile. Eight of them (stenophyllanin C, malabathrin A, heterophylliin E, pterocarinin B, eucalbanin A, cornusiin B, reginin A and alienanin B), as far as we know, have been identified for the first time in walnuts.

Although significant work has been previously reported in the identification of walnut polyphenols, most of it has been carried out by NMR techniques. Therefore, this research constitutes the first comprehensive identification of phenolic compounds in walnuts by LC coupled to high-resolution mass spectrometry. It provides useful information to further develop new methods for the reliable quantification of these compounds in such a complex matrix, especially for ellagitannins, which levels might be underestimated due to the difficulty associated with their analysis.

Acknowledgments

This work was supported by a grant from California Walnut Commission. J.R. was supported by Juan de la Cierva post-doctoral contract from the Ministry of Science and Innovation (MICINN) of Spain. C.S. was supported by "Consejo Nacional de Ciencia y Tecnología(CONACYT)" and by the "Dirección General de Relaciones Internacionales de la Secretaría de la Educación Pública (DGRI-SEP)" from Mexico. A.V. received support from the MICINN of Spain as well. The authors acknowledge the technical assistance of Dr Olga Jauregui from the "Scientific and Technical Services" of the University of Barcelona (Spain).

References

Abe, L. T., Lajolo, F. M., & Genovese, M. I. (2010). Comparison of phenol content and antioxidant capacity of nuts. *Ciência e Tecnologia de Alimentos, 30*, 254–259.

Amaral, J. S., Seabra, R. M., Andrade, P. B., Valentão, P. C., Pereira, J. A., & Ferreres, F. (2004). Phenolic profile in the quality control of walnut (*Juglans regia* L.) leaves. *Food Chemistry, 88*, 373–379.

Anderson, K. J., Teuber, S. S., Gobeille, A., Cremin, P., Waterhouse, A. L., & Steinberg, F. M. (2001). Walnut polyphenolics inhibit in vitro human plasma and LDL oxidation. *The Journal of Nutrition, 131*, 2837–2842.

Boulekbache-Makhlouf, L., Meudec, E., Mazauric, J.-P., Madani, K., & Cheynier, V. (2013). Qualitative and semi-quantitative analysis of phenolics in eucalyptus globulus leaves by high-performance liquid chromatography coupled with diode array detection and electrospray ionisation mass spectrometry. *Phytochemical Analysis, 24*, 162–170.

Bulló, M., Lamuela-Raventós, R., & Salas-Salvadó, J. (2011). Mediterranean diet and oxidation: Nuts and olive oil as important sources of fat and antioxidants. *Current Topics in Medicinal Chemistry, 11*, 1797–1810.

Cerda, B., Tomas-Barberan, F. A., & Espin, J. C. (2004). Metabolism of antioxidant and chemopreventive ellagitannins from strawberries, raspberries, walnuts, and oak-aged wine in humans: identification of biomarkers and individual variability. *Journal of Agricultural and Food Chemistry, 53*, 227–235.

Clifford, M. N., Johnston, K. L., Knight, S., & Kuhnert, N. (2003). Hierarchical scheme for LC–MSn identification of chlorogenic acids. *Journal of Agricultural and Food Chemistry, 51*, 2900–2911.

Estruch, R., Ros, E., Salas-Salvadó, J., Covas, M.-I., Corella, D., Arós, F., et al. (2013). Primary prevention of cardiovascular disease with a Mediterranean diet. *New England Journal of Medicine, 368*, 1279–1290.

Fukuda, T. (2008). Walnut polyphenols: structures and functions. In C. Alasalvar & F. Shahidi (Eds.), *Tree Nuts: Composition, Phytochemicals, and Health Effects*. Boca Raton, FL: CRC Press.

Fukuda, T., Ito, H., & Yoshida, T. (2003). Antioxidative polyphenols from walnuts (*Juglans regia* L.). *Phytochemistry, 63*, 795–801.

Gil, M. I., Tomas-Barberan, F. A., Hess-Pierce, B., Holcroft, D. M., & Kader, A. A. (2000). Antioxidant activity of pomegranate juice and its relationship with phenolic composition and processing. *Journal of Agricultural and Food Chemistry, 48*, 4581–4589.

Gómez-Caravaca, A. M., Verardo, V., Segura-Carretero, A., Caboni, M. F., & Fernández-Gutiérrez, A. (2008). Development of a rapid method to determine phenolic and other polar compounds in walnut by capillary electrophoresis–electrospray ionization time-of-flight mass spectrometry. *Journal of Chromatography A, 1209*, 238–245.

Hanhineva, K., Rogachev, I., Kokko, H., Mintz-Oron, S., Venger, I., Kärenlampi, S., et al. (2008). Non-targeted analysis of spatial metabolite composition in strawberry (*Fragaria ananassa*) flowers. *Phytochemistry, 69*, 2463–2481.

Hou, A. J., Liu, Y. Z., Yang, H., Lin, Z. W., & Sun, H. D. (2000). Hydrolyzable tannins and related polyphenols from *Eucalyptus globulus*. *Journal of Asian Natural Products Research, 2*, 205–212.

Ito, H., Okuda, T., Fukuda, T., Hatano, T., & Yoshida, T. (2007). Two novel dicarboxylic acid derivatives and a new dimeric hydrolyzable tannin from walnuts. *Journal of Agricultural and Food Chemistry, 55*, 672–679.

Larrosa, M., García-Conesa, M. T., Espín, J. C., & Tomás-Barberán, F. A. (2010). Ellagitannins, ellagic acid and vascular health. *Molecular Aspects of Medicine, 31*, 513–539.

Maguire, L. S., O'Sullivan, S. M., Galvin, K., O'Connor, T. P., & O'Brien, N. M. (2004). Fatty acid profile, tocopherol, squalene and phytosterol content of walnuts, almonds, peanuts, hazelnuts and the macadamia nut. *International Journal of Food Sciences and Nutrition, 55*, 171–178.

Meyers, K. J., Swiecki, T. J., & Mitchell, A. E. (2006). Understanding the Native Californian diet: Identification of condensed and hydrolyzable tannins in tanoak acorns (*Lithocarpus densiflorus*). *Journal of Agricultural and Food Chemistry, 54*, 7686–7691.

Minoggio, M., Bramati, L., Simonetti, P., Gardana, C., Iemoli, L., Santangelo, E., et al. (2003). Polyphenol pattern and antioxidant activity of different tomato lines and cultivars. *Annals of Nutrition and Metabolism, 47*, 64–69.

Mullen, W., Yokota, T., Lean, M. E. J., & Crozier, A. (2003). Analysis of ellagitannins and conjugates of ellagic acid and quercetin in raspberry fruits by LC–MSn. *Phytochemistry, 64*, 617–624.

Nagasawa, T., Tabata, N., Ito, Y., Aiba, Y., Nishizawa, N., & Kitts, D. (2003). Dietary G-rutin suppresses glycation in tissue proteins of streptozotocin-induced diabetic rats. *Molecular and Cellular Biochemistry, 252*, 141–147.

Nonaka, G., Nishimura, H., & Nishioka, I. (1985). Tannins and related compounds. Part 26. Isolation and structures of stenophyllanins A, B, and C, novel tannins from *Quercus stenophylla*. *Journal of the Chemical Society, Perkin Transactions, 1*, 163–172.

Odriozola-Serrano, I., Soliva-Fortuny, R., & Martin-Belloso, O. (2008). Effect of minimal processing on bioactive compounds and color attributes of fresh-cut tomatoes. *LWT-Food Science and Technology, 41*, 217–226.

Okuda, T., Yoshida, T., Hatano, T., & Ito, H. (2009). Ellagitannins renewed the concept of tannins. In S. Quideau (Ed.), *Chemistry and Biology of Ellagitannins: An Underestimated Class of Bioactive Plant Polyphenols* (pp. 1–54). Singapore: World Scientific Publishing Company.

Pan, A., Sun, Q., Manson, J. E., Willett, W. C., & Hu, F. B. (2013). Walnut consumption is associated with lower risk of Type 2 Diabetes in women. *The Journal of Nutrition, 143*, 512–518.

Pellegrini, N., Serafini, M., Salvatore, S., Del Rio, D., Bianchi, M., & Brighenti, F. (2006). Total antioxidant capacity of spices, dried fruits, nuts, pulses, cereals and sweets consumed in Italy assessed by three different in vitro assays. *Molecular Nutrition & Food Research, 50*, 1030–1038.

Pereira, J. A., Oliveira, I., Sousa, A., Valentão, P., Andrade, P. B., Ferreira, I. R., et al. (2007). Walnut (*Juglans regia* L.) leaves: Phenolic compounds, antibacterial activity and antioxidant potential of different cultivars. *Food and Chemical Toxicology, 45*, 2287–2295.

Prior, R. L., & Gu, L. (2005). Occurrence and biological significance of proanthocyanidins in the American diet. *Phytochemistry, 66*, 2264–2280.

Quideau, S., Jourdes, M., Saucier, C., Glories, Y., Pardon, P., & Baudry, C. (2003). DNA Topoisomerase inhibitor acutissimin a and other flavano-ellagitannins in red wine. *Angewandte Chemie International Edition, 42*, 6012–6014.

Ros, E., Núñez, I., Pérez-Heras, A., Serra, M., Gilabert, R., Casals, E., et al. (2004). A walnut diet improves endothelial function in hypercholesterolemic subjects: A randomized crossover trial. *Circulation, 109*, 1609–1614.

Scalbert, A., Manach, C., Morand, C., Rémésy, C., & Jiménez, L. (2005). Dietary polyphenols and the prevention of diseases. *Critical Reviews in Food Science and Nutrition, 45*, 287–306.

Seeram, N. P., Aronson, W. J., Zhang, Y., Henning, S. M., Moro, A., Lee, R., et al. (2007). Pomegranate ellagitannin-derived metabolites inhibit prostate cancer growth and localize to the mouse prostate gland. *Journal of Agricultural and Food Chemistry, 55*, 7732–7737.

Silva, F. A. M., Borges, F., Guimarães, C., Lima, J. L., Matos, C., & Reis, S. (2000). Phenolic acids and derivatives: studies on the relationship among structure, radical scavenging activity, and physicochemical parameters. *Journal of Agricultural and Food Chemistry, 48*, 2122–2126.

Tanaka, T., Kirihara, S., Nonaka, G. I., & Nishioka, I. (1993). Five new ellagitannins, platycaryanins A, B, C, and D, and platycariin, and a new complex tannin, strobilanin, from the fruits and bark of *Platycarya strobilacea* Sieb et Zucc., and biomimetic synthesis of C-glycosidic ellagitannins from glucopyranose-based ellagitannins. *Chemical and Pharmaceutical Bulletin, 41*, 1708–1716.

Vallverdú-Queralt, A., Jáuregui, O., Medina-Remón, A., Andrés-Lacueva, C., & Lamuela-Raventós, R. M. (2010). Improved characterization of tomato polyphenols using liquid chromatography/electrospray ionization linear ion trap quadrupole Orbitrap mass spectrometry and liquid chromatography/electrospray ionization tandem mass spectrometry. *Rapid Communications in Mass Spectrometry, 24*, 2986–2992.

Vallverdú-Queralt, A., Medina-Remón, A., Andres-Lacueva, C., & Lamuela-Raventos, R. M. (2011). Changes in phenolic profile and antioxidant activity during production of diced tomatoes. *Food Chemistry, 126*, 1700–1707.

Vinson, J. A., & Cai, Y. (2012). Nuts, especially walnuts, have both antioxidant quantity and efficacy and exhibit significant potential health benefits. *Food & Function, 3*, 134–140.

4.2 ARTICLE II:

Walnut polyphenol metabolites, urolithins A and B, inhibit the expression of prostate-specific antigen and the androgen receptor in prostate cancer cells.

Claudia Sánchez-González, Carlos J. Ciudad, Verónica Noé, María Izquierdo-Pulido

Food & Function 2014; 5(11):2922-2930.

Impact Factor (JCR): 2.907.

Ranking in Food Science and Technology: 16/123 (Q1)

.

ABSTRACT

Introduction: Prostate cancer is the sixth cause of cancer-related death in men worldwide; therefore the identification of new agents that may prevent and/or regulate the progression of cancer cell growth is of great interest. **Walnuts** contain several bioactive compounds shown to slow down cancer progression including pedunculagin, a polyphenol that is metabolized by gut microbiota to **urolithins A** and **B**. An important target in prostate cancer is the androgen receptor (AR), which is required for the development of prostate carcinogenesis from early prostate intraepithelial neoplasia to organ-confined or locally invasive primary tumors. This study used a **prostate cancer cell** model to elucidate the effects that urolithins A and B exert over the expression and activity of the **AR** and **Prostate Specific Antigen** (PSA).

Materials and methods: LNCaP cells were treated with 40 µM urolithins A and B or a mix (M) of both at several time points. AR and PSA mRNA and protein levels were determined by RT-Real Time PCR and Western Blot, respectively. PSA promoter activity was assessed after transient transfection of PC3 cells with a luciferase construct of the PSA-promoter containing

three AREs. Electrophoretic mobility shift assays were performed to evaluate the potential role of urolithins on AR–ARE binding. Apoptosis was measured by flow cytometry after 24 hour incubation with either UA or UB or both compounds. The levels of the anti-apoptotic protein BCL-2 were determined by Western Blot.

Results: A **decrease in AR and PSA mRNA** and protein levels was observed after treatment with urolithins A and B and a mix of both metabolites at every time-point. The inhibition of PSA promoter activity after 24 hour incubation with urolithins indicated a possible effect at the transcription level on AR-mediated PSA expression. This could be related to a decreased binding of AR to the consensus AREs sequence as determined by EMSA. AR and PSA have been shown to play an important role in prostate cancer cell viability. Some authors have associated high PSA levels with increased levels of the anti-apoptotic protein BCL-2. Hence, we measured the effect that UA, UB and M had on apoptosis and BCL-2 levels. An increase in the apoptotic cell population was observed upon treatment with UA, UB and M, which correlated with a decrease in BCL-2 protein levels.

Conclusion: Our results suggest that **urolithins A** and **B** attenuate the function of the AR by repressing its expression. A down-regulation of AR and PSA mRNA and protein levels could provoke an interruption of the interaction between PSA and AR, with a proven role in prostate cancer development and progression. The modulatory effect of **urolithins** on the AR receptor also causes an apoptotic effect on LNCaP cells. The aforementioned results indicate **a potential role of walnuts as a chemo-preventive and/or chemo-therapeutic agent for prostate cancer.**

Food & Function

PAPER

Cite this: *Food Funct.*, 2014, **5**, 2922

Walnut polyphenol metabolites, urolithins A and B, inhibit the expression of the prostate-specific antigen and the androgen receptor in prostate cancer cells

Claudia Sánchez-González,[a] Carlos J. Ciudad,[b] Véronique Noé[b] and Maria Izquierdo-Pulido*[a,c]

Walnuts have been gathering attention for their health-promoting properties. They are rich in polyphenols, mainly ellagitannins (ETs) that after consumption are hydrolyzed to release ellagic acid (EA). EA is further metabolized by microbiota to form urolithins, such as A and B, which are absorbed. ETs, EA and urolithins have shown to slow the proliferation and growth of different types of cancer cells but the mechanisms remain unclear. We investigate the role of urolithins in the regulatory mechanisms in prostate cancer, specifically those related to the androgen receptor (AR), which have been linked to the development of this type of cancer. In our study, urolithins down-regulated the mRNA and protein levels of both prostate specific antigen (PSA) and AR in LNCaP cells. The luciferase assay performed with a construct containing three androgen response elements (AREs) showed that urolithins inhibit AR-mediated PSA expression at the transcriptional level. Electrophoretic mobility shift assays revealed that urolithins decreased AR binding to its consensus response element. Additionally, urolithins induced apoptosis in LNCaP cells, and this effect correlated with a decrease in Bcl-2 protein levels. In summary, urolithins attenuate the function of the AR by repressing its expression, causing a down-regulation of PSA levels and inducing apoptosis. Our results suggest that a diet rich in ET-containing foods, such as walnuts, could contribute to the prevention of prostate cancer.

Received 19th June 2014,
Accepted 18th August 2014

DOI: 10.1039/c4fo00542b

www.rsc.org/foodfunction

1. Introduction

Prostate cancer is the second most frequently diagnosed cancer and the sixth leading cause of cancer death among men. Generally, the highest rates are recorded in North America, Oceania, and Northern and Western Europe.[1] Epidemiology supports the important role of nutrition in prostate cancer prevention.[2] A number of protective compounds have been identified in the diet, including selenium, sulforane from cruciferous, carotenoids, and polyphenols. These food phytochemicals may affect the biological process of cancer development *via* different mechanisms. *In vitro* and *in vivo* evidence has pointed out that phytochemicals affect a broad range of intracellular molecular targets.[3–7] In particular, polyphenols may exert anticancer effects by several mechanisms such as reducing the pro-oxidative effect of carcinogenic agents,[8,9] modulation of cancer cell signaling,[10,11] cell cycle progression,[12,13] promotion of apoptosis,[14,15] and modulation of enzymatic activities.[16] Regarding prostate cancer progression, a recent clinical trial assessed the effect of a polyphenol-blend dietary supplement over prostate-specific antigen (PSA) levels in men with localized prostate carcinoma; this study found a significant favorable effect on the percentage rise in PSA levels, an important indicator of prostate cancer progression.[17] Polyphenols have also been shown to act on multiple targets in pathways not only related to cancer progression, cellular proliferation and death,[18] but also in inflammation,[19] angiogenesis,[20] and drug and radiation resistance.[21]

Walnuts (*Juglans regia* L.) have been gathering increasing attention for their health-promoting properties, which have been reported to improve lifestyle-related diseases such as arteriosclerosis, hypercholesterolemia, hypertriglyceridemia, cardiovascular disease, diabetes, and cancer.[22–24] Walnuts are rich in bioactive polyphenols (total contents ranging from 1575 mg to 2500 mg per 100 g) and they represent, on a serving size basis, the seventh largest source of total polyphenols among common foods and beverages.[25] The most

[a]*Nutrition and Food Science Department, School of Pharmacy, University of Barcelona, Barcelona, Spain*
[b]*Biochemistry and Molecular Biology Department, School of Pharmacy, University of Barcelona, Barcelona, Spain*
[c]*CIBER Fisiopatología de la Obesidad y la Nutrición (CIBEROBN), Spain.*
E-mail: maria_izquierdo@ub.edu

This journal is © The Royal Society of Chemistry 2014

abundant polyphenols in walnuts are ellagitannins (ETs), mainly pedunculagin.[26] ETs are tannins that release ellagic acid (EA) upon hydrolysis, which are further metabolized by gut flora to form urolithins, mainly urolithins A and B.[27] These urolithins circulate in blood and can reach many of the target organs where the effects of ellagitannins are noted.[27,28] Although the occurrence of ETs and EA in the bloodstream is almost negligible, urolithins can reach a concentration at micromolar levels in plasma,[29] their maximum concentration is reached 24 to 48 hours after consumption of ET-rich foods, although urolithins can be found in plasma and urine up to 72 hours after consumption in both free and conjugated forms;[27] urolithins and their conjugates have also been found in the human prostate after walnut and pomegranate juice consumption.[30] Like other polyphenols, ETs, EA and their derived metabolites possess a wide range of biological activities which suggest that they could have beneficial effects on human health.[31] Moreover, ETs and EA seem to exhibit anticancer properties *in vitro* and *in vivo*. Recent research *in vitro* has shown that walnut extracts have dose-dependent inhibitory effects on colon cancer cell growth[32] and it has been observed that walnuts delay the growth rate of breast cancer cells[33] and prostate cancer cells[30] implanted in mice. ET-rich herbal extracts have been shown to inhibit LNCaP cell proliferation and reduce PSA secretion.[34] Other authors have also attributed estrogenic and anti-estrogenic activity to urolithins based on their binding affinity to the estrogen receptor in MCF-7 cells, labeling urolithins as potential endocrine-disruptive molecules.[29]

Prostate-specific antigen is a well-known prostate tumor marker, expressed at a high level in the luminal epithelial cells of the prostate and is absent or expressed at very low levels in other tissues.[35] However recent data suggest that PSA is not only a biomarker, but that it also has a biological role in the development and progression of prostate cancer, since it is involved in tumor growth, invasion and metastasis.[36] PSA is encoded by the *KLK3* gene and its expression is tightly controlled by androgen through the action of the androgen receptor (AR).[37] Upon binding to androgen, AR translocates into the nucleus and binds to the androgen response elements (AREs) on the PSA promoter, interacting with other transcription factors and activating PSA gene transcription.[38] The expression of PSA in prostate cancer generally reflects the transcriptional activity of AR, but additional factors regulating the PSA promoter have also been identified.[39–41]

Considering all of the above, we hypothesized that the main walnut polyphenol metabolites, urolithins A and B, could exert a role over regulatory mechanisms in prostate cancer, specifically those related to the androgen receptor, which have been linked to the development and progression of this type of cancer. To this purpose, and using a prostate cancer cell model (LNCaP cells), we investigated the effects of urolithins A and B on the gene expression of PSA and AR and their protein expression. We also assayed the ability of those compounds to modify the PSA promoter activity and to bind AR. In addition, the effect of both urolithins on apoptosis was also explored.

2. Experimental

2.1 Materials and chemicals

Urolithin A (UA; 3,8-dihydroxy-6*H*-dibenzo[*b*,*d*]pyran-6-one, 95% purity) and urolithin B (UB; 3-dihydroxy-6*H*-dibenzo[*b*,*d*]-pyran-6-one, 98% purity) were synthesized by the Department of Organic Chemistry, School of Pharmacy at the University of Barcelona (Barcelona, Spain). Urolithins and dehydrotestosterone (DHT) (Sigma-Aldrich, Madrid, Spain) were suspended in DMSO.

2.2 Cell culture

LNCaP (androgen responsive) and PC3 (androgen independent) human prostate adenocarcinoma cell lines were routinely grown in Ham's F-12 medium, supplemented with 7% (v/v) fetal bovine serum (FBS, both from GIBCO, Invitrogen, Barcelona, Spain), sodium penicillin G and streptomycin, and were maintained at 37 °C under a humidified atmosphere containing 5% CO_2. 250 000–500 000 cells were incubated with 40 μM of either urolithin A or urolithin B, or a combination composed of 20 μM UA and 20 μM UB (named MIX). This concentration was chosen because it can be found in plasma after consumption of ET-rich foods,[26–28] and it is within the range used to assay the biological activity of urolithins.[42,43] In addition, this concentration was not cytotoxic (data not shown). Incubations were also performed, depending upon the experiment, with 1 nM of DHT. The final concentration of DMSO in the culture medium was always ≤0.5%.

2.3 RT-real time PCR

Total RNA was extracted from LNCaP using the Trizol reagent (Life Technologies, Madrid, Spain) in accordance with the manufacturer's instructions. Complementary DNA (cDNA) was synthesized as described by Oleaga *et al.* (2013).[44] RNA concentration and purity was checked using a Nanodrop spectrophotometer system (ND-1000 3·3 Nanodrop Technologies, Wilmington, DE, USA). mRNA levels were determined with StepOnePlus™ real-time PCR systems (Applied Biosystems, Barcelona, Spain) using 3 μL of cDNA and Taqman probes (Applied Biosystems, Barcelona, Spain), for *KLK3* (Hs02576345) and *AR* (Hs00171172) genes and *APRT* (Hs00975725) as an endogenous control. Changes in gene expression were calculated using the quantitative $^{\Delta\Delta}$Ct method and normalized against APRT in each sample.

2.4 Western blot

LNCaP cells (350 000) were plated on 35 mm dishes and treated the day after with the different compounds. Twenty-four hours after incubation cells were collected and centrifuged for 5 min at 800*g* at 4 °C. The cell pellets were suspended in 200 μL of lysis buffer (0.5 M NaCl, 1.5 mM $MgCl_2$, 1 mM EGTA, 10% glycerol 1% Triton x_100, 50 mM HEPES, pH 7.9 all from Applichem, Barcelona, Spain), and 10 μL protease inhibitor cocktail (from Sigma-Aldrich, Madrid, Spain). The cell lysate was kept on ice for 60 min vortexing every 15 min. Cellular debris was removed by centrifugation at

15 000*g* at 4 °C for 10 min. A 5 μL aliquot of the extract was used to determine the protein concentration using the Bradford assay (Bio-Rad, Barcelona, Spain).

Whole cell extracts (100 μg) were resolved in 12% SDS-polyacrylamide gels and transferred to PVDF membranes (Immobilon P, Millipore, Madrid, Spain) using a semidry electroblotter. Membranes were probed overnight at 4 °C with primary antibodies against AR (1 : 200 dilution; sc-816 from Santa-Cruz Biotechnology Inc., Heidelberg, Germany), PSA (1 : 300 dilution; A0562 from Dako, Denmark) or Bcl-2 (1 : 200 dilution; sc-492 from Santa-Cruz Biotechnology Inc., Heidelberg, Germany). Signals were detected by secondary horseradish peroxidase-conjugated antibody, either anti-rabbit (1 : 2500; Dako, Denmark) or anti-mouse (1 : 2500 dilution, sc-2005 Santa Cruz Biotechnology Inc., Heidelberg, Germany) and enhanced chemiluminescence using the ECL™ Prime Western blotting detection reagent, as recommended by the manufacturer (GE Healthcare, Barcelona, Spain). Chemiluminescence was detected with ImageQuant LAS 4000 Mini technology (GE Healthcare, Barcelona, Spain). Normalization of the blots was performed by incubation with an antibody against tubulin (1 : 800 dilution, sc-5286 from Santa-Cruz Biotechnology Inc., Heidelberg, Germany).

2.5 Transfection and luciferase assay

PC3 cells (350 000) were plated in 35 mm dishes the day before transfection. The medium (2 ml) was renewed before transfection, which was performed using FuGENE 6 (Roche, Barcelona, Spain). For each well, the transfection reagent was incubated for 5 minutes in 100 μL of antibiotic and serum free medium, followed by the addition of plasmid DNA and incubated for another 20 min at a ratio of 3 : 1 (μL of transfection reagent : μg of plasmid DNA). One μg of plasmid DNA, either pGL3 basic vector or PSAp, a 6 kb PSA promoter construct containing three AREs in front of a luciferase reporter gene were used for transfection.

Incubation with 40 μM of UA, UB or MIX and 1 nM of DHT was performed 6 hours after transfection, and the luciferase activity was determined 24 hours after transfection. Cell extracts were prepared by lysing cells with 100 μL of reporter lysis buffer (2 mM DTT, 2 mM EDTA, 10% glycerol, 1% Triton X_100, 25 mM Tris-phosphate, pH 7.8). The lysate was centrifuged at 12 000*g* for 2 min at 4 °C to pellet cell debris and supernatants were transferred to a fresh tube. Fifteen μL of the extract were added to 15 μL of the luciferase assay substrate (Promega, Madrid, Spain) at room temperature. Luminescence was measured using the Glomax™ 20/20 luminometer (Promega, Madrid, Spain) and expressed as relative luminescence units (RLU). Luciferase results were normalized by the total protein concentration in the cell lysates. Protein concentration was determined by the Bradford assay (Bio-Rad, Barcelona, Spain) according to the manufacturer's protocol.

2.6 Nuclear extracts

Nuclear extracts were prepared according to the protocol described by Andrews and Faller (1991).[45] Briefly, 500 000 cells were plated and incubated the following day with urolithins A, B or MIX and 1 nM DHT. Cells were collected in cold PBS after being treated for 24 hours. Cells were pelleted and suspended in a cold hypotonic buffer (1.5 mM $MgCl_2$, 10 mM KCl (AppliChem, Barcelona, Spain), 0.5 mM DTT, 0.2 mM PMSF, 10 mM HEPES-KOH, pH 8.0 from Sigma-Aldrich, Madrid, Spain). Cells were then allowed to swell for 10 minutes, vortexed and pelleted by centrifugation. The resulting pellet was then suspended in a cold high-salt buffer (25% glycerol, 420 mM NaCl, 1.5 mM $MgCl_2$, 10 mM KCl, 0.5 mM DTT, 0.2 mM PMSF, 20 mM HEPES-KOH, pH 8.0) for 20 minutes. Cellular debris was removed by centrifugation and the supernatant fraction was stored at −80 °C until further use.

2.7 Electrophoretic mobility shift assay

EMSA assay was performed using LNCaP nuclear extracts prepared as previously described. AR consensus double-stranded oligonucleotide 5′-CTA GAA GTC T**GG TAC A**GG GTG TTC TTT TTG CA-3′ (binding site in bold) was obtained from Santa Cruz Biotechnology, Heidelberg, Germany (sc-2551). One hundred nanograms of the AR consensus sequence was 5′-end-labeled with T4 polynucleotide kinase (New England Biolabs, Beverly, MA) and [γ-^{32}P]ATP (3000 Ci mmol^{-1}, Perkin Elmer, Madrid, Spain) as described by Rodríguez *et al.* (2013).[46]

The radiolabeled probe (20 000 cpm) was incubated in a 20 μL reaction mixture also containing 1 μg of Herring sperm DNA (Invitrogen, Barcelona, Spain) as an unspecific competitor, 2 μg of nuclear extract protein, 5% glycerol, 4 mM $MgCI_2$, 60 mM KCl and 25 mM Tris-HCl, pH 8.0 (AppliChem, Barcelona, Spain). Samples were resolved by gel electrophoresis (5% polyacrylamide, 5% glycerol, 1 mM EDTA and 45 mM Tris-borate, pH 8.0; AppliChem, Barcelona, Spain). The gel was dried for 90 minutes, exposed to europium plates overnight and analyzed using a Storm 840 Phosphorimager (Molecular Dynamics, GE Healthcare Life Sciences, Barcelona, Spain).

To determine the binding specificity, the radiolabeled ARE probe was competed either with 3 ng (5-fold) of unlabeled ARE consensus or a mutant ARE oligonucleotide. The mutant AR oligonucleotide had two "GT" to "CA" substitutions in the AR binding motif 5′-CTA GAA GTC T**GC CAC A**GG **GTC ATC T**TT TTG CA-3′ (binding site in bold) (sc-2552, Santa Cruz Biotechnology, Heidelberg, Germany). These experiments were performed using NE from LNCaP cells treated with 1 nM DHT.

2.8 Apoptosis

Apoptosis was determined by the rhodamine method. LNCaP cells (250 000) were plated in 35 mm dishes with 2 ml complete F-12 medium and after 24 h, they were treated with 40 μM UA, UB or MIX. Staurosporine (1 μM) (Sigma-Aldrich, Madrid, Spain) was used as a positive control. Rhodamine (final concentration 5 ng ml^{-1}) (Sigma-Aldrich, Madrid, Spain) was added for 30 min and the cells were collected, centrifuged at 800*g* at 4 °C for 5 min, and washed once with PBS. The pellet was suspended in 500 ml PBS plus propidium iodide (PI) (final concentration 5 mg ml^{-1}) (Sigma-Aldrich, Madrid,

This journal is © The Royal Society of Chemistry 2014

Spain). Flow cytometry data were analyzed using the Summit v4.3 software. The percentage of Rho-negative, PI negative cells corresponds to the apoptotic population.

2.9 Statistical analyses

All data are reported as mean ± SE and are representative of at least three independent experiments. Data were analyzed using one-way ANOVA followed by the Bonferroni *post hoc* multiple range test using the SPSS software v.21. The difference between groups was considered statistically significant at $p < 0.05$.

3. Results

3.1 Urolithins A and B decrease PSA mRNA and protein levels in LNCaP cells

Taking into account the role of prostate specific antigen in prostate cancer, we analyzed the effect of urolithins on PSA mRNA expression. LNCaP cells were incubated with urolithins during different time periods (12, 24, and 48 h). Total RNA was extracted and PSA expression was analyzed by RT-real time PCR (Fig. 1A). On average, urolithins induced the major decrease in PSA mRNA levels after 24 hours; urolithin A provoked an 85% reduction, a similar effect was observed after incubation with MIX at the same time point, while UB exerted a 50% inhibition. To examine whether the effects observed at the mRNA level were translated into the protein, we performed Western blot analyses in LNCaP cells after 24 hour incubation with urolithins. As shown in Fig. 1B, cells incubated with UA exhibited a 63% decrease in PSA protein levels compared to the untreated control, followed by cells treated with MIX or UB.

3.2 Urolithins A and B decrease AR mRNA and protein expression

To determine whether urolithins were able to modulate AR mRNA expression, LNCaP cells were incubated for several time periods, between 9 and 24 hours; total RNA was extracted and AR expression was analyzed by RT-real time PCR. A decrease in AR mRNA levels was observed at every time point (Fig. 2A). The major decrease was observed after the incubation with UA and MIX, obtaining on average a reduction of 60% for both 9 and 12 hours. Androgen receptor protein levels were also determined in LNCaP cells treated with urolithins, inducing a decrease between 50% and 60% (Fig. 2B).

3.3 Urolithins A and B inhibit the PSA promoter activity

To assess whether urolithins affected the transcriptional activation of PSA, transient transfections in PC3 cells using a luciferase reporter vector carrying 6 kb of the PSA promoter were performed.[47] PC3 cells were chosen because they are PSA negative and although they are considered AR-negative they do express low AR mRNA and protein levels[48] in addition to retaining co-regulators necessary for AR activity in prostate tumor progression.[49] Therefore, changes in PSA promoter activity would be accurately reflected after incubation with urolithins and/or DHT in these reporter assays. Six hours after transfection with the reporter vector, cells were incubated with urolithins, either in the absence or in the presence of DHT. As expected, treatment with 1 nM DHT increased the luciferase activity by 83% compared to cells incubated in the absence of DHT, which exhibited similar activity to the basic pGL3 vector (Fig. 3). DHT-incubated cells treated with UA, UB or MIX showed a reduction in luciferase activity. UA-incubated cells showed a slightly higher inhibition in luciferase activity than UB and MIX when compared to the DHT-induced promoter, although this was not statistically

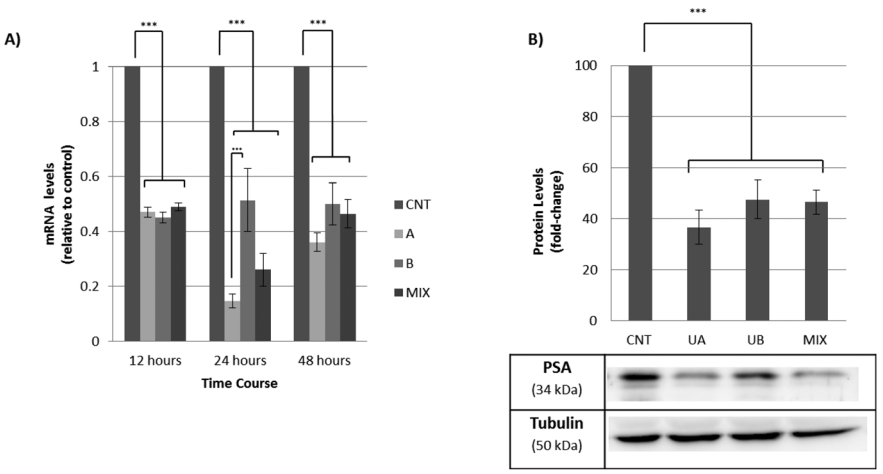

Fig. 1 (A) PSA mRNA levels determined by real time RT-PCR. Bars represent PSA mRNA levels in LNCaP cells either control (0.10% of DMSO) or incubated with UA, UB or MIX. The different incubation conditions are indicated in the figure. Results are expressed in fold changes compared to the untreated cells and normalized using APRT as an endogenous control. They are the mean ± SE of 3 different experiments. ***$p < 0.001$. (B) Determination of PSA protein levels by Western blotting. Bars represent PSA protein levels in LNCaP cells either control (0.10% of DMSO) or incubated with UA, UB or MIX. Results are expressed in fold changes compared to the untreated cells and represent the mean ± SE of 3 different experiments. ***$p < 0.001$.

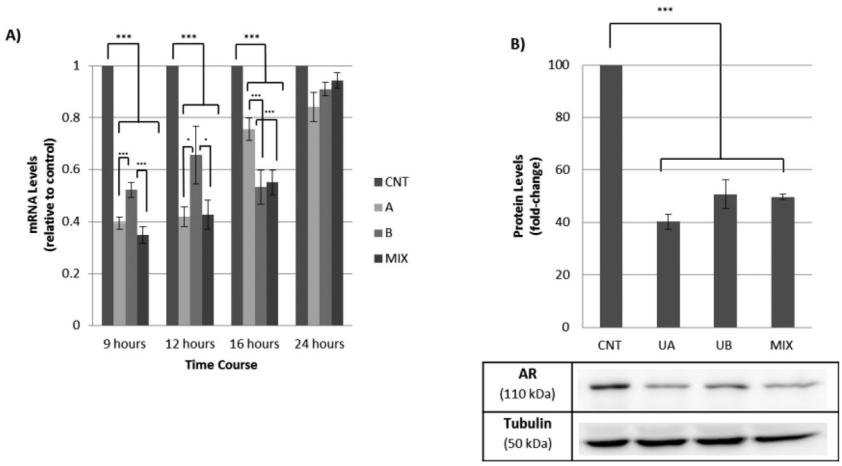

Fig. 2 (A) AR mRNA levels determined by real time RT-PCR. Incubation conditions are the same as described in Fig. 1A. Results are expressed in fold changes compared to the untreated cells and normalized using APRT as an endogenous control. They are the mean ± SE of 3 different experiments. ***$p < 0.001$. (B) Determination of AR protein levels by Western blotting. Results are expressed in fold changes compared to the untreated cells and represent the mean ± SE of 3 different experiments. ***$p < 0.001$.

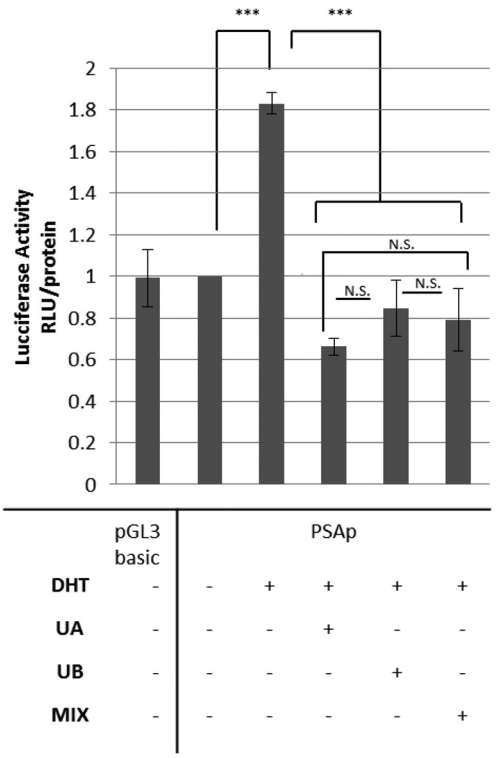

Fig. 3 PSA promoter activity in PC3 cells. Cells were transfected with a luciferase reporter vector carrying 6 kb of the PSA promoter, and 6 h later they were treated with UA, UB and MIX in the presence or absence of 1 nM DHT. Results are expressed as luciferase relative units/total protein compared to control. They are the mean ± SE of 3 different experiments. ***$p < 0.001$. N.S., not significant.

significant (Fig. 3). These results indicated a repression of DHT-induced PSA promoter activation by urolithins. Cells incubated only with UA, UB or MIX exhibited basal luciferase activity, similar to the activity observed for pGL3 and PSAp in the absence of DHT (inactive PSAp, data not shown).

3.4 PSA expression correlates with the binding of nuclear extracts to an ARE

The regulation of PSA by androgens takes place through the ARE sequences in its promoter region.[38] The effect of

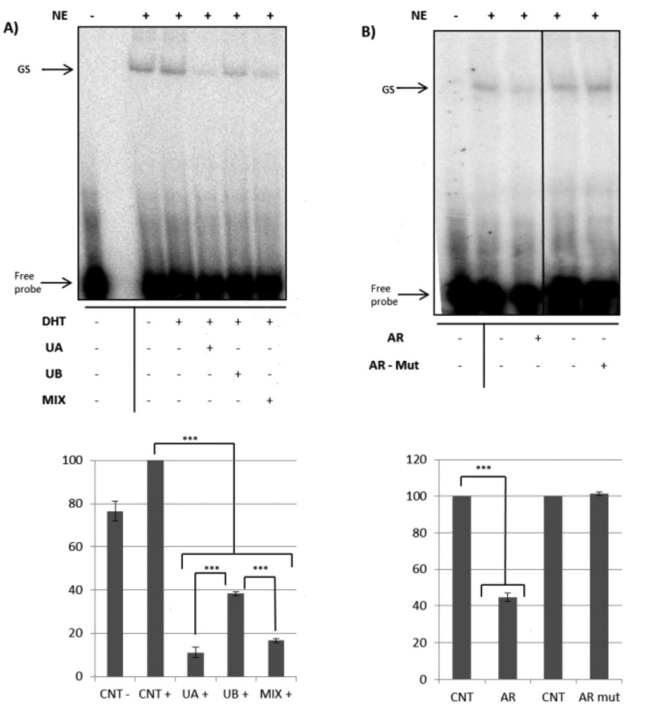

Fig. 4 (A) Effect of urolithins on AR binding to nuclear proteins. EMSA was performed using the AR consensus sequence as a probe and nuclear extracts from LNCaP cells. First lane corresponds to the probe alone. Nuclear extracts were either control or treated cells with 1 nM DHT and 40 μM of UA, UB or MIX for 24 hours. ***$p < 0.001$. N.S., not significant. (B) Competition assays. The binding of untreated LNCaP nuclear extracts to the AR consensus sequence was competed with the addition of either 3 ng (5-fold excess) of unlabeled AR or unlabeled mutated AR in the binding reaction.

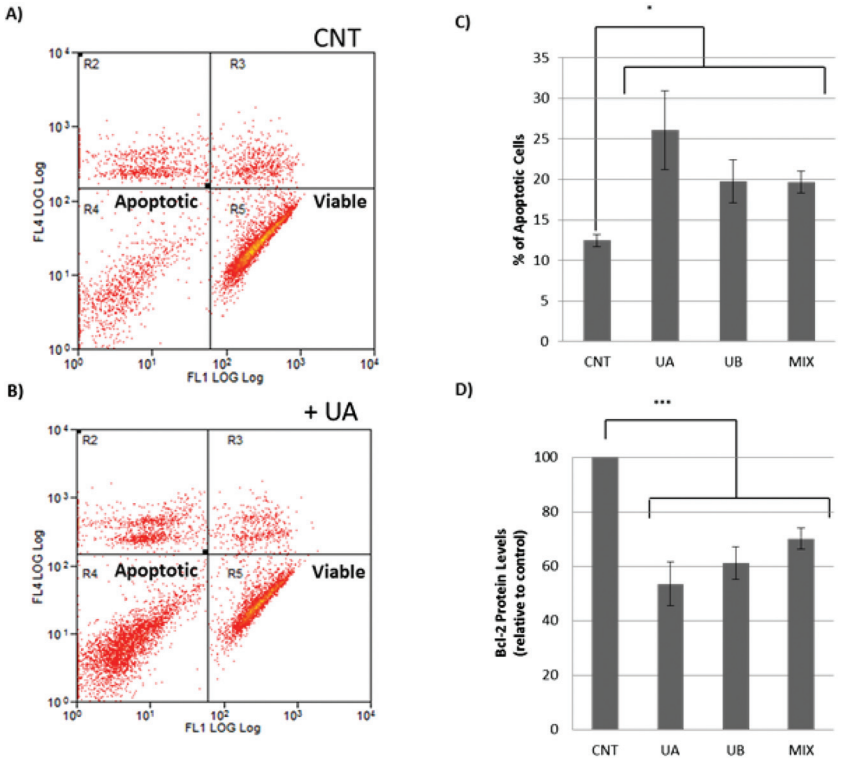

Fig. 5 Apoptosis determined by flow cytometry. (A) Representative flow cytometer histograms displaying the cell population in the untreated control sample (0.12% DMSO) and (B) in cells incubated with 40 μM UA. (C) Percentage of apoptotic cells determined by flow cytometry. Bars represent LNCaP cells either untreated control (0.12% of DMSO), or incubated with UA, UB or MIX (40 μM) after 24 hour of exposure. Results represent the mean ± SE of 3 different experiments. *$p < 0.05$. (D) Bcl-2 protein levels in cells incubated with UA, UB or MIX for 24 hours. ***$p < 0.001$.

urolithins on ARE binding to nuclear proteins was determined using electrophoretic mobility shift assays (EMSAs). EMSAs were performed using an ARE consensus sequence as the probe and nuclear extracts from untreated (control) and treated LNCaP cells. Cells were incubated with 1 nM DHT and urolithins for 24 hours. As shown in Fig. 4A, the interaction of nuclear extracts from control cells with the radiolabelled probe originated a shifted band, the intensity of which was clearly decreased upon incubation with UA, UB or MIX. The highest reduction was seen after UA and MIX incubation (Fig. 4A), with an 85% decrease in band intensity, followed by UB.

To assess the binding specificity, 3 ng of unlabeled consensus ARE (corresponding to a 5-fold excess compared to the probe) or unlabeled mutated AR were added to the binding reaction. As shown in Fig. 4B, a 56% reduction in band intensity was observed when the binding to the ARE labeled probe was competed with the unlabeled probe, whereas the competition with the unlabeled mutated AR did not affect the intensity of the shifted band.

3.5 Urolithins A and B induce apoptosis and a decrease of Bcl-2 protein levels in LNCaP cells

We examined the effect of urolithins on apoptosis using the rhodamine method. Following incubation of LNCaP cells with UA, UB and MIX for 24 hours, the percentage of apoptotic cells increased compared with the control (0.20% DMSO). A 14% increase in apoptotic cell population was observed after incubation with UA, whereas UB and MIX caused a 7% increase, although this difference was not statistically significant (Fig. 5A–5C). Both *in vitro* and *in vivo* studies have established that Bcl-2 expression confers anti-apoptotic activity in prostate cancer and its overexpression is linked to progression into advanced prostate cancer.[50] Bcl-2 overexpression has also been correlated with high PSA levels in prostate cancer.[36] Hence, Bcl-2 protein levels were measured after urolithin incubation. UA, UB and MIX induced a decrease in Bcl-2 protein levels after 24 hour treatment (Fig. 5D).

4. Discussion

The main objective of our study was to determine the potential role of the major polyphenol metabolites in walnuts, urolithins, in the modulation of the prostate-specific antigen and the androgen receptor in prostate cancer cells. A great number of dietary components such as lycopene, vitamin E, selenium, isoflavones and polyphenols potentially affect a range of carcinogenic pathways in the prostate, including androgen metabolism, cell cycle processes and apoptosis, maintenance of mitochondrial membrane potentials, insulin-like growth factor

(IGF)-Akt signaling, and response to oxidative stress.[51] Although, these dietary components have been assessed for their chemo-preventive capacities, there are a limited number of studies focusing on the role that walnut polyphenols have in the prevention of prostate cancer, especially those addressed to elucidate the molecular mechanisms involved. As an example, the anticancer activity for urolithins A, B, C, and D through the inhibition of CYP1B1[52] was reported in human prostate carcinoma 22Rv1 cells, while pedunculagin,[30] ellagic acid[42] and extracts from the green husk of walnuts[53] showed an anti-proliferative and apoptotic effect on LNCaP cells. Other authors have also observed that urolithins localized to the mouse prostate gland and inhibited the growth of both androgen-dependent and androgen-independent prostate cancer cell lines.[54]

In our study, there was a clear repression of PSA transcription by urolithins A and B, as well as a decrease in PSA protein levels. The aforementioned decrease in PSA levels upon treatment with urolithins correlated with the down-regulation of the androgen receptor. The decrease in PSA and AR levels after incubation with urolithins is in agreement with the effects reported for other phenolic compounds, such as epigallocatechin gallate (EGCG), grape seed procyanidins or caffeic acid. PSA and AR play a pivotal role in prostate cancer development and progression and a potential cross-talk between these two genes has been postulated by several authors.[55,56] In a recent study, Saxena *et al.* (2012)[55] pointed out that PSA is not only a biomarker of prostate cancer and a known downstream target of the androgen receptor, but it is also required for AR mRNA and protein expression. Similarly, several authors reported that AR inhibition resulted in a marked decrease in cell proliferation.[57,58] Thus, the observed effect of urolithins on prostate cancer cells could be due to their possible interference in this cross-talk and the reduction of PSA and AR levels.

A possible manner by which urolithins could interfere with the previously mentioned AR-PSA cross-talk is by displaying phytoestrogen-like activity. In this direction, the modulation of hormone receptors by phenolic dietary components, such as isoflavones, has been widely studied. Some authors compared urolithins with several phytoestrogens, such as genistein, daidzein, resveratrol and enterolactone. These authors reported an interference caused by urolithins in endocrine pathways proposing them as possible phytoestrogens.[29] In this sense, the estrogenic and anti-estrogenic activity reported for urolithins has been related to their interaction with the estrogen receptor in human breast cancer cells (MCF-7).[29] However, phytoestrogens, such as genistein, do not only interact with the estrogen receptor but have also been shown to decrease AR levels in LNCaP cells, and to cause a reduction in the binding of nuclear proteins to an ARE.[59] Considering all of the above, we explored if urolithins were able to exert an effect over the androgen receptor, similar to that induced by phytoestrogens. In our study we demonstrate that the activation of the PSA promoter by DHT was blocked upon incubation with urolithins. The reduced activation of PSA, which is an AR-regulated promoter, could be explained by the decrease in the binding of nuclear proteins to a consensus ARE, which under our conditions was an 86% reduction. In addition, the binding of AR to AREs was reduced by 32% after direct incubation of untreated nuclear proteins with UA (data not shown). Hence, the decrease in transcription caused by urolithins over PSA levels was due to a direct effect on the PSA promoter. Our results are in keeping with those observed by Larrosa (2006)[28,29] and colleagues who studied the binding affinity of urolithins to the estrogen receptor in breast adenocarcinoma cells. These authors observed a higher binding affinity for urolithin A than for urolithin B, similar to our results in which a higher decrease in binding was observed upon incubation with UA when compared to UB.

It is important to note that PSA is fundamental in the pathophysiology of prostate cancer. It stimulates oxidative stress in LNCaP and PC3 cells,[60] and is also involved in tumor invasion and metastasis.[61] Considering its role in prostate cancer progression, we explored if the pronounced decrease of PSA levels upon urolithin incubation would result in an increase in apoptosis. Urolithins indeed caused an increase in apoptotic activity in LNCaP cells. Moreover, the increase in apoptosis upon incubation with urolithins was correlated with a decrease in the expression of Bcl-2, a critical regulator of the apoptotic pathway, and a potent suppressor of apoptosis.[62] Human tumors usually express high levels of Bcl-2 protein and in prostate cancer its levels correlate with high levels of PSA.[36] Thus, the decrease in Bcl-2 and the apoptotic activity induced upon incubation with urolithins could be linked to the inhibition of PSA by these compounds. Other authors have reported that juglone, a non-polyphenolic compound found in roots and leaves of the walnut tree, can cause apoptosis in prostate cancer cells, in this case, associated with mitochondrial dysfunction and activation of caspases 3 and 9.[63]

5. Conclusion

Our results provide new insights into the effect metabolites of a common dietary component have on molecular mechanisms involved in prostate carcinogenesis, which could in turn provide a foundation for developing strategies for disease prevention. The effect of dietary agents on cancer can be used to identify molecular therapeutic targets, and used as part of a chemo-preventive strategy. Dietary intervention targeting multiple pathways might, therefore, be an effective therapeutic approach, either alone, or in conjunction with targeted pharmaceutical agents.

In summary, we demonstrated a reduction in PSA and AR levels induced by urolithins. This effect could be due to a decreased binding of the AR to AREs, and to decreased levels of the androgen receptor resulting in PSA transcription inhibition. An induction of apoptosis in LNCaP cells was also observed, which may be caused by the down-regulation of AR and PSA, as well as a decrease of Bcl-2 protein levels. A diet high in ET-rich foods, such as walnuts, provides a considerable

 This journal is © The Royal Society of Chemistry 2014

intake of pedunculagin and its metabolites, urolithins, which could assist in the prevention of prostate cancer in men.

Conflict of interest

The authors have no potential conflict of interest.

Acknowledgements

The 6 kb PSA promoter construct containing three AREs in front of a luciferase reporter gene (PSAp) was graciously provided by Dr Charles Young from the Mayo Clinic, Rochester, MN.

This work was supported by grants from the California Walnut Commission (FBG-306913) and the Spanish Government of Science and Innovation (SAF2011-23582). C.S.G. was supported by scholarships from the "Consejo Nacional de Ciencia y Tecnología, CONACYT" and the "Dirección General de Relaciones Internacionales de la Secretaría de Educación Pública, DGRI-SEP" from Mexico. Our group holds the Quality Mention from the Government of Catalonia, Spain (SGR2009-118).

References

1 American Cancer Society, *Am. Cancer Soc.*, 2011, 9–18.
2 M. Stacewicz-Sapuntzakis, G. Borthakur, J. L. Burns and P. E. Bowen, *Mol. Nutr. Food Res.*, 2008, **52**, 114–130.
3 J. Dai and R. J. Mumper, *Molecules*, 2010, **15**, 7313–7352.
4 S. Ramos, *Mol. Nutr. Food Res.*, 2008, **52**, 507–526.
5 P. Signorelli and R. Ghidoni, *J. Nutr. Biochem.*, 2005, **16**, 449–466.
6 R. Tsao, *Nutrients*, 2010, **2**, 1231–1246.
7 D. T. Verhoeven, H. Verhagen, R. A. Goldbohm, P. A. van den Brandt and G. van Poppel, *Chem.-Biol. Interact.*, 1997, **103**, 79–129.
8 S. J. Duthie and V. L. Dobson, *Eur. J. Nutr.*, 1999, **38**, 28–34.
9 R. W. Owen, A. Giacosa, W. E. Hull, R. Haubner, B. Spiegelhalder and H. Bartsch, *Eur. J. Cancer*, 2000, **36**, 1235–1247.
10 N. Khan, F. Afaq, M. Saleem, N. Ahmad and H. Mukhtar, *Cancer Res.*, 2006, **66**, 2500–2505.
11 G. Corona, M. Deiana, A. Incani, D. Vauzour, M. A. Dessì and J. P. E. Spencer, *Biochem. Biophys. Res. Commun.*, 2007, **362**, 606–611.
12 G. Corona, M. Deiana, A. Incani, D. Vauzour, M. A. Dessì and J. P. E. Spencer, *Mol. Nutr. Food Res.*, 2009, **53**, 897–903.
13 W. Wang, L. Heideman, C. S. Chung, J. C. Pelling, K. J. Koehler and D. F. Birt, *Mol. Carcinog.*, 2000, **28**, 102–110.
14 S. K. Mantena, M. S. Baliga and S. K. Katiyar, *Carcinogenesis*, 2006, **27**, 1682–1691.
15 R. Fabiani, A. De Bartolomeo, P. Rosignoli, M. Servili, G. F. Montedoro and G. Morozzi, *Eur. J. Cancer Prev.*, 2002, **11**, 351–358.
16 D. Vauzour, A. Rodriguez-Mateos, G. Corona, M. J. Oruna-Concha and J. P. E. Spencer, *Nutrients*, 2010, **2**, 1106–1131.
17 R. Thomas, M. Williams, H. Sharma, A. Chaudry and P. Bellamy, *Prostate Cancer Prostatic Dis.*, 2014, **17**, 180–186.
18 L. Fini, E. Hotchkiss, V. Fogliano, G. Graziani, M. Romano, E. B. De Vol, H. Qin, M. Selgrad, C. R. Boland and L. Ricciardiello, *Carcinogenesis*, 2008, **29**, 139–146.
19 S. U. Mertens-Talcott, P. Jilma-Stohlawetz, J. Rios, L. Hingorani and H. Derendorf, *J. Agric. Food Chem.*, 2006, **54**, 8956–8961.
20 V. Granci, Y. M. Dupertuis and C. Pichard, *Curr. Opin. Clin. Nutr. Metab. Care*, 2010, **13**, 417–422.
21 A. K. Garg, T. A. Buchholz and B. B. Aggarwal, *Antioxid. Redox Signaling*, 2005, **7**, 1630–1647.
22 R. Estruch, E. Ros, J. Salas-Salvadó, M.-I. Covas, D. Corella, F. Arós, E. Gómez-Gracia, V. Ruiz-Gutiérrez, M. Fiol, J. Lapetra, R. M. Lamuela-Raventos, L. Serra-Majem, X. Pintó, J. Basora, M. A. Muñoz, J. V. Sorlí, J. A. Martínez and M. A. Martínez-González, *N. Engl. J. Med.*, 2013, **368**, 1279–1290.
23 A. Pan, Q. Sun and J. Manson, *J. Nutr.*, 2013, 512–518.
24 E. Ros, I. Núñez, A. Pérez-Heras, M. Serra, R. Gilabert, E. Casals and R. Deulofeu, *Circulation*, 2004, **109**, 1609–1614.
25 J. A. Vinson and Y. Cai, *Food Funct.*, 2012, **3**, 134–140.
26 J. Regueiro, C. Sánchez-González, A. Vallverdú-Queralt, J. Simal-Gándara, R. Lamuela-Raventós and M. Izquierdo-Pulido, *Food Chem.*, 2014, **152**, 340–348.
27 J. M. Landete, *Food Res. Int.*, 2011, **44**, 1150–1160.
28 M. Larrosa, F. A. Tomás-Barberán and J. C. Espín, *J. Nutr. Biochem.*, 2006, **17**, 611–625.
29 M. Larrosa, A. González-Sarrías, M. T. García-Conesa, F. A. Tomás-Barberán and J. C. Espín, *J. Agric. Food Chem.*, 2006, **54**, 1611–1620.
30 A. González-Sarrías, J. A. Giménez-Bastida, M. T. García-Conesa, M. B. Gómez-Sánchez, N. V. García-Talavera, A. Gil-Izquierdo, C. Sánchez-Alvarez, L. O. Fontana-Compiano, J. P. Morga-Egea, F. A. Pastor-Quirante, F. Martínez-Díaz, F. A. Tomás-Barberán and J. C. Espín, *Mol. Nutr. Food Res.*, 2010, **54**, 311–322.
31 J. C. Espín, M. Larrosa, M. T. García-Conesa and F. Tomás-Barberán, *Evid. Based Complement. Alternat. Med.*, 2013, **2013**, 270418.
32 M. Carvalho, P. J. Ferreira, V. S. Mendes, R. Silva, J. A. Pereira, C. Jerónimo and B. M. Silva, *Food Chem. Toxicol.*, 2010, **48**, 441–447.
33 W. E. Hardman, G. Ion, J. A. Akinsete and T. R. Witte, *Nutr. Cancer*, 2011, **63**, 960–970.
34 M. Stolarczyk, J. P. Piwowarski, S. Granica, J. Stefańska, M. Naruszewicz and A. K. Kiss, *Phytother. Res.*, 2013, **27**, 1842–1848.

35 K. B. Cleutjens, H. A. van der Korput, C. C. van Eekelen, H. C. van Rooij, P. W. Faber and J. Trapman, *Mol. Endocrinol.*, 1997, **11**, 148–161.
36 S. Altuwaijri, *J. Cancer Ther.*, 2012, **03**, 331–336.
37 F. Yeung, X. Li, J. Ellett, J. Trapman, C. Kao and L. W. Chung, *J. Biol. Chem.*, 2000, **275**, 40846–40855.
38 S. P. Balk, *J. Clin. Oncol.*, 2003, **21**, 383–391.
39 A. Magklara, A. Scorilas and C. Stephan, *Urology*, 2000, **2**, 527–532.
40 Z. Sun, J. Pan and S. P. Balk, *Nucleic Acids Res.*, 1997, **25**, 3318–3325.
41 P. Oettgen, E. Finger and Z. Sun, *J. Biol. Chem.*, 2000, **275**, 1216–1225.
42 R. Vicinanza, Y. Zhang, S. M. Henning and D. Heber, *Evid. Based Complement Alternat. Med.*, 2013, **2013**, 247504.
43 A. González-Sarrías, J.-C. Espín, F. A. Tomás-Barberán and M.-T. García-Conesa, *Mol. Nutr. Food Res.*, 2009, **53**, 686–698.
44 C. Oleaga, C. J. Ciudad, M. Izquierdo-Pulido and V. Noé, *Mol. Nutr. Food Res.*, 2013, **57**, 986–995.
45 N. C. Andrews and D. V. Faller, *Nucleic Acids Res.*, 1991, **19**, 2499.
46 L. Rodríguez, X. Villalobos, S. Dakhel, L. Padilla, R. Hervas, J. L. Hernández, C. J. Ciudad and V. Noé, *Biochem. Pharmacol.*, 2013, **86**, 1541–1554.
47 N. Xing, Y. Chen, S. Mitchell and C. Young, *Carcinogenesis*, 2001, **22**, 409–414.
48 F. Alimirah, J. Chen, Z. Basrawala, H. Xin and D. Choubey, *FEBS Lett.*, 2006, **580**, 2294–2300.
49 I. V. Litvinov, L. Antony, S. L. Dalrymple, R. Becker, L. Cheng and J. T. Isaacs, *Prostate*, 2006, 1338.
50 K. Chaudhary, P. Abel and E. Lalanil, *Environ. Health Perspect.*, 1999, **107**, 49–57.
51 V. Venkateswaran and L. H. Klotz, *Nat. Rev. Urol.*, 2010, **7**, 442–453.
52 S. G. Kasimsetty, D. Bialonska, M. K. Reddy, C. Thornton, K. L. Willett and D. Ferreira, *J. Agric. Food Chem.*, 2009, **57**, 10636–10644.
53 A. A. Alshatwi, T. N. Hasan, G. Shafi, N. A. Syed, A. H. Al-Assaf, M. S. Alamri and A. S. Al-Khalifa, *Evid. Based Complement Alternat. Med.*, 2012, **2012**, 103026.
54 N. P. Seeram, W. J. Aronson, Y. Zhang, S. M. Henning, A. Moro, R.-P. Lee, M. Sartippour, D. M. Harris, M. Rettig, M. A. Suchard, A. J. Pantuck, A. Belldegrun and D. Heber, *J. Agric. Food Chem.*, 2007, **55**, 7732–7737.
55 P. Saxena, M. Trerotola, T. Wang, J. Li, A. Sayeed, J. Vanoudenhove, D. S. Adams, T. J. Fitzgerald, D. C. Altieri and L. R. Languino, *Prostate*, 2012, **72**, 769–776.
56 Y. Niu, S. Yeh, H. Miyamoto, G. Li, S. Altuwaijri, J. Yuan, R. Han, T. Ma, H. Kuo and C. Chang, *Cancer Res.*, 2008, **68**, 7110–7119.
57 L. Kong, Q. Yuan, H. Zhu, Y. Li, Q. Guo, Q. Wang, X. Bi and X. Gao, *Biomaterials*, 2011, **32**, 6515–6522.
58 H. L. Oh and C.-H. Lee, *Bioorg. Med. Chem. Lett.*, 2011, **21**, 1347–1349.
59 J. N. Davis, O. Kucuk and F. H. Sarkar, *Mol. Carcinog.*, 2002, **34**, 91–101.
60 S. Williams, P. Singh, J. Isaacs and S. Denmeade, *Prostate*, 2007, **329**, 312–329.
61 M. M. Webber, A. Waghray and D. Bello, *Clin. Cancer Res.*, 1995, **1**, 1089–1094.
62 A. Malik, S. Afaq, M. Shahid, K. Akhtar and A. Assiri, *Asian Pac. J. Trop. Med.*, 2011, **4**, 550–555.
63 H. Xu, X. Yu, S. Qu and D. Sui, *Bioorg. Med. Chem. Lett.*, 2013, **23**, 3631–3634.

This journal is © The Royal Society of Chemistry 2014

4.3 ARTICLE III:

Urolithin A causes p21 upregulation in prostate cancer cells.

Claudia Sánchez-González, Carlos J. Ciudad*, Maria Izquierdo-Pulido[#], Véronique Noé[#]

[#] Dr. Véronique Noé and Dr. Maria Izquierdo-Pulido share senior authorship.

* Dr. Carlos J. Ciudad is corresponding author.

European Journal of Nutrition 2015 [e-pub ahead of print]; **DOI: 10.1007/s00394-015-0924-z.**

Impact Factor (JCR): 3.840.

Ranking in Nutrition and Dietetics: 17/79 (Q1).

ABSTRACT

Introduction: Walnuts contain several bioactive compounds, including pedunculagin, a polyphenol metabolized by microbiota to form **urolithins** such as urolithin A. Urolithin A has several known biological effects on cancer cell models, but its effect on whole genome expression in prostate cancer cells is unknown. The aim of this study was to determine **gene expression changes** in **prostate cancer cells** upon incubation with urolithin A.

Material and Methods: We performed a **genomic analysis** to study the effect of urolithin A on **LNCaP prostate cells**. Cells were incubated with 40 μM UA for 24 hours. Then, total RNA was extracted and hybridized to Affymetrix Human Genome U219 Array. Microarray results were analyzed using the GeneSpring v13 software. Differentially expressed genes ($p < 0.05$, Fold

Change > 2) were used to perform Biological Association Networks. The activation of p21 promoter was assessed by luciferase activity. Cell cycle was analyzed by flow cytometry and apoptosis was measured both by the rhodamine method and by caspase 3/7 activation. Cell viability was determined by the MTT assay.

Results: We identified two gene nodes, FN-1 and CDKN1A, among the differentially expressed genes upon UA treatment. The overexpression of CDKN1A was validated at the mRNA and protein levels and p21 promoter activation was also observed. Cell cycle analyses showed an increase in G1-phase cell population upon incubation with UA, which also resulted in apoptosis and caspase 3/7 activation.

Conclusion: Our results indicate a clear effect of **urolithin A** on whole genome expression in a prostate cancer cell model. The **significant up regulation of p21**, which has a known role in cell cycle and apoptosis, correlated with an increased percentage of cells in the G1 phase of the cell cycle and in apoptosis. These results further validate the multi-targeted effects of urolithins and the potential role of **urolithin A as a chemo-preventive agent for prostate cancer**.

Eur J Nutr
DOI 10.1007/s00394-015-0924-z

ORIGINAL CONTRIBUTION

Urolithin A causes p21 up-regulation in prostate cancer cells

Claudia Sánchez-González[1] · Carlos J. Ciudad[2] · Maria Izquierdo-Pulido[1,3] · Véronique Noé[2]

Received: 11 March 2015 / Accepted: 5 May 2015
© Springer-Verlag Berlin Heidelberg 2015

Abstract
Purpose Walnuts contain several bioactive compounds, including pedunculagin, a polyphenol metabolized by microbiota to form urolithins, namely urolithin A (UA). The aim of this study was to determine gene expression changes in prostate cancer cells after incubation with UA.
Methods We performed a genomic analysis to study the effect of UA on LNCaP prostate cells. Cells were incubated with 40 μM UA for 24 h, and RNA was extracted and hybridized to Affymetrix Human Genome U219 array. Microarray results were analyzed using GeneSpring v13 software. Differentially expressed genes ($p < 0.05$, fold change > 2) were used to perform biological association networks. Cell cycle was analyzed by flow cytometry and apoptosis measured by the rhodamine method and by caspases 3 and 7 activation. Cell viability was determined by MTT assay.
Results We identified two nodes, FN-1 and CDKN1A, among the differentially expressed genes upon UA treatment. CDKN1A was validated, its mRNA and protein levels were significantly up-regulated, and the promoter activation measured by luciferase. Cell cycle analysis showed an increase in G1-phase, and we also observed an induction of apoptosis and caspases 3 and 7 activation upon UA treatment.
Conclusion Our results indicate a potential role of UA as a chemopreventive agent for prostate cancer.

Keywords Urolithin A · Walnuts · Ellagitannins cancer prevention

Introduction

Compounds with anticancer activity that are naturally found in the diet can represent a particularly efficient therapeutic adjuvant. One such type of bioactive compounds is polyphenols, which exert their anticancer effects by several mechanisms, such as decreasing the pro-oxidative effect of carcinogenic agents [1, 2], modulation of cancer cell signaling [3, 4], altering cell cycle progression [5], promoting apoptosis [6, 7] and modulating enzymatic activities [8]. Polyphenols have also been shown to act on multiple targets involved in inflammation (tumor necrosis factor, TNF) [9], angiogenesis (vascular endothelial growth factor, VEGF) [10], and drug and radiation resistance (multi-drug resistance protein, MDR) [11].

Walnuts are a common dietary component in many places around the world. It is well documented that the most abundant polyphenols in walnuts are ellagitannins (ETs), mainly pedunculagin [12, 13]. ETs exhibit structural diversity according to food source [12]. Previous studies of rat intestinal contents showed that ETs could be hydrolyzed to ellagic acid (EA) at the pH found in the small intestine and cecum [14, 15]. EA is further metabolized by gut flora to urolithins, mainly urolithin A (UA) and B (UB) [16] and is probably formed in the colon [15]. These

Véronique Noé and Maria Izquierdo-Pulido share senior authorship.

✉ Carlos J. Ciudad
cciudad@ub.edu

[1] Nutrition and Food Science Department, University of Barcelona, 08028 Barcelona, Spain

[2] Biochemistry and Molecular Biology Department, School of Pharmacy, University of Barcelona, Av. Joan XXIII s/n, 08028 Barcelona, Spain

[3] CIBER Fisiopatología de la Obesidad y la Nutrición (CIBEROBN), Barcelona, Spain

Published online: 12 May 2015

urolithins circulate in blood and can reach many of the target organs where the effects of ellagitannins are observed [17]. The occurrence of ETs and EA in the bloodstream is almost negligible, but their derived metabolites, urolithins, can reach micromolar concentrations in plasma [18]. It is important to note that urolithin levels in plasma and urine after ingestion of ETs-rich foods can differ between individuals due to their gut microbiota [15].

Like other polyphenols, ETs, EA and their derived metabolites possess varied biological activities which suggest that they could have beneficial effects on human health [18]. The role of ETs in several molecular pathways related to cancer initiation, development and progression has been assessed in in vitro [19, 20] and in vivo studies [21]. Our group has previously assessed the effect that UA and UB exert on LNCaP prostate adenocarcinoma cells. We observed a clear down-regulation especially by UA of androgen receptor (AR) and prostate-specific antigen (PSA) expression, both important targets in prostate cancer progression [22].

Even though there is emerging evidence that walnut polyphenols can reduce the risk of developing certain cancers, the molecular mechanisms underlying their chemopreventive effect still remain poorly known. Nutrigenomics is an approach that favors the understanding of how dietary components influence molecular pathways, and how this influence can modulate signaling in early phases of disease, such as in cancer. Nutrients and food bioactive compounds are considered to be "signaling molecules" that, through cellular sensing mechanisms, can produce changes in gene expression at the transcriptomic, proteomic, and metabolomic levels [23]. Therefore, considering our previous results, we were encouraged to further explore the effect of UA upon LNCaP gene expression through a genomic approach. The aim of our study was to determine the effect of urolithin A, the main human metabolite of walnut polyphenols, on gene expression in a prostate cancer cell line using microarrays. We also performed biological association networks (BANS) to generate node genes that constituted important targets for further exploration. Furthermore, we evaluated the effect of UA on cell cycle, apoptosis and proliferation.

Materials and methods

Chemicals

Urolithin A (UA; 3,8-dihydroxy-6H-dibenzo[b,d]pyran-6-one, 95 % purity) was synthesized by the Department of Organic Chemistry, School of Pharmacy at the University of Barcelona (Barcelona, Spain). Urolithin A was resuspended in DMSO.

Cell culture

LNCaP (androgen responsive) human prostate adenocarcinoma cell line was routinely grown in Ham's F-12 medium, supplemented with 7 % (V/V) fetal bovine serum (FBS, both from GIBCO, Invitrogen, Barcelona, Spain), sodium penicillin G and streptomycin, and was maintained at 37 °C in a humidified atmosphere containing 5 % CO_2. Different number of cells, depending on the assay, were incubated with 40 μM urolithin A since we have previously used at this concentration [22] which can be found in plasma after consumption of pedunculagin-rich foods [18]. The final concentration of DMSO in the culture medium was always ≤0.2 %.

Microarrays

Gene expression was analyzed by hybridization to Affymetrix Human Genome U219 array plate, which measures gene expression of more than 36,000 transcripts and variants that represent more than 20,000 genes. LNCaP cells (350,000) were incubated with 40 μM urolithin A for 24 h. Total RNA was prepared from triplicate samples using RNAeasy minikit (Qiagen) following the recommendations of the manufacturer. RNA quality was tested by Agilent Technologies using 2100 Bioanalyzer Eukaryote Total RNA Nano Series II. Labeling, hybridization and detection were carried out following the manufacturer's specifications at the IDIBAPS Genomic Service from Hospital Clínic, Barcelona. In brief, cRNA was labeled with biotin, purified, fragmented and hybridized onto the platform, using the GeneChip HT 3′IVT Express Kit. Afterward, the GeneTitan® Multi-Channel Instrument (Affymetrix) was used to hybridize, wash and stain. Microarrays were scanned using the Genechip Scanner 3000.

Microarray data analyses

Genomic analyses were carried out using the GeneSpring GX software v.13 (Agilent Technologies). Data were processed by RMA (robust multi-array average) normalization in log2 base scale and using a baseline transformation to the median of control samples. Differentially expressed genes were obtained by applying a p value cutoff of less than 0.05, and a fold change of expression of at least two-fold as described in Selga et al. [24]. Normalized and raw data were submitted to the Gene Expression Omnibus database (GEO). The GEO series GSE65527 was assigned for the data set.

Generation of biological association networks (BANs)

BANs were constructed with the aid of the pathway analysis within the GeneSpring v.13 (Agilent) as described

by Selga et al. [25] starting with the list of differentially expressed genes after 24 h of incubation with UA. NLP network discovery was performed using an advanced analysis with an expand interactions algorithm to assess relations among entities. The software builds an association network using our data and bibliographic interaction databases. Relevant network associations were curated.

Real-time RT-PCR

Total RNA was extracted from LNCaP using RNAeasy minikit (Qiagen) in accordance with the manufacturer's instructions. Complementary DNA (cDNA) was synthesized as described by Oleaga et al. [26]. RNA concentration and purity was checked using a Nanodrop spectrophotometer system (ND-1000 3.3 Nanodrop Technologies, Wilmington, DE, USA). mRNA levels were determined by StepOnePlus™ Real-Time PCR Systems (Applied Biosystems, Barcelona, Spain) using 3 μL of cDNA and specific Taqman probes (Applied Biosystems, Barcelona, Spain) for *CDKN1A* (Hs00355782) and *FN-1* (Hs00365052) genes and *APRT* (Hs00975725) as an endogenous control.

Western blot

LNCaP cells (350,000) were plated on 35 mm/well 6-well dishes and treated the day after with UA. After 24 h of incubation, cells were collected and centrifuged for 5 min at 800×*g* at 4 °C. The cell pellets were suspended in 200 μL of Lyss buffer (0.5 M NaCl, 1.5 mM $MgCl_2$, 1 mM EGTA, 10 % glycerol 1 % Triton x_100, 50 mM HEPES, pH 7.9 all from Applichem, Barcelona, Spain), and 10 μL protease inhibitor cocktail (from Sigma-Aldrich, Madrid, Spain). The cell lysate was kept on ice for 60 min vortexing every 15 min. Cellular debris was removed by centrifugation at 15,000×*g* at 4 °C for 10 min. A 5 μL aliquot of the extract was used to determine the protein concentration using the Bradford assay (Bio-Rad, Barcelona, Spain).

Whole-cell extracts (100 μg) were resolved in 12 % SDS–polyacrylamide gels and transferred to PVDF membranes (Immobilon P, Millipore, Madrid, Spain) using a semidry electroblotter. Membranes were probed overnight at 4 °C with primary antibody against p21 (1:200 dilution; sc-397 from Santa-Cruz Biotechnology Inc., Heidelberg, Germany). Signal was detected by secondary horseradish peroxidase-conjugated anti-rabbit (1:2500; Dako, Denmark) antibody and enhanced chemiluminescence using the ECL™ Prime Western Blotting Detection Reagent, as recommended by the manufacturer (GE Healthcare, Barcelona, Spain). Chemiluminescence was detected with ImageQuant LAS 4000 Mini technology (GE Healthcare, Barcelona, Spain). Normalization of the blots was performed by incubation with an antibody against tubulin (1:800 dilution, sc-5286 from Santa-Cruz Biotechnology Inc., Heidelberg, Germany).

Transfection and luciferase assay

LNCaP cells (350,000) were plated in 35 mm/well 6-well dishes the day before transfection. Medium (2 mL) was renewed before transfection, which was performed using FuGENE 6 (Roche, Barcelona, Spain). For each well, transfection reagent was incubated for 5 min in 100 μL of antibiotic and serum-free medium, followed by the addition of plasmid DNA and incubated for another 20 min at a ratio of 3:1 (μL of transfection reagent: μg of plasmid DNA). One microgram of plasmid DNA, either the basic vector or WWP-Luc promoter, a p21 promoter construction in front of a luciferase reporter gene, was used for transfection. WWP-Luc (p21/WAF1 promoter) was obtained from Dr. Bert Vogelstein from the Johns Hopkins School of Medicine.

Incubation with 40 μM of UA was performed 6 h after transfection, and luciferase activity was determined 24 h after transfection. Cell extracts were prepared by lysing cells with 100 μL of Reporter Lysis Buffer (2 mM DTT, 2 mM EDTA, 10 % glycerol, 1 % Triton X_100, 25 mM Tris–phosphate, pH 7.8). The lysate was centrifuged at 12,000×*g* for 2 min at 4 °C to pellet cell debris, and supernatants were transferred to a fresh tube. Fifteen microliters of the extract was added to 15 μL of the luciferase assay substrate (Promega, Madrid, Spain) at room temperature. Luminescence was measured using the Glomax™ 20/20 Luminometer (Promega, Madrid, Spain) and expressed as relative luminescence units (RLU). Luciferase results were normalized by total protein concentration in the cell lysates. Protein concentration was determined by the Bradford assay (Bio-Rad, Barcelona, Spain) according to the manufacturer's protocol.

Cell cycle analysis

After treating cells with for 24 h, cells were recovered by centrifugation (800×*g*, 3 min) and washed once with cold PBS. The pellet was resuspended in 500 μL cold PBS and 4500 μL cold 70 % ethanol and left at −20 °C overnight. The cells were then centrifuged, and the pellet was washed once with cold PBS, resuspended in PBS, RNAse A (2 mg/mL, final concentration), 0.1 % Triton X_100 and stained with propidium iodide (5 mg/mL final concentration) for 1 h and analyzed by flow cytometry. Flow cytometric experiments were carried out using an Epics XL flow cytometer (Coulter Corporation, Hialeah, Florida). Excitation of the sample was done using a standard 488-nm

air-cooled argon-ion laser at 15 mW power. Forward scatter (FSC), side scatter (SSC) and red (620 nm) fluorescence for PI were acquired. Aggregates were excluded gating single cells by their area versus peak fluorescence signal. DNA analysis on single fluorescence histograms was done using Multicycle software (Phoenix Flow Systems, San Diego, CA).

Apoptosis

Apoptosis was determined by two methods: Rhodamine method and Caspase-Glo 3/7 assay (Promega, Madrid, Spain) which measures caspase activation. For the rhodamine method, LNCaP cells (250,000) were plated in 35 mm/well 6-well dishes with 2 mL complete F-12 medium and 24 h after, they were treated with increasing concentrations of UA. Staurosporine (1 μM) (Sigma-Aldrich, Madrid, Spain) was used as a positive control. Rhodamine (final concentration 5 ng/mL) (Sigma-Aldrich, Madrid, Spain) was added for 30 min, and the cells were collected, centrifuged at 800×*g* at 4 °C for 5 min, and washed once in PBS. The pellet was suspended in 500 mL PBS plus propidium iodide (PI) (final concentration 5 mg/mL) (Sigma-Aldrich, Madrid, Spain). Flow cytometry data were analyzed using the Summit v4.3 software. The percentage of Rho-negative and PI negative cells corresponds to the apoptotic population.

For the Caspase-Glo 3/7 assay, 10,000 cells per well were plated in a 96-well plate in 100 μL F12-complete medium. After 24 h, cells were incubated with UA for 24 h. The following day, 100 μL of Caspase-Glo 3/7 reagent was added. After 1 h of incubation, luminescence was measured using a Modulus™ Microplate luminometer (Turner Biosystems, Promega, Madrid, Spain). F12-complete medium and the reagent were considered the blank control and untreated cells as background.

Cell viability

Cell viability was measured by MTT assay. Cells were plated in 35 mm/well 6-well dishes in F12 medium, and cells were incubated with increasing concentrations of UA for 24 h. After incubation, 0.63 mM of 3-(4,5-dimethylthiazol-2-yl)-2,5-diphenyltetrazolium bromide and 18.4 mM of sodium succinate (both from Sigma-Aldrich, Madrid, Spain) were added to the culture medium and incubated for 3 h at 37 °C. Then, the medium was removed and the solubilization reagent (0.57 % acetic acid and 10 % sodium dodecyl sulfate in dimethyl sulfoxide) (Sigma-Aldrich, Madrid, Spain) was added. Cell viability was measured at 570 nm in a WPA S2100 Diode Array spectrophotometer (Biochrom Ltd., Cambridge, UK).

Statistical analyses

For the RT-PCR determinations, western blot analyses and apoptosis assays, values are expressed as the mean ± SE of three independent experiments. Data were analyzed using one-way ANOVA followed by Tukey's post hoc multiple range test by using the SPSS software v.21. The difference between groups was considered statistically significant at $p < 0.05$.

Results

Effect of urolithin A incubation in LNCaP gene expression

Gene expression profile was compared between LNCaP cells incubated with 40 μM UA for 24 h versus control (vehicle-treated cells). GeneSpring GX software v.13 was used to analyze the results and a list of twofold differentially expressed genes and a *p* value cutoff of <0.05 was created. UA incubation caused the up-regulation of 37 genes and down-regulation of 74 genes. Differentially expressed genes are presented in Table 1A, B. The data reported in this paper are accessible through GEO series accession number [GSE65527].

Generation of biological association networks

A biological association network (BAN) was constructed using pathway architect within GeneSpring v.13 using the list of differentially expressed genes (Table 1A, B) upon incubation with UA. In the generated network, CDKN1A that encodes for p21 appeared as a prominent node and was chosen for further validation due to its relation to cancer progression (Fig. 1), another gene to note in the BAN was fibronectin-1 (FN-1). Changes in gene expression of both nodes are shown in Table 1A, B. CDKN1A was up-regulated by 260 %, while FN-1 was down-regulated by 48 %.

Validation of p21 changes at the mRNA and protein levels

For the validation of CDKN1A, LNCaP cells were incubated with 40 μM UA for 24 h. Total RNA was extracted, and p21 expression was analyzed by real-time RT-PCR. A 2.6-fold increase in CDKN1A mRNA levels was observed after 24-h incubation with UA (Fig. 2a). P21 protein levels were also determined upon incubation of LNCaP cells with UA, and an 8.6-fold increase was observed in these conditions (Fig. 2b).

Table 1 (A) List of overexpressed genes, (B) list of underexpressed genes

Gene symbol	Gene title	*p* value (corrected)	FC	Raw value
(A)				
ANTXR1	Anthrax toxin receptor 1	0.018071683	3.9283698	33–131
HMGCS2	3-hydroxy-3-methylglutaryl-CoA synthase 2 (mitochondrial)	0.041272584	3.2182467	311–1001
SLC1A1	Solute carrier family 1 (neuronal/epithelial high affinity glutamate transporter, system Xag), member 1	0.04198332	2.9483755	69–203
RBKS	Ribokinase	0.04065924	2.890072	82–238
SFRS11	Serine/arginine-rich splicing factor 11	0.049647037	2.8698597	285–819
FTH1	Ferritin, heavy polypeptide 1	0.029451594	2.8085105	890–2502
RPL31	Ribosomal protein L31	0.048858333	2.7897265	264–736
RNFT2	Ring finger protein, transmembrane 2	0.04847244	2.6944962	102–276
ABCG1	ATP-binding cassette, sub-family G (WHITE), member 1	0.041132696	2.6784973	79–212
SNORD72	Small nucleolar RNA, C/D box 72	0.041381806	2.6759524	377–1010
CDKN1A	Cyclin-dependent kinase inhibitor 1A (p21, Cip1)	0.03852722	2.605698	1449–3776
TCTEX1D2	Tctex1 domain containing 2	0.033454563	2.5897472	152–395
C6orf52	Chromosome 6 open reading frame 52	0.041132696	2.5859122	180.93625
SDC4	Syndecan 4	0.018071683	2.5526035	253–645
NUTF2	Nuclear transport factor 2	0.03852722	2.5449026	59–152
PIK3R3	Phosphoinositide-3-kinase, regulatory subunit 3 (gamma)	0.039309744	2.4860854	667–1658
HSPA5	Heat shock 70 kDa protein 5 (glucose-regulated protein, 78 kDa)	0.048546728	2.4627695	145–358
DNAJC21	DnaJ (Hsp40) homolog, subfamily C, member 21	0.04065924	2.3872724	27–65
ARMCX3	Armadillo repeat containing, X-linked 3	0.048788916	2.3852787	159–380
C17orf108	LYR motif containing 9	0.048965555	2.3784144	111–266
SAP18	Sin3A-associated protein, 18 kDa	0.044830944	2.3029501	59–137
C9orf103	idnK, gluconokinase homolog (*E. coli*)	0.021912582	2.2767186	108–247
SERPINB5	Serpin peptidase inhibitor, clade B (ovalbumin), member 5	0.039116967	2.1881664	87–192
KRCC1	Lysine-rich coiled-coil 1	0.04073255	2.178822	95–209
DDB2	Damage-specific DNA binding protein 2, 48 kDa	0.039309744	2.1729174	229–481
PLRG1	Pleiotropic regulator 1	0.046348132	2.158798	151–326
GNG7	Guanine nucleotide binding protein (G protein), gamma 7	0.048489492	2.1230555	92–196
RNF32	Ring finger protein 32	0.03852722	2.1158345	43–92
DDB2	Damage-specific DNA binding protein 2, 48 kDa	0.029451594	2.096718	222–482
SIPA1L1	Signal-induced proliferation-associated 1 like 1	0.046348132	2.0962265	40–84
KANK1	KN motif and ankyrin repeat domains 1	0.046864968	2.0880623	35–75
GSTA4	Glutathione *S*-transferase alpha 4	0.044622324	2.0603788	324–669
BBC3	BCL2 binding component 3	0.048489492	2.059085	128–264
UGT2B15	UDP glucuronosyltransferase 2 family, polypeptide B15	0.03852722	2.0504327	4175–8561
SESN1	Sestrin 1	0.039309744	2.0473588	674–1381
PGRMC2	Progesterone receptor membrane component 2	0.048489492	2.0238128	645–1305
C11orf95	Chromosome 11 open reading frame 95	0.04801972	2.013529	43–88
(B)				
TARP	TCR gamma alternate reading frame protein	0.0411327	−20.279497	832–41
LAMA1	Laminin, alpha 1	0.03482863	−10.690396	336–31
TRPM8	Transient receptor potential cation channel subfamily M member 8	0.04127258	−9.334312	344–36
SEMA6D	Sema domain, transmembrane domain (TM), and cytoplasmic domain, (semaphorin) 6D	0.04854673	−6.9679465	287–41
TM4SF1	Transmembrane 4 L six family member	0.04653614	−6.4500413	288–44
NKX3-1	NK3 homeobox 1	0.03345456	−6.02152	5460–1414
KLK2	Kallikrein 2	0.03345456	−5.918217	2539–447
ARHGAP28	Rho GTPase activating protein 28	0.03930974	−5.5213523	483–196

Table 1 continued

Gene symbol	Gene title	*p* value (corrected)	FC	Raw value
TMPRSS2	Transmembrane protease, serine 2	0.04127258	−4.916592	50–102
MAF	v-maf avian musculoaponeurotic fibrosarcoma oncogene homolog	0.03852722	−4.5020537	168–37
FKBP5	FK506 binding protein 5	0.04127258	−4.393235	345–78
STK39	Serine threonine kinase 39	0.04653614	−4.3851995	2229–807
HPGD	Hydroxyprostaglandin dehydrogenase 15-(NAD)	0.03852722	−4.188455	48–11
TMEM100	Transmembrane protein 100	0.03345456	−4.053033	57–14
PLA1A	Phospholipase A1 member A	0.03852722	−4.0299063	112–27
MCCC2	Methylcrotonoyl-CoA carboxylase 2 (beta)	0.04896556	−4.0113063	1789–446
CENPN	Centromere protein N	0.0481307	−3.989921	4778–1918
PMEPA1	Prostate transmembrane protein, androgen induced 1	0.04198332	−3.935241	1204–306
EAF2	ELL associated factor 2	0.04848949	−3.7372491	442–118
TUBA3D	Tubulin, alpha 3d	0.04878892	−3.7160873	159–42
ABCC4	ATP-binding cassette, sub-family C (CFTR/MRP), member 4	0.04713093	−3.51927	79–22
IGF1R	Insulin-like growth factor 1 receptor	0.0411327	−3.3870313	254–84
SLC38A4	Solute carrier family 38, member 4	0.04848949	−3.297615	38–11
INPP4B	Inositol polyphosphate-4-phosphatase, type II	0.03852722	−3.2538679	80–24
FAM65B	Family with sequence similarity 65, member B	0.02945159	−3.0884745	657–228
HOMER2	Homer homolog 2 (drosophila)	0.04554693	−3.0316038	178–59
TNFAIP8	Tumor necrosis factor, alpha-induced protein 8	0.04854673	−2.9435992	64–22
CAB39L	Calcium binding protein 39-like	0.03852722	−2.9318016	814–279
ELL2	Elongation factor, RNA polymerase II, 2	0.04651458	−2.9182982	275–94
SLC16A6	SLC16A6 pseudogene 1	0.04964704	−2.8450818	436–153
NTNG1	Netrin G1	0.04653614	−2.84009	130–45
STK39	Serine threonine kinase 39	0.04848949	−2.762043	2229–807
NDRG1	N-myc downstream regulated 1	0.04847244	−2.6652703	1049–393
SLC4A4	Solute carrier family 4 (sodium bicarbonate cotransporter), member 4	0.04462232	−2.5919237	634–244
ELOVL7	ELOVL fatty acid elongase 7	0.04964704	−2.5912743	113–43
MBOAT2	Membrane bound *O*-acyltransferase domain containing 2	0.04127258	−2.5849755	2675–1034
RAB3B	RAB3B, member RAS oncogene family	0.04847244	−2.5677748	180–70
TMPO	Thymopoietin	0.04462232	−2.519366	238–94
PDLIM5	PDZ and LIM domain 5	0.04854673	−2.502937	429–171
TBRG1	Transforming growth factor beta regulator 1	0.02191258	−2.5027993	614–245
LAMC1	Laminin, gamma 1	0.04127258	−2.4839528	1687–679
NEDD4L	Neural precursor cell expressed, developmentally down-regulated 4-like, E3 ubiquitin protein ligase	0.04686497	−2.4582028	1155–495
KCND2	Potassium voltage-gated channel, Shal-related subfamily, member 2	0.04854673	−2.4482534	80–32
LANCL1	LanC lantibiotic synthetase component C-like 1 (bacterial)	0.04848949	−2.4360988	180–74
LCP1	Lymphocyte cytosolic protein 1 (L-plastin)	0.04848949	−2.3906643	1808–756
KCNMA1	Potassium large conductance calcium-activated channel, subfamily M, alpha member 1	0.02945159	−2.3443553	430–183
TFPI	Tissue factor pathway inhibitor (lipoprotein-associated coagulation inhibitor)	0.04848949	−2.3411489	1841–786
IGSF5	Immunoglobulin superfamily, member 5	0.0411327	−2.2933848	55–25
TBRG1	Transforming growth factor beta regulator 1	0.04550014	−2.2920535	1645–717
AGL	Amylo-alpha-1, 6-glucosidase, 4-alpha-glucanotransferase	0.04089165	−2.274828	167–73
SYT4	Synaptotagmin IV	0.04848949	−2.237817	2523–1226
SOAT1	Sterol *O*-acyltransferase 1	0.04360254	−2.228152	689–313
GCNT1	Glucosaminyl (*N*-acetyl) transferase 1, core 2	0.03852722	−2.2103882	82–37
HES1	Hes family bHLH transcription factor	0.03852722	−2.1978023	121–55
FKBP1A	FK506 binding protein 1A	0.04848949	−2.1769133	353–162

Table 1 continued

Gene symbol	Gene title	*p* value (corrected)	FC	Raw value
TJP1	Tight junction protein 1	0.02945159	−2.11793	341–161
LIN7B	Lin-7 homolog B (*C. elegans*)	0.04847244	−2.1050866	174–83
ADAMTS1	ADAM metallopeptidase with thrombospondin type 1 motif, 1	0.0379042	−2.0998979	2939–1399
GNB4	Guanine nucleotide binding protein (G protein), beta polypeptide 4	0.0411327	−2.096679	1230–587
DHFR	Dihydrofolate reductase	0.04964704	−2.090263	779–373
FN1	Fibronectin 1	0.02945159	−2.0699394	1475–711
FGFR1OP	FGFR1 oncogene partner	0.04211903	−2.069577	787–380
PPAP2A	Phosphatidic acid phosphatase type 2A	0.04848949	−2.0578847	4149–2016
C3orf58	Chromosome 3 open reading frame 58	0.0450805	−2.0526423	162–79
LIMCH1	LIM and calponin homology domains 1	0.04686497	−2.0517795	1748–852
LOC81691	Exonuclease NEF-sp	0.03852722	−2.0482614	189–92
PPFIA2	Protein tyrosine phosphatase, receptor type, f polypeptide (PTPRF)	0.04964704	−2.0405033	284–139
TMEM79	Transmembrane protein 79	0.02945159	−2.0395525	289–141
SCARB2	Scavenger receptor class B, member 2	0.04854673	−2.0371418	1189–583
MPHOSPH9	M-phase phosphoprotein 9	0.041381806	−2.024088	496–245
FAM3B	Family with sequence similarity 3, member B	0.018071683	−2.0137253	38–18
ACTR3	ARP3 actin-related protein 3 homolog (yeast)	0.048858333	−2.01066	1516–754
KIF22	Kinesin family member 22	0.046348132	−2.0081372	576–287
ZNF385B	Zinc finger protein 385B	0.044830944	−2.0049856	708–353

The table shows the list of differently expressed genes by 2.0-fold with a p value <0.05 obtained after cells treated with 40 μM UA and includes the gene symbol for all genes, and their associated title. The additional columns correspond to the corrected p value, the fold change in expression relative to the control group, and the changes in raw values

Effect of urolithin A on p21 promoter activity

To assess whether UA modulates the transcriptional activation of p21, we performed transient transfections in LNCaP cells using a luciferase reporter vector carrying the p21 promoter construct (WWP-luc) in the absence and in the presence of UA. UA-incubated cells (40 μM) showed a 3.5-fold increase on luciferase activity when compared to the vehicle-treated cells (Fig. 2c). As a control, cells transfected with the empty vector and un-transfected cells showed basal luminescence (Fig. 2c).

Urolithin A causes changes in the cell cycle

LNCaP cells were incubated with 40 μM UA to evaluate its effect over cell cycle. The results show a statistically significant increase in cells in the G1-phase after 24 h of incubation (Fig. 3a). Consequently, the increase in the percentage of G1 cells was accompanied by a decrease in cell number in both the S and G2/M phases.

Urolithin A causes apoptosis and caspases 3 and 7 activation

We assessed the effect of urolithins on apoptosis using the rhodamine method. After incubating LNCaP cells with UA at two concentrations (10 and 40 μM) for 24 h, the percentage of apoptotic cells increased compared with the control (Fig. 4a). A dose-dependent increase in apoptotic cell population was observed, although a statistically significant increase (14 %) was seen only after incubation with 40 μM UA (Fig. 4b). In addition, we also measured caspases 3 and 7 activation. Using the Caspase-Glo 3/7 assay, no apparent change was determined after incubation with 10 μM, but in accordance with the results using the rhodamine method, caspases 3 and 7 activation was significantly higher after incubation with 40 μM UA (Fig. 4c).

Effect of urolithin A on cell viability

Since UA caused changes in cell cycle distribution and induced apoptosis, we also measured cell viability after incubation with increasing concentrations of UA. UA caused a dose-dependent decrease in LNCaP cell viability. This effect became particularly evident after incubation with 60 μM UA (Fig. 5).

Discussion

The main objective of this study was to investigate, through functional genomics, the effect of UA, a known metabolite

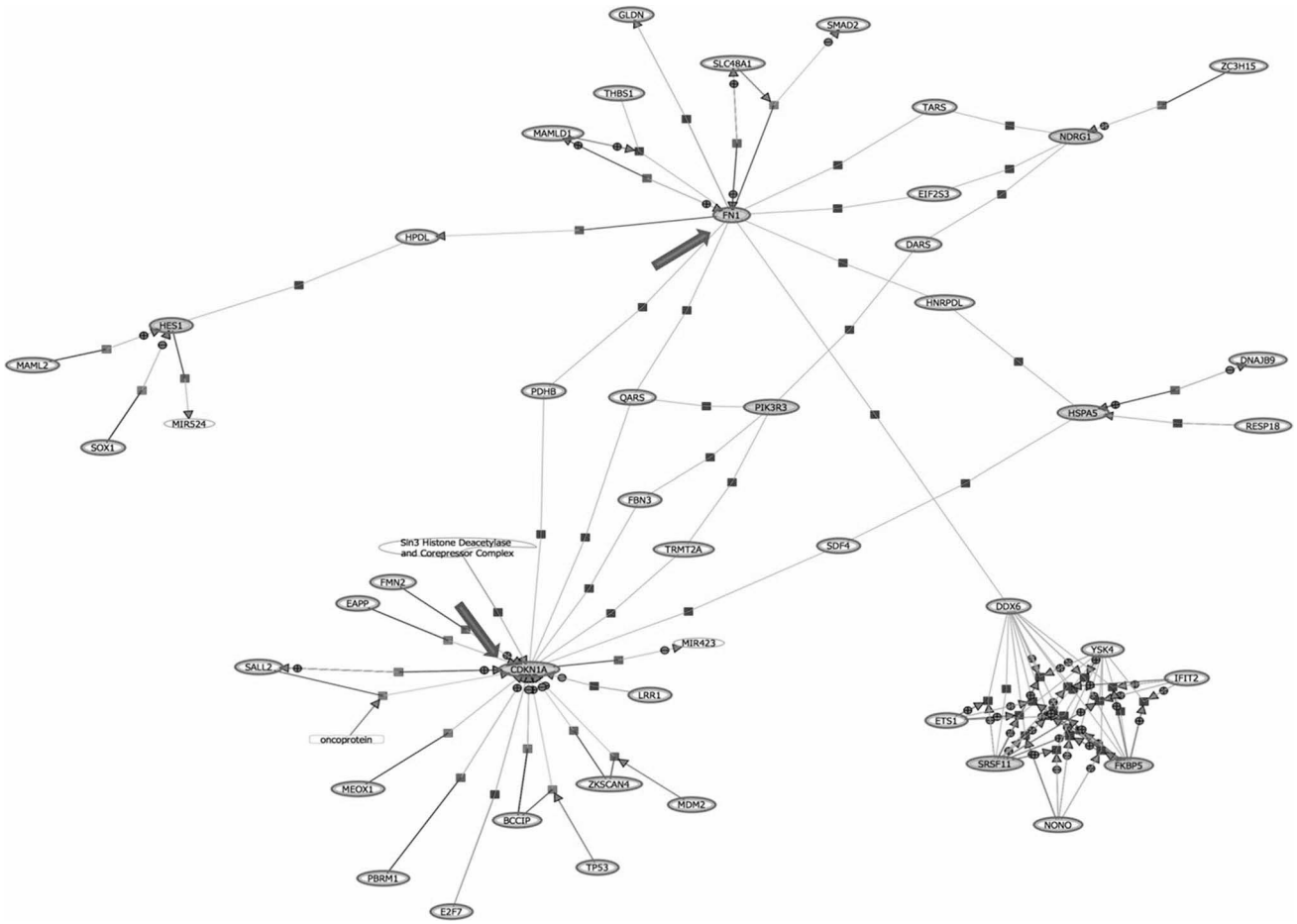

Fig. 1 Biological association network. The list of differentially expressed genes after 24-h incubation with 40 μM urolithin A was used to construct a BAN using the pathway analysis software within GeneSpring v13. The expanded BAN shows CDKN1A and FN-1 as node genes

of ETs, on gene expression in LNCaP prostate adenocarcinoma cells. To do so, microarray analyses were performed obtaining lists of differentially expressed genes. Then, a biological association network (BANs) analysis was performed to establish the relationship among the differentially expressed genes and whether these interactions resulted in important nodes. Two main nodes were found, namely CDKN1A (encoding for p21 protein), which was overexpressed, and FN-1 (encoding for the extracellular glycoprotein, fibronectin), which was underexpressed. Due to the well-known anti-proliferative role of p21 in tumor cells, we decided to focus on exploring the effects that UA has on the transcriptional regulation of p21 and its role on the cell cycle and apoptosis.

The role of ETs in prostate cancer progression has been reported by several authors including ourselves [22, 27–30]. Using a pomegranate fruit extract, Malik et al. [30] determined the increase in Bax and p21, and the decrease in Bcl-2 in PC3 androgen-independent cells. In a xenograft model, the pomegranate extract was able to reduce PSA secretion and tumor growth. Albrecht et al. [28] used four different pomegranate extracts (fruit, pericarp and 2 oils) to assess cell cycle progression and apoptosis in LNCaP, PC-3 and DU 145. These authors observed a twofold increase in p21 in prostate cancer cells with fermented juice polyphenols. Punicalagin, ellagic acid (EA) and total pomegranate tannin (TPT) were able to decrease the viability of human oral, prostate and colon tumor cells; however, superior activity was obtained with pure pomegranate juice (PJ). Similarly, PJ, punicalagin, EA and TPT induced apoptosis in HT-29 cells Seeram et al. [19]. González-Sarrias et al. [27] analyzed prostate tissue from volunteers after intake of ET-rich foods. The authors did not observe significant differences between benign prostate hyperplasia and prostate cancer. They concluded that the results obtained in the different groups might be influenced by the high variability between individuals, by the heterogeneity of the prostate tissues obtained by different procedures and by the use of small specimens that may not be representative of neighboring tissues. It is important to note that other variables such

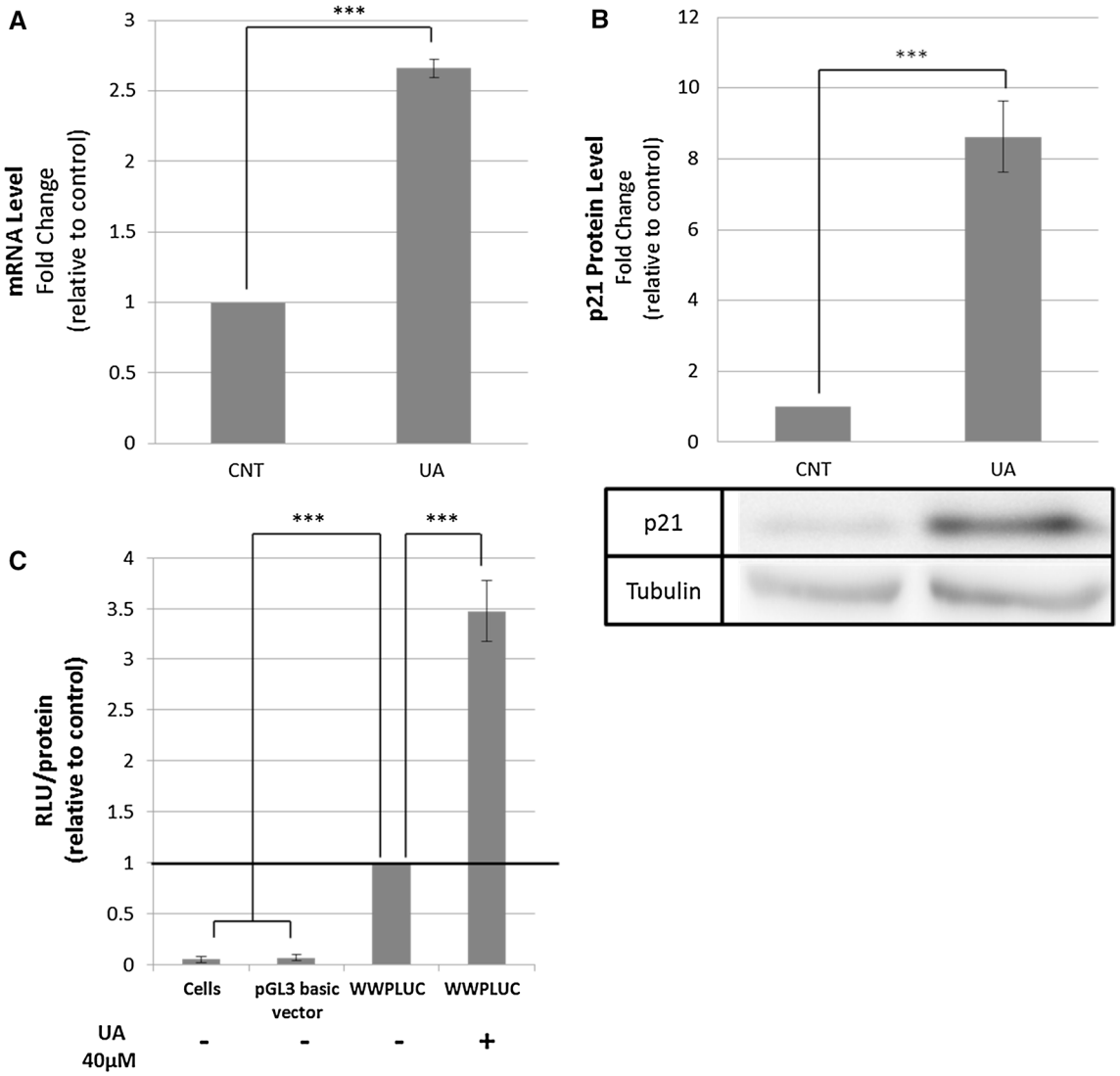

Fig. 2 CDKN1A mRNA and protein levels. **a** CDKN1A mRNA levels determined by real-time RT-PCR. *Bars* represent CDKN1A mRNA levels in LNCaP cells either control (0.10 % of DMSO) or treated with 40 μM UA during 24 h. Results are expressed in fold changes compared to the untreated cells and normalized using APRT as an endogenous control. They are the mean ± SE of three different experiments. ***$p < 0.001$. **b** Determination of p21 protein levels by western blot. *Bars* represent p21 protein levels in LNCaP cells either control (0.10 % of DMSO) or treated with 40 μM UA. Results are expressed as fold change compared to the untreated cells and represent the mean ± SE of three different experiments. ***$p < 0.001$. **c** p21 promoter activity in LNCaP cells. Cells were transfected with a luciferase reporter vector carrying the p21 promoter, and 6 h later, they were incubated with 40 μM UA. Results are expressed as luciferase relative units/total protein compared to control. They are the mean ± SE of three different experiments. ***$p < 0.001$

as disease stage and treatment could influence the effect of ETs over proliferation and other markers of PCa development and progression, including CDKN1A. In addition, in vivo levels of ET metabolites are highly variable and dependent on host's microbiota. In this direction, Seeram et al. [31] determined that ET metabolites were concentrated at high levels in mouse prostate, colon and intestinal tissues after administration of pomegranate extract and UA. Furthermore, they determined that pomegranate extract was able to inhibit the growth of a tumor xenograft performed with LAPC-4 prostate cancer cells by more of 50 %.

In the present study, we are able to associate the effects of the specific metabolite of ET, UA, with the changes in cell cycle distribution, proliferation and apoptosis in prostate cancer cells. We began our approach using a genomic strategy that allowed us to identify p21 as a relevant gene node in the network of differentially expressed genes provoked by UA action. The concentration of 40 μM UA was chosen because it is in the order of low micromolar levels, similar to what can be found in plasma after consumption of ET-rich foods [16, 17, 32] and was not cytotoxic to LNCaP cells [22]. In addition, most of the biological

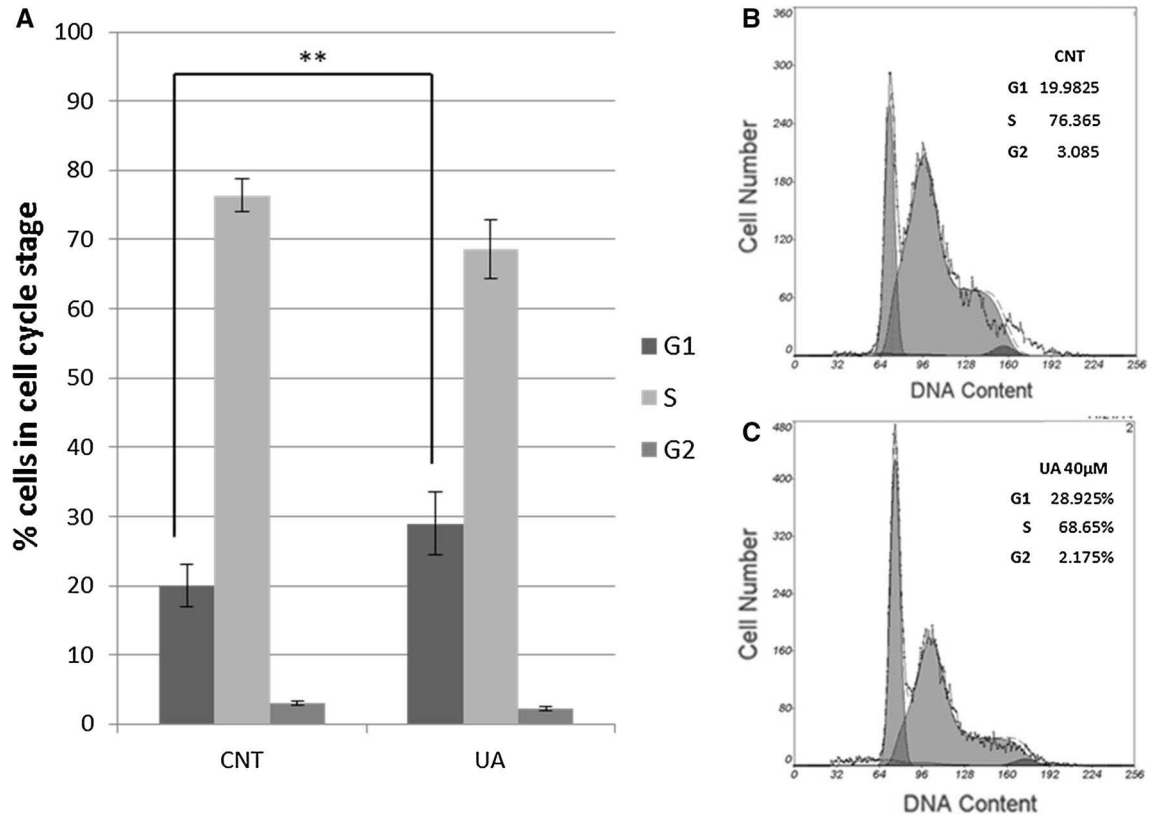

Fig. 3 Cell cycle distribution after incubation with urolithin A. **a** *Bars* represent the cell cycle phase distribution of control or UA-treated cells. Results are expressed as the mean of three experiments ± SE of relative cell population (%) $^{**}p < 0.005$. Representative flow cytometry histograms of cell cycle of LNCaP cells upon incubation with either DMSO (**b**) or with UA 40 µM (**c**) for 24 h

experiments with urolithins using human cell lines are performed in this range of concentrations [18, 31, 33]. In our approach with cultured cells, a single dose of the minimum concentration of UA in order to see a transcriptional effect was used. Given that the study was performed for a period of 24 h, one single dose was enough to observe changes in mRNA expression levels.

P21 is a cell cycle arrest inductor that functions as both a sensor and an effector of multiple anti-proliferative signals. It should be noted that under certain conditions, p21 has also been shown to have an oncogenic role, though this effect depends on the cellular localization, apoptotic stimuli and type of cancer [34]. Specifically, in prostate cancer, forced expression of p21 by transfection of adenoviral a vector had inhibitory effects on cancer cell growth [35]. Taking into account the significant up-regulation of p21 by UA, both at mRNA and protein levels, we decided to further explore the potential effect of this metabolite on cell cycle progression, particularly since this interaction has not been previously assessed in an androgen-dependent prostate cancer cell model. P21 inhibits cell cycle progression primarily through the inhibition of cyclin-dependent kinases resulting in G1 cell cycle arrest and a block in the transition in S phase [36]. Accordingly, our results show that UA caused an alteration in the cell cycle with an accumulation of cells in G1 and a reduction in S and G2. The role of p21 in cancer is complex, and among its well-known activities, p21 mediates p53-dependent G1 growth arrest, although recent evidence also indicates that p21 is an effector of multiple tumor suppressor pathways independent of p53 [36]. In CaSki cervical carcinoma cells, EA, the precursor of UA, induced an elevation of p21 mRNA and protein levels, but no relevant increase level in p53 mRNA and protein levels were detected. These authors suggested the activation of p21 by EA could be either through a p53-independent mechanism or by a p53-dependent mechanism that does not involve changes in p53 protein levels [37]. Therefore, although p21 activation can depend on p53, it appears that the induction of p21 by ETs is not dependent upon p53 levels.

We had previously assessed the effect that urolithins have on the modulation of the AR, which is fundamental in prostate cancer carcinogenesis and determined the inhibition in AR and PSA expression after incubating LNCaP cells with urolithins A and B. Down-regulation of PSA (KLK3) by UA was also detected in the microarray

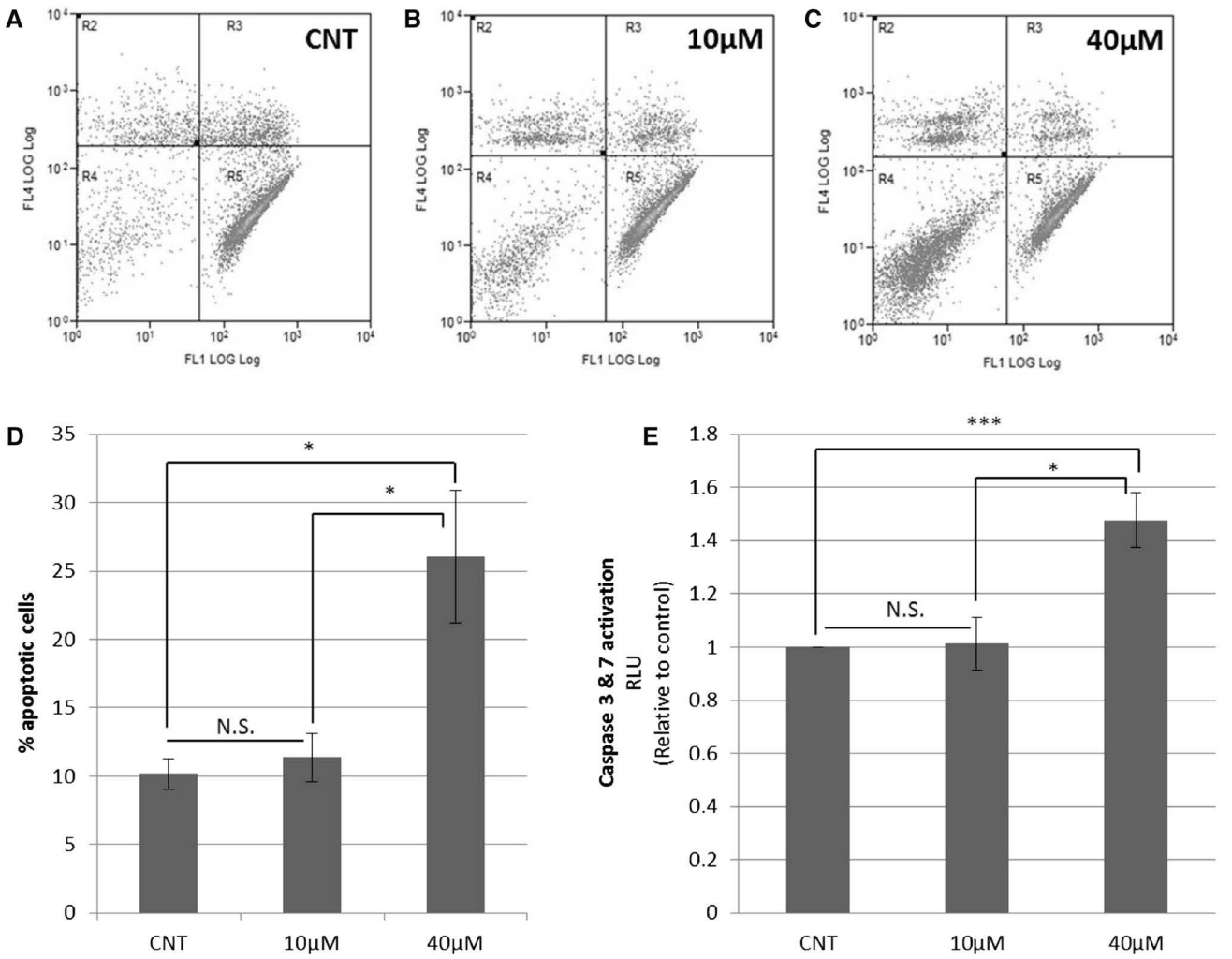

Fig. 4 Apoptosis levels determined by flow cytometry. Representative flow cytometer histograms displaying the cell populations. **a** Untreated control sample (0.12 % DMSO), **b** 10 μM UA and **c** 40 μM UA. **d** Percentage of apoptotic cells determined by flow cytometry. *Bars* represent LNCaP cells either untreated control (0.12 % of DMSO), or treated with increasing concentrations of UA for 24 h. Results represent the mean ± SE of three different experiments. $*p < 0.05$. **e** Caspases 3 and 7 activation by urolithin A. *Bars* represent relative luciferase units (RLU) relative to untreated control after incubation with either 10 or 40 μM UA. Results represent the mean ± SE of three different experiments. $***p < 0.001$. *NS* no significant difference

experiments. However, the decrease in fold change was -1.93 with a p value of less than 0.05; therefore, it was not included in Table 1A, B corresponding to fold changes higher than 2. In the case of AR, its down-regulation, as previously described [22], takes place between 9 and 12 h of treatment with UA, and it does not appear underexpressed in the microarray at 24 h.

Taking into account that a link between AR, PSA levels and p21 in a prostate cancer cell model had been explored through mechanistic studies [35], it was of interest to explore the role that urolithins might have in the possible interaction between AR, PSA and p21. Wang and colleagues [35] described that overexpression of the AR was responsible for p21 silencing and possibly for creating resistance to apoptosis in advanced prostate cancer. This inhibition of p21 by AR levels was androgen response element (ARE) and androgen dependent, which might negatively impact the sensitivity to apoptosis. In their study, a 50 % reduction in AR levels was accompanied by a 12-fold increase in p21 promoter activity in LNCaP cells. Although the study by Wang et al. was not performed using dietary bioactive compounds, their results can serve to link our previous observation that UA caused a significant down-regulation of both PSA and AR levels and a decrease in binding between AR and ARE [22] with the changes in p21 levels seen in the present work. Transfection of the p21 promoter in LNCaP cells led to an increase in its activity after UA incubation. Therefore, it is plausible to conclude that one

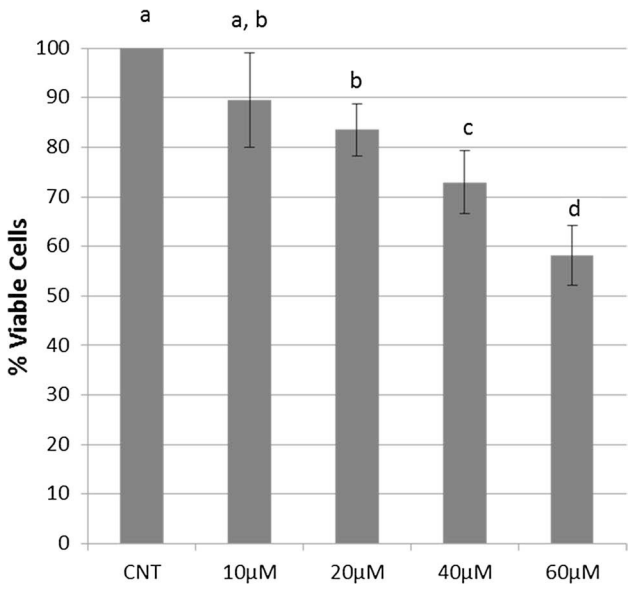

Fig. 5 Effect of urolithin A on cell viability. MTT assays were performed to determine cell viability upon incubation with increasing concentrations of urolithin A in LNCaP cells. They are the mean ± SE of 3 different experiments. Columns bearing *different letters* differ significantly at $p < 0.05$

of the mechanisms by which UA exerts its effects on p21 levels is through its transcriptional activation.

Many factors may modulate apoptosis, including growth factors, intracellular mediators of signal transduction and nuclear proteins regulating gene expression, DNA replication and cell cycle regulatory genes [38]. P21 displays a dual-face behavior as anti- or pro-apoptotic factor depending on the cellular localization and other stimulus [34]. ETs have been linked to suppressing prostate cancer cell proliferation and inducing apoptosis [20, 39]. As previously mentioned, AR has been associated with prostate cancer progression; some authors suggest that a down-regulation of AR expression might be responsible for inducing apoptosis in prostate cancer cells incubated with walnut bioactive compounds such as juglone, ellagic acid and urolithins A and B [22, 37, 40]. However, the induction of apoptosis by ETs has also been observed in androgen-independent PC3 and DU-145 prostate adenocarcinoma cells [20, 39].

We previously observed an induction of apoptosis and a decrease in Bcl-2 levels after incubation with urolithins [22]. Bcl-2 is an anti-apoptotic protein, localized to mitochondria, endoplasmic reticulum and the nuclear envelope, which interferes with the activation of caspases by preventing the release of cytochrome c [41]. Thus, in the present study, we measured caspases 3 and 7 activation to assess whether UA could promote the activity of these enzymes. UA caused apoptosis in a dose-dependent manner, and induction of caspases 3 and 7 was evident upon incubation with 40 μM UA, observation that to our knowledge had not been previously described. Naiki-Ito et al. [42] also reported that ellagic acid, the precursor of UA, at high concentrations (75–125 μM) promotes apoptosis, activates caspase 3 and reduces Bcl-2 protein levels in LNCaP cells. Interestingly, some studies assessed that cross talk between tumor cells and extracellular matrix proteins, when present in culture systems, leads to behavioral changes in tumor cell biology, such as increased adherence to substrates, increased resistance to chemotherapeutic agents and resistance to apoptosis [43]. Thus, the effect of UA on tumor cell survival is probably multifactorial, considering that the extracellular protein, fibronectin (encoded by FN-1), was down-regulated by UA incubation and appeared as a node gene in our BAN.

In summary, in this work, we present novel findings on UA, a major polyphenol metabolite in walnuts, which modulates the expression of a wide array of genes involved in prostate cancer development, progression and metastasis. Additionally, UA exerts chemopreventive effects against prostate carcinogenesis in a prostate cancer cell model. These effects include the inhibition of cell proliferation and cell cycle progression through the up-regulation of p21 and induction of apoptosis coupled to caspases 3 and 7 activation.

Acknowledgments This work was supported by grants from the California Walnut Commission (FBG-306913) and Spanish Government of Science and Innovation (SAF2011-23582 and SAF2014-51825-R). C.S.G. was supported by a scholarship from the "Consejo Nacional de Ciencia y Tecnología, CONACYT" from Mexico. Our group holds the Quality Mention from the Government of Catalonia, Spain (2014SGR96).

Conflict of interest Authors have no potential conflict of interest.

References

1. Duthie SJ, Dobson VL (1999) Dietary flavonoids protect human colonocyte DNA from oxidative attack in vitro. Eur J Nutr 38:28–34
2. Owen RW, Giacosa A, Hull WE et al (2000) The antioxidant/anticancer potential of phenolic compounds isolated from olive oil. Eur J Cancer 36:1235–1247
3. Khan N, Mukhtar H (2013) Modulation of signaling pathways in prostate cancer by green tea polyphenols. Biochem Pharmacol 85:667–672. doi:10.1016/j.bcp.2012.09.027
4. Corona G, Deiana M, Incani A et al (2007) Inhibition of p38/CREB phosphorylation and COX-2 expression by olive oil polyphenols underlies their anti-proliferative effects. Biochem Biophys Res Commun 362:606–611. doi:10.1016/j.bbrc.2007.08.049
5. Corona G, Deiana M, Incani A et al (2009) Hydroxytyrosol inhibits the proliferation of human colon adenocarcinoma cells through inhibition of ERK1/2 and cyclin D1. Mol Nutr Food Res 53:897–903. doi:10.1002/mnfr.200800269
6. Mantena SK, Baliga MS, Katiyar SK (2006) Grape seed proanthocyanidins induce apoptosis and inhibit metastasis of highly

metastatic breast carcinoma cells. Carcinogenesis 27:1682–1691. doi:10.1093/carcin/bgl030
7. Fabiani R, De Bartolomeo A, Rosignoli P et al (2002) Cancer chemoprevention by hydroxytyrosol isolated from virgin olive oil through G1 cell cycle arrest and apoptosis. Eur J Cancer Prev 11:351–358
8. Adams LS, Zhang Y, Seeram NP et al (2010) Pomegranate ellagitannin-derived compounds exhibit anti-proliferative and anti-aromatase activity in breast cancer cells in vitro. Cancer Prev Res (Phila) 3:108–113. doi:10.1158/1940-6207.CAPR-08-0225. Pomegranate
9. Kang NJ, Shin SH, Lee HJ, Lee KW (2011) Polyphenols as small molecular inhibitors of signaling cascades in carcinogenesis. Pharmacol Ther 130:310–324. doi:10.1016/j.pharmthera.2011.02.004
10. Granci V, Dupertuis YM, Pichard C (2010) Angiogenesis as a potential target of pharmaconutrients in cancer therapy. Curr Opin Clin Nutr Metab Care 13:417–422. doi:10.1097/MCO.0b013e3283392656
11. Garg AK, Buchholz TA, Aggarwal BB (2005) Chemosensitization and radiosensitization of tumors by plant polyphenols. Antioxid Redox Signal 7:1630–1647
12. Regueiro J, Sánchez-González C, Vallverdú-Queralt A et al (2014) Comprehensive identification of walnut polyphenols by liquid chromatography coupled to linear ion trap-Orbitrap mass spectrometry. Food Chem 152:340–348. doi:10.1016/j.foodchem.2013.11.158
13. Cerdá B, Periago P, Espín JC, Tomás-Barberán FA (2005) Identification of urolithin a as a metabolite produced by human colon microflora from ellagic acid and related compounds. J Agric Food Chem 53:5571–5576. doi:10.1021/jf050384i
14. Daniel EM, Kfcjpnick AS, Heur Y et al (1989) Extraction, stability, and quantitation of ellagic acid in various fruits and nuts. J Food Compos Anal 349:338–349
15. Garcia-Muñoz C, Vaillant F (2014) Metabolic fate of ellagitannins: implications for health, and research perspectives for innovative functional foods. Crit Rev Food Sci Nutr 54:1584–1598. doi:10.1080/10408398.2011.644643
16. Landete JM (2011) Ellagitannins, ellagic acid and their derived metabolites: a review about source, metabolism, functions and health. Food Res Int 44:1150–1160. doi:10.1016/j.foodres.2011.04.027
17. Larrosa M, Tomás-Barberán FA, Espín JC (2006) The dietary hydrolysable tannin punicalagin releases ellagic acid that induces apoptosis in human colon adenocarcinoma Caco-2 cells by using the mitochondrial pathway. J Nutr Biochem 17:611–625. doi:10.1016/j.jnutbio.2005.09.004
18. Espín JC, Larrosa M, García-Conesa MT, Tomás-Barberán F (2013) Biological significance of urolithins, the gut microbial ellagic acid-derived metabolites: the evidence so far. Evid Based Complement Altern Med 2013:270418. doi:10.1155/2013/270418
19. Seeram NP, Adams LS, Henning SM et al (2005) In vitro antiproliferative, apoptotic and antioxidant activities of punicalagin, ellagic acid and a total pomegranate tannin extract are enhanced in combination with other polyphenols as found in pomegranate juice. J Nutr Biochem 16:360–367. doi:10.1016/j.jnutbio.2005.01.006
20. Vicinanza R, Zhang Y, Henning SM, Heber D (2013) Pomegranate juice metabolites, ellagic acid and urolithin A, synergistically inhibit androgen-independent prostate cancer cell growth via distinct effects on cell cycle control and apoptosis. Evid Based Complement Altern Med 2013:247504. doi:10.1155/2013/247504
21. Hardman WE, Ion G, Akinsete JA, Witte TR (2011) Dietary walnut suppressed mammary gland tumorigenesis in the C(3)1 TAg mouse. Nutr Cancer 63:960–970. doi:10.1080/01635581.2011.589959
22. Sánchez-González C, Ciudad CJ, Noé V, Izquierdo-Pulido M (2014) Walnut polyphenol metabolites, urolithins A and B, inhibit the expression of the prostate-specific antigen and the androgen receptor in prostate cancer cells. Food Funct 5:2922–2930. doi:10.1039/c4fo00542b
23. Afman L, Müller M (2006) Nutrigenomics: from molecular nutrition to prevention of disease. J Am Diet Assoc 106:569–576. doi:10.1016/j.jada.2006.01.001
24. Selga E, Morales C, Noé V et al (2008) Role of caveolin 1, E-cadherin, Enolase 2 and PKCalpha on resistance to methotrexate in human HT29 colon cancer cells. BMC Med Genomics 1:35. doi:10.1186/1755-8794-1-35
25. Selga E, Oleaga C, Ramírez S et al (2009) Networking of differentially expressed genes in human cancer cells resistant to methotrexate. Genome Med 1:83. doi:10.1186/gm83
26. Oleaga C, Ciudad CJ, Izquierdo-Pulido M, Noé V (2013) Cocoa flavanol metabolites activate HNF-3β, Sp1, and NFY-mediated transcription of apolipoprotein AI in human cells. Mol Nutr Food Res 57:986–995. doi:10.1002/mnfr.201200507
27. González-Sarrías A, Giménez-Bastida JA, García-Conesa MT et al (2010) Occurrence of urolithins, gut microbiota ellagic acid metabolites and proliferation markers expression response in the human prostate gland upon consumption of walnuts and pomegranate juice. Mol Nutr Food Res 54:311–322. doi:10.1002/mnfr.200900152
28. Albrecht M, Jiang W, Kumi-Diaka J et al (2004) Pomegranate extracts potently suppress proliferation, xenograft growth, and invasion of human prostate cancer cells. J Med Food 7:274–283. doi:10.1089/1096620041938704
29. Bell C, Hawthorne S (2008) Ellagic acid, pomegranate and prostate cancer—a mini review. J Pharm Pharmacol 60:139–144. doi:10.1211/jpp.60.2.0001
30. Malik A, Afaq F, Sarfaraz S et al (2005) Pomegranate fruit juice for chemoprevention and chemotherapy of prostate cancer. Proc Natl Acad Sci 102:14813–14818. doi:10.1073/pnas.0505870102
31. Seeram NP, Aronson WJ, Zhang Y et al (2007) Pomegranate ellagitannin-derived metabolites inhibit prostate cancer growth and localize to the mouse prostate gland. J Agric Food Chem 55:7732–7737. doi:10.1021/jf071303g
32. Espín JC, González-Barrio R, Cerdá B et al (2007) Iberian pig as a model to clarify obscure points in the bioavailability and metabolism of ellagitannins in humans. J Agric Food Chem 55:10476–10485. doi:10.1021/jf0723864
33. González-Sarrías A, Giménez-Bastida JA, Núñez-Sánchez MA et al (2013) Phase-II metabolism limits the antiproliferative activity of urolithins in human colon cancer cells. Eur J Nutr. doi:10.1007/s00394-013-0589-4
34. Dutto I, Tillhon M, Cazzalini O et al (2014) Biology of the cell cycle inhibitor p21(CDKN1A): molecular mechanisms and relevance in chemical toxicology. Arch Toxicol. doi:10.1007/s00204-014-1430-4
35. Wang LG, Ossowski L, Ferrari AC (2001) Overexpressed androgen receptor linked to p21 WAF1 silencing may be responsible for androgen independence and resistance to apoptosis of a prostate cancer cell line. Cancer Res 61:7544–7551
36. Piccolo M, Crispi S (2012) The dual role played by p21 may influence the apoptotic or anti-apoptotic fate in cancer. J Can Res Updates 1:189–202
37. Narayanan BA, Geoffroy O, Willingham MC et al (1999) p53/p21(WAF1/CIP1) expression and its possible role in G1 arrest and apoptosis in ellagic acid treated cancer cells. Cancer Lett 136:215–221
38. Zaridze DG (2008) Molecular epidemiology of cancer. Biochemistry 73:532–542. doi:10.1134/S0006297908050064

39. Alshatwi AA, Hasan TN, Shafi G et al (2012) Validation of the antiproliferative effects of organic extracts from the green husk of *Juglans regia* L. on PC-3 human prostate cancer cells by assessment of apoptosis-related genes. Evid Based Complement Altern Med 2012:103026. doi:10.1155/2012/103026
40. Xu H, Yu X, Qu S, Sui D (2013) Juglone, isolated from *Juglans mandshurica* Maxim, induces apoptosis via down-regulation of AR expression in human prostate cancer LNCaP cells. Bioorg Med Chem Lett 23:3631–3634. doi:10.1016/j.bmcl.2013.04.007
41. Kang MH, Reynolds CP (2009) Bcl-2 inhibitors: targeting mitochondrial apoptotic pathways in cancer therapy. Clin Cancer Res 15:1126–1132. doi:10.1158/1078-0432.CCR-08-0144
42. Naiki-Ito A, Chewonarin T, Tang M, Pitchakarn P, Kuno T, Ogawa K, Asamoto M, Shirai T,Takahashi S (2015) Ellagic acid, a component of pomegranate fruit juice, suppresses androgen-dependentprostate carcinogenesis via induction of apoptosis. Prostate 75:151–160. doi:10.1002/pros.22900
43. Moroz A, Delella FK, Lacorte LM et al (2013) Fibronectin induces MMP2 expression in human prostate cancer cells. Biochem Biophys Res Commun 430:1319–1321. doi:10.1016/j.bbrc.2012.12.031

5. DISCUSSION

The **main objective** of this thesis was to explore the effect of walnut polyphenol metabolites on the expression of genes related to cancer development and progression. To achieve this goal, first it was necessary to identify the specific polyphenolic profile of walnuts using a sensitive analytical approach. After such identification, a nutrigenomic approach was used to study the effects of the main human ellagitannin metabolites, urolithins A and B, on key pathways related to prostate carcinogenesis and progression.

5.1 Identification of walnut polyphenols and their antioxidant capacity

The identification of phenolic compounds in food matrixes is a complicated task when compared to supplements or drugs because of the wide variety of structures present in nature and the lack of standard polyphenols commercially available. Several methods have been used for the determination of polyphenols, such as capillary electrophoresis, gas chromatography, nuclear magnetic resonance, and, most commonly, high-performance liquid chromatography (HPLC) coupled to ultraviolet and mass spectrometry (Vallverdú-Queralt, 2010).

Using linear ion trap quadrupole-Orbitrap-mass spectrometry (LTQ-Orbitrap-MS), walnuts were found to contain a highly complex mixture of gallotannins, ellagitannins, flavonoids and phenolic acids. Our analytic approach allowed us to tentatively identify more than 100 individual phenolics. Corresponding molecular formulas, their MS/MS fragments, mass measurement errors and retention times are shown in Table 1 of Article I. Many of these compounds had been previously detected in walnuts. However, the high-resolution MS analyses revealed the presence of other polyphenols that have never been reported in walnuts before. **Major phenolic compounds found in walnut extracts belonged to the family of ellagitannins.** The polyphenol content determined by the Folin-Ciocalteu method ranged from 1,576 mg to 2,499 mg GAE per 100 g, which represents the seventh largest source of ETs in common foods and beverages (Vinson & Cai, 2012).

Using ABTS+ and DPPH assays we determined average values for antioxidant capacity in a walnut polyphenol extract, which were 21.4 ± 2.0 mmol TE/100g and 25.7 ± 2.1 mmol TE/100g respectively. This was in agreement to other authors (Vinson & Cai, 2012) who also

reported that walnuts showed high scavenging activities, much higher than other nuts, such as hazelnuts, almonds or peanuts. Therefore, **walnuts consolidate as an important food source of polyphenols with a significant antioxidant activity**.

Several studies have assessed the antioxidant capacity of ellagitannins and their impact on oxidative-stress and inflammation-induced disease, which are summarized in Figure D.1 (Hseu et al., 2012; Sudheer, Muthukumaran, Devipriya, & Menon, 2007). Oxidative stress can be defined as an imbalance between free radical and reactive metabolites, such as reactive oxygen species (ROS), production and their elimination. This lack of balance can lead to cell damage potentially creating an impact in an organism as a whole. Over the years, epidemiologic and observational evidence has encouraged belief in the use of bioactive compounds with antioxidant potential for disease prevention (Stanner, Hughes, Kelly, & Buttriss, 2007).

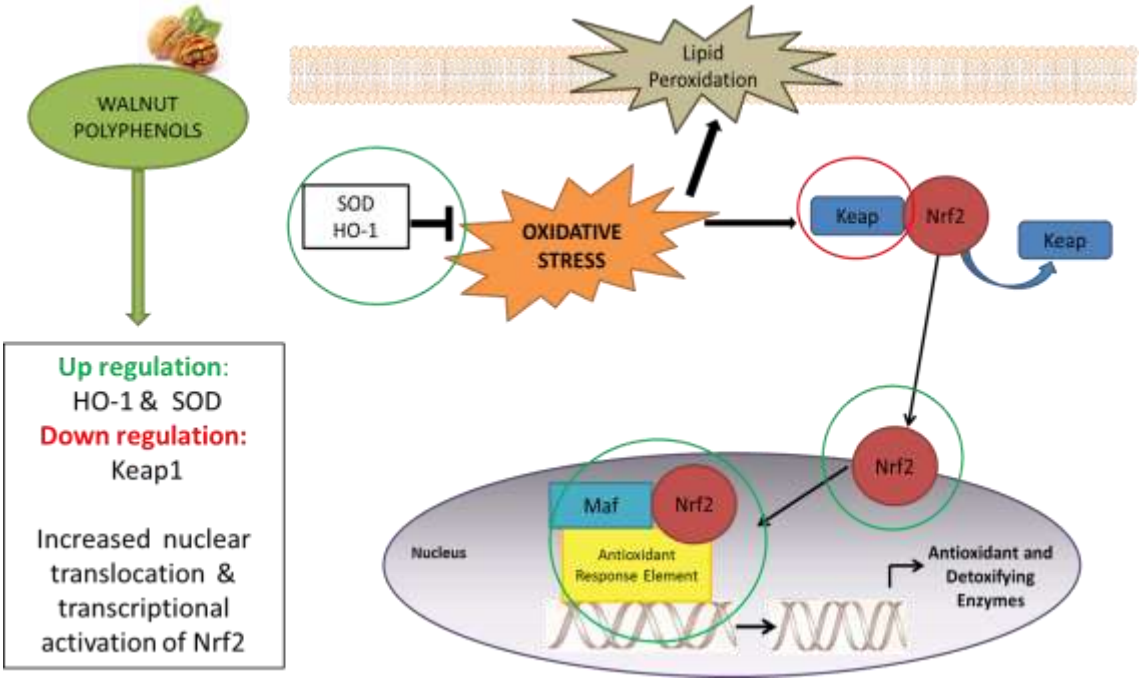

Figure D.1: Antioxidant activity of walnut polyphenols.

Several works have explored the antioxidant effects of ellagic acid, including, the role it may have in the modulation of the Keap1-Nrf2 pathway, a major regulator of cytoprotective responses to oxidative stress. In a study by Hseu et al. the antioxidant potential of ellagic acid was directly correlated with the increased expression of both heme oxygenase 1 (HO-1) and superoxide dismutase (SOD), which was followed by the down regulation of Keap1 (kelch-like ECH-associated protein 1) and the increased nuclear translocation and transcriptional activation of Nrf2 (nuclear factor erythroid 2-related factor 2) in HaCaT human keratocyte cells (Hseu et al., 2012). In addition, ellagic acid seemed to modulate lipid peroxidation index, severity in DNA damage and micronuclei number in nicotine-incubated lymphocytes (Sudheer et al., 2007). These results further confirm the role of ellagic acid in activating a response against oxidative stress.

The antioxidant capacity of ellagitannins is particularly promising due to the increasing evidence from epidemiological studies and large clinical prevention trials that suggest that oxidative stress and DNA damage play an important role in carcinogenesis (Bell & Hawthorne, 2008). Reactive oxygen species are generated during cell metabolism and it is thought that they mediate cytotoxicity by reacting with lipids, DNA and proteins to cause cell damage (Hussain, Hofseth, & Harris, 2003; Khan, Afaq, & Mukhtar, 2008). Moreover, research suggests that antioxidant levels have an inverse relationship with cancer incidence.

Unraveling links between diet and cancer is difficult since thousands of dietary components are consumed each day, a typical diet may provide more than 25,000 bioactive food compounds. This relationship is further complicated since a single bioactive compound can modify multiple processes in both normal and cancerous cells. To determine the contribution of our diet to cancer it is necessary to understand the biological processes related to cancer development. Nutrigenomics is a new approach that allows us to clarify the impact of dietary components and nutrition in the development and progression of diseases such as cancer.

Considering the intricate relationship between dietary bioactive compounds and cancer, we worked with a prostate cancer model and focused on the interaction of **urolithins A and B,**

with carcinogenic pathways in the prostate, including, androgen receptor function, cell cycle and apoptosis.

5.2 Androgen Receptor and Prostate Specific Antigen: key players in prostate carcinogenesis and development

For our first nutrigenomic approach we explored the role of urolithins A and UB in the modulation of the androgen receptor (AR) and prostate-specific antigen (PSA) in prostate cancer cells. Upon androgen binding, the AR translocates to the nucleus and binds to androgen response elements (AREs) within the regulatory regions of target genes. The specific combination of cofactors that are recruited to AREs provides for tissue- and ligand-specific gene expression. AR has a central role in the normal growth and development of the prostate gland, in prostate carcinogenesis and in androgen-dependent (AD) or androgen-independent (AI) progression of the disease (Koochekpour, 2010).

A staple characteristic of prostate cancer is the continual dependence on the AR for growth and survival. Patients with advanced prostate cancer initially benefit from androgen-ablation therapy, which leads to a decreased level of androgens and temporary tumor remission due to apoptosis of androgen-sensitive tumor cells. However, relapse of disease due to the growth of castrate-resistant tumors is frequently observed in patients, which makes the conventional hormone ablation therapy ineffective (Saxena et al., 2012). AR signaling is active in most castrate resistant prostate cancer (CRPC) or androgen independent prostate cancer. PSA, an AR-dependent gene, is widely used as a marker for disease activity. PSA declines after initiation of hormone depletion therapy and a subsequent rise is commonly the first sign of disease progression. In addition, it has also been proposed that PSA may directly participate in prostate cancer development, potentially by promoting AR signaling, although this potential interaction is still highly elusive (Altuwaijri, 2012). In our study (**article II**), there was a clear repression of PSA transcription caused by urolithins A and B, as well as a decrease in PSA protein levels. The aforementioned decrease in PSA levels upon treatment with urolithins correlated with the down-regulation of AR. The decrease in PSA and AR levels after incubation with urolithins is in agreement with the effects reported for other phenolic compounds, such as

epigallocatechin gallate (EGCG), grape seed procyanidins or caffeic acid (Lin, Jiang, & Chuu, 2012; Mantena et al., 2006; Ren, Zhang, Mitchell, Butler, & Young, 2000). In *in vitro* models, knockdown of AR results in cell death in both human and murine androgen independent-castration resistant prostate cancer cell lines (Chen, Sawyers, & Scher, 2008). In addition, several authors have reported that in androgen-dependent models, AR inhibition resulted in a marked decrease in cell proliferation as well (Kong et al., 2011; Oh & Lee, 2011). Thus, it is evident that both PSA and AR play a pivotal role in prostate cancer development and progression and the potential cross-talk between these two genes may have important implications as an additional aspect of AR function, contributing to both androgen-dependent and independent disease, and reinforce the potential relevance of PSA as a valid molecular target for prostate cancer therapy (Niu et al., 2008; Saxena et al., 2012). As such, a compound that can modulate the expression and activity of both AR and PSA, such as urolithins, could represent an important preventive approach against prostate carcinogenesis.

5.3 The hormone-disruptive role of urolithins

A possible manner by which urolithins could interfere with the aforementioned AR-PSA cross-talk is by displaying phytoestrogen-like activity. The modulation of hormone receptors by dietary components, such as isoflavones, has been widely studied (Bilal, Chowdhury, Davidson, & Whitehead, 2014; J. N. Davis, Kucuk, & Sarkar, 2002; Signorelli & Ghidoni, 2005). Some authors have compared urolithins with several phytoestrogens, such as genistein, daidzein, resveratrol and enterolactone, and have reported that urolithins modulate endocrine pathways labeling them as **phytoestrogens** (Larrosa et al., 2006). The estrogenic and anti-estrogenic activity induced by urolithins has been related to their interaction with the estrogen receptor (ER) in MCF-7 human breast cancer cells (Larrosa et al., 2006). Larrosa (2006) and colleagues performed structure analyses, which revealed that both urolithin A and B exhibited structural characteristics that made these molecules able to bind with the α- and β-estrogen receptors. However, phytoestrogens like genistein, do not only interact with the estrogen receptor but have also been shown to interact with the androgen receptor. In a prostate cancer model

(LNCaP cells) 12 hour incubation with genistein caused a decrease in AR levels, as well as a reduction in binding of nuclear proteins to a consensus ARE (J. N. Davis et al., 2002).

Considering all of the above, we explored whether urolithins were able to exert an effect over AR, similar to the effect induced by phytoestrogens. Transient transfections of PC-3 cells with a PSA promoter construct, containing functional AREs, resulted in an 83% increase in promoter activity upon incubation with DHT and this induction was blocked in the presence of urolithins. The reduced activation of PSA, an AR-regulated promoter, could be explained by the decrease in the binding of nuclear proteins to a consensus ARE. In our study, urolithins' modulatory actions over PSA levels were transcriptionally induced due to a direct effect on the PSA promoter. In this regard, the binding of nuclear proteins from urolithin A-treated cells to AREs was reduced by 86% in an LNCaP cell model as shown in EMSAs (**Article II**). An ER competitive binding assay performed by Larrosa and colleagues (2006) in MCF-7 cells showed that both urolithins had affinity for ERα and ERβ receptors, which could result in the inhibition of estradiol-ER binding and the subsequent binding to its response elements in the promoter region of target genes. These authors observed a higher binding affinity for urolithin A than for urolithin B, which is in agreement with our results in which a higher decrease in AR-ARE binding was observed upon incubation with UA when compared to UB. Therefore, given the decrease in AR expression levels and decreased AR-ARE binding, it would be plausible to conclude that urolithins interact with AR as well, displaying a modulatory effect over steroid receptors similar to isoflavones and other phytoestrogens.

In view of the aforementioned evidence it is possible to conclude that urolithins can play a key role in the modulation of hormone and hormone-receptor dependent diseases, such as breast and prostate cancers. The urolithin-hormone receptor interaction in prostate and breast cancer models proposed by ourselves and other authors (Larrosa et al., 2006; Sánchez-González et al., 2014) is summarized in Figure D.2.

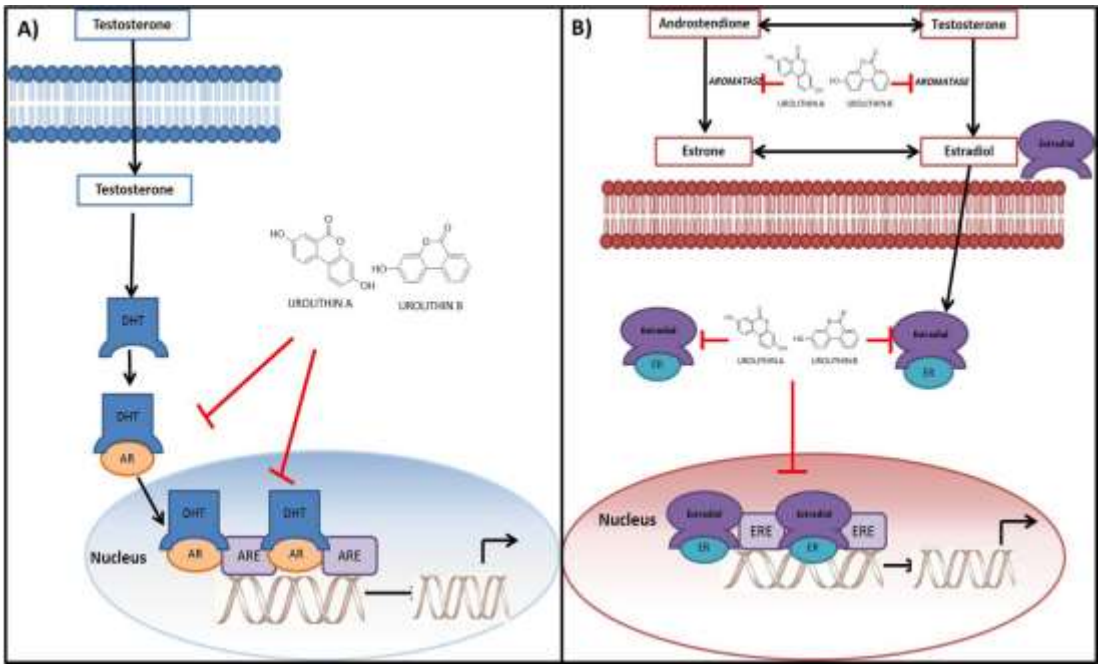

Figure D.2: Urolithin Interaction in hormone-dependent signaling in a) prostate and b) breast cancer.

5.4 AR and p21 interaction: Influence over cell cycle progression and apoptosis

Taking into account the results obtained in our previous study (**Article II**), in which urolithin A seemed to exert marked effects over expression and function, we decided to further explore the effect of this metabolite on genome expression in LNCaP prostate adenocarcinoma cells. To do so, **functional genomic analyses** were performed obtaining lists of differentially expressed genes. Using a Biological Association Network (BAN) analysis, the relationship among the differentially expressed genes was established. These interactions resulted in two main gene nodes, namely **CDKN1A** that encodes for **p21 protein**, which was overexpressed, and **FN-1** that encodes for the extracellular glycoprotein, fibronectin, which was underexpressed.

Ellagic acid has been reported to induce cell cycle arrest and/or apoptosis in several cancer cell lines. Suggested molecular targets for ellagic acid effects are amongst others NF-kβ, cyclin D1, p21 and p53, all involved in regulation of cell cycle and apoptosis (Fjaeraa & Nånberg, 2009). In view of the role that p21 has in human cancer development, its interaction with

ellagic acid (urolithin A precursor) and the BAN results, we validated its expression at mRNA and protein levels after urolithin A incubation. A significant up-regulation of p21 was observed by this bioactive compound. Thus, we decided to further explore the potential effect of this metabolite over cell cycle progression. P21 is a cell cycle arrest inductor that functions as both a sensor and an effector of multiple anti-proliferative signals. P21 inhibits cell cycle progression primarily through the inhibition of cyclin-dependent kinases resulting in G1 cell cycle arrest and a block in the transition to S phase (Piccolo & Crispi, 2012), as shown in Figure D.3. Accordingly, our results show that urolithin A caused an alteration in the cell cycle with an accumulation of cells in G1 and a reduction in S and G2.

The role of p21 in cancer is complex, among its well-known activities, p21 mediates p53-dependent G1 growth arrest, although recent evidence also indicates that p21 is an effector of multiple tumor suppressor pathways independent of p53 (Piccolo & Crispi, 2012). In CaSki cervical carcinoma cells, ellagic acid, the UA precursor, induced an elevation of p21 mRNA and protein levels, but no relevant increase level in p53 mRNA and protein levels were detected. These authors suggested the activation of p21 by ellagic acid could be either through a p53-independent mechanism or by a p53-dependent mechanism that does not involve changes in p53 protein levels (Narayanan, Geoffroy, Willingham, Re, & Nixon, 1999). Therefore, although p21 activation can depend on p53, it appears that the induction of p21 by ellagitannins is not dependent upon p53 levels.

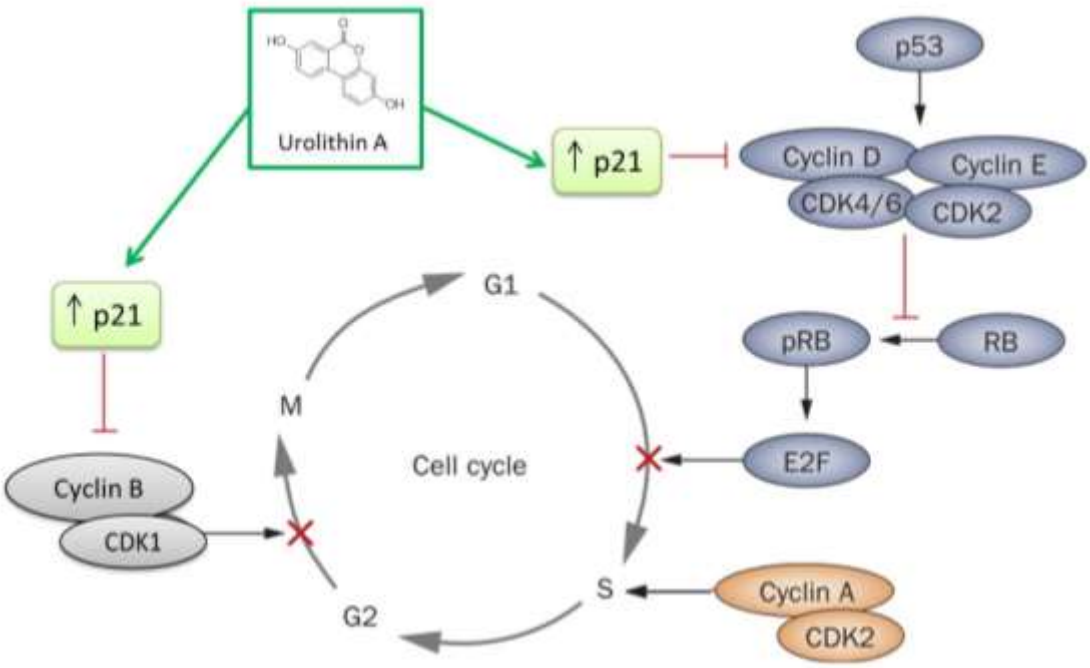

Figure D.3. p21 and urolithin interaction in cell cycle. Adapted from (Venkateswaran & Klotz, 2010).

A link between AR, PSA and p21 levels has been explored in a prostate cancer cell model through mechanistic studies (L. G. Wang, Ossowski, & Ferrari, 2001). Thus, it was of interest to study the role that urolithins might have in the possible interaction between these proteins. Wang et al. (2001) described that overexpression of AR was responsible for p21 silencing and possibly for creating resistance to apoptosis in advanced prostate cancer. AR regulation of cell survival or death depends on the nature of cellular context and extracellular stimuli. The pro-survival function of AR is mediated mainly by transcriptional regulation of its target genes. By contrast, the pro-death function of AR can be transcription-dependent or independent. Although the underlying death-promoting mechanism of AR is not completely understood (Y. Lin, Lu, Kokontis, & Xiang, 2013), it could be related to p21 levels. In the study by Wang et al. (2001), a 50% reduction in AR was accompanied by a 12-fold increase in p21 promoter activity in LNCaP cells. This inhibition of p21 by AR levels was ARE and androgen dependent, which might negatively impact the sensitivity to apoptosis. Although the study by Wang et al. (2001) was not performed using dietary bioactive compounds, their results can serve to associate our

previous observation that urolithin A caused a significant down-regulation of both PSA and AR levels and a decrease in binding of AR to ARE (**Article II**) with the increase in p21 levels observed in our second nutrigenomic study (**Article III**).

To further explore the modulation of p21 expression by urolithin A, we transfected the p21 promoter in LNCaP cells, and we observed an increase in promoter activity upon urolithin A incubation. It should be noted that unlike the inhibition of p21 by AR, which was ARE and androgen dependent, the induced up-regulation of p21-promoter activity was ARE-independent (L. G. Wang et al., 2001). Therefore, it is reasonable to conclude that urolithins may exert a dual effect in this AR-ARE-P21 interaction, first through AR and ARE inhibition and secondly, by increasing p21 levels through its transcriptional regulation.

Taking into consideration that the expression of several genes related to cell cycle progression and prostate cancer cell growth were modulated by urolithins, we examined if these metabolites could also provoke an increase in apoptosis. **Urolithins** did **induce apoptosis** in LNCaP cells, though this effect could be caused by a possible interaction in several pathways, first by decreasing the expression of AR target genes (such as PSA) thus inhibiting the pro-survival role of AR and secondly by increasing p21 levels. PSA is fundamental in the pathophysiology of prostate cancer. It stimulates oxidative stress in LNCaP and PC3 cells (Williams, Singh, Isaacs, & Denmeade, 2007), and it is also involved in tumor invasion and metastasis (Webber, Waghray, & Bello, 1995). Human tumors usually express high levels of the anti-apoptotic protein Bcl-2 and in prostate cancer its levels correlate with high levels of PSA (Altuwaijri, 2012). We explored if the pronounced decrease of AR and PSA levels upon urolithin incubation would result in an increase in apoptosis. Urolithins did cause an increase in apoptotic activity in LNCaP cells. Moreover, the increase in apoptosis upon incubation with urolithins was correlated with a decrease in the expression of Bcl-2. Bcl-2 is localized into the mitochondria, endoplasmic reticulum and the nuclear envelope, and it interferes with the activation of caspases by preventing the release of cytochrome c (M. H. Kang & Reynolds, 2009). Therefore, in our second nutrigenomic study (**Article III**), we measured caspase 3 and 7

activation to assess whether the decrease in Bcl-2 levels by UA could also promote the activity of these enzymes. An induction on caspase 3 and 7 was indeed observed after UA incubation.

In addition, as mentioned, some authors (L. G. Wang et al., 2001) have described that AR overexpression was responsible for p21 silencing and possibly for creating resistance to apoptosis in advanced prostate cancer. The induction of apoptotic activity could be linked to the multi-target effect of urolithins, which caused inhibition of PSA and AR and an increase in p21 levels, this resulted in decreased Bcl-2 levels and increased caspase 3 and 7 activities. The effect of urolithins on apoptosis is summarized in Figure D.4 shown below.

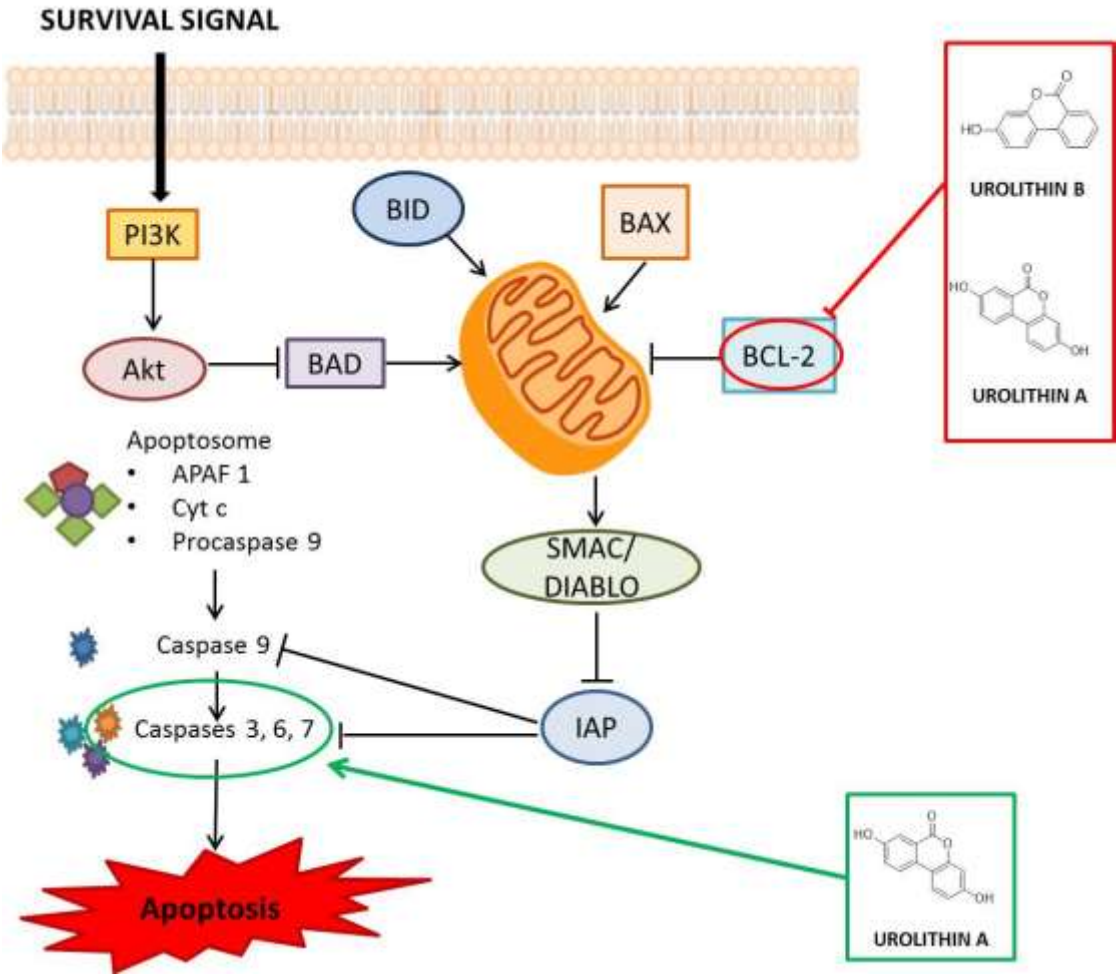

Figure D.4: Urolithin interaction with effectors of the apoptotic pathway. Adapted from (Igney & Krammer, 2002).

In summary, the results obtained in this work expose novel findings on the effect **urolithins** have over the expression of a **wide array of genes** involved in **prostate cancer** development and progression. In particular, urolithin A and urolithin B reduced PSA and AR levels possibly due to a decreased binding of the AR to AREs, as well as decreased levels of AR resulting in PSA transcription inhibition. Additionally, urolithin A exerts chemo-preventive effects which include the inhibition of cell proliferation and cell cycle progression through the up-regulation of p21, thus inhibiting cyclin dependent kinases, and the induction of apoptosis, coupled to Bcl-2 inhibition and caspase 3 activation. It is evident that **walnut ellagitannins** like other phytochemicals **work through multiple targeted pathways**. The results obtained by our *in vitro* approaches, in addition to the observed effects by other authors, warrant further analyses of the role that ellagitannins could have in cancer prevention using *in vivo* studies and human trials.

Our results provide new insights in the effect that metabolites of a common dietary component have on molecular mechanisms involved in prostate carcinogenesis, which could in turn provide a foundation for developing strategies for disease prevention. The effect of dietary agents in cancer can be used to identify molecular therapeutic targets, and used as part of a chemo-preventive strategy. Dietary intervention targeting multiple pathways might, therefore, be an effective therapeutic approach, either alone, or in conjunction with targeted pharmaceutical agents.

6. CONCLUSIONS

1. An analytical methodology for the determination of polyphenols in walnuts using HPLC-MS has been developed, which has allowed the identification of 120 compounds, mainly hydrolysable and condensed tannins, flavonoids and phenolic acids. The MS analyses revealed the presence of eight polyphenols that have never been reported before in walnuts: stenophyllanin C, malabathrin A, eucalbanin A, cornusiin B, heterophylliin E, pterocarinin B, reginin A and alienanin B.

2. The average polyphenol content in walnut extracts is 2,464 ± 22 mg GAE/ 100 g according to the Folin-Ciocalteau method, with an antioxidant capacity of 25.7 ± 2.1 mmol TE/100 g by the DPPH method and 21.4 ± 2.0 mmol TE/100 g as determined by the $ABTS^{+}$ method. Therefore, walnuts would represent the seventh largest source of ETs in common foods and beverages.

3. Urolithins A and B induced a reduction of PSA (prostate specific antigen) and AR (androgen receptor) levels in LNCaP cells. This effect could be due to the decrease in binding of AR to androgen response elements (AREs), and to the down regulation of AR levels resulting in the inhibition of PSA transcription.

4. PSA transcriptional activation is modulated by urolithin A and B, through the inhibition of the agonist activity of dehydrotestosterone (DHT) on the PSA promoter, possibly due to the decreased binding of AR to the AREs present in this promoter.

5. Urolithins A and B induced apoptosis in LNCaP cells, probably due to the down-regulation of Bcl-2 protein levels and the increase in caspase 3 and 7 activities, caused specifically by urolithin A.

6. Two main gene nodes have been identified after performing a biological association network (BAN) upon LNCaP cell treatment with urolithin A: CDKN1A (encoding for p21 protein) which was overexpressed and FN-1 (encoding for the extracellular glycoprotein, fibronectin), which was underexpressed.

7. Urolithin A caused the activation of p21 promoter in LNCaP cells, possibly due to its interaction with the AR-ARE dimer. Furthermore urolithin A induced an alteration in the cell cycle with an accumulation of cells in G1 and a reduction in S and G2 phases.

8. The effect of urolithin A on tumor cell survival is probably multifactorial, including the inhibition of cell proliferation and cell cycle progression through the up-regulation of p21, the down-regulation of fibronectin and the induction of apoptosis.

9. In summary, it has been shown that urolithins A and B, major polyphenol metabolites of walnuts, modulate the expression of a wide array of genes involved in prostate cancer development, progression and metastasis. A diet high in ellagitannins-rich foods, such as walnuts, would provide a considerable intake of pedunculagin and its metabolites, urolithins, which could contribute to the prevention of prostate cancer.

7. BIBLIOGRAPHY

Abe, L., Lajolo, F., & Genovese, M. (2010). Comparison of phenol content and antioxidant capacity of nuts. *Ciência E Tecnologia de Alimentos*, *30*(Supl 1), 254–259. Retrieved from http://www.scielo.br/scielo.php?pid=S0101-20612010000500038&script=sci_arttext

Afman, L., & Müller, M. (2006). Nutrigenomics: from molecular nutrition to prevention of disease. *Journal of the American Dietetic Association*, *106*(4), 569–76. doi:10.1016/j.jada.2006.01.001

Alshatwi, A. a, Hasan, T. N., Shafi, G., Syed, N. A., Al-Assaf, A. H., Alamri, M. S., & Al-Khalifa, A. S. (2012). Validation of the Antiproliferative Effects of Organic Extracts from the Green Husk of Juglans regia L. on PC-3 Human Prostate Cancer Cells by Assessment of Apoptosis-Related Genes. *Evidence-Based Complementary and Alternative Medicine : eCAM*, *2012*, 103026. doi:10.1155/2012/103026

Altuwaijri, S. (2012). Role of Prostate Specific Antigen (PSA) in Pathogenesis of Prostate Cancer. *Journal of Cancer Therapy*, *03*(04), 331–336. doi:10.4236/jct.2012.34043

American Cancer Society. (2011). Cancer Facts & Figures 2011. *American Cancer Society*, 9–18.

Anari, M. R., Sanchez, R. I., Bakhtiar, R., Franklin, R. B., & Baillie, T. a. (2004). Integration of knowledge-based metabolic predictions with liquid chromatography data-dependent tandem mass spectrometry for drug metabolism studies: application to studies on the biotransformation of indinavir. *Analytical Chemistry*, *76*(3), 823–32. doi:10.1021/ac034980s

Andrews, N. C., & Faller, D. V. (1991). A rapid micropreparation technique for extraction of DNA-binding proteins from limiting numbers of mammalian cells. *Nucleic Acids Research*, *19*(9), 2499. Retrieved from http://www.pubmedcentral.nih.gov/articlerender.fcgi?artid=329467&tool=pmcentrez&rendertype=abstract

Bell, C., & Hawthorne, S. (2008). Ellagic acid, pomegranate and prostate cancer -- a mini review. *The Journal of Pharmacy and Pharmacology*, *60*(2), 139–44. doi:10.1211/jpp.60.2.0001

Biesalski, H.-K., Dragsted, L. O., Elmadfa, I., Grossklaus, R., Müller, M., Schrenk, D., … Weber, P. (2009). Bioactive compounds: definition and assessment of activity. *Nutrition*, *25*(11-12), 1202–5. doi:10.1016/j.nut.2009.04.023

Bilal, I., Chowdhury, A., Davidson, J., & Whitehead, S. (2014). Phytoestrogens and prevention of breast cancer: The contentious debate. *World Journal of Clinical Oncology*, *5*(4), 705–12. doi:10.5306/wjco.v5.i4.705

Cerdá, B., Periago, P., Espín, J. C., & Tomás-Barberán, F. A. (2005). Identification of urolithin a as a metabolite produced by human colon microflora from ellagic acid and related

compounds. *Journal of Agricultural and Food Chemistry*, *53*(14), 5571–6. doi:10.1021/jf050384i

Chen, Y., Sawyers, C., & Scher, H. (2008). Targeting the androgen receptor pathway in prostate cancer. *Current Opinion in Pharmacology*, *8*(4), 440–448. doi:10.1016/j.coph.2008.07.005.Targeting

Corona, G., Deiana, M., Incani, A., Vauzour, D., Dessì, M. A., & Spencer, J. P. E. (2007). Inhibition of p38/CREB phosphorylation and COX-2 expression by olive oil polyphenols underlies their anti-proliferative effects. *Biochemical and Biophysical Research Communications*, *362*(3), 606–11. doi:10.1016/j.bbrc.2007.08.049

Corona, G., Deiana, M., Incani, A., Vauzour, D., Dessì, M. A., & Spencer, J. P. E. (2009). Hydroxytyrosol inhibits the proliferation of human colon adenocarcinoma cells through inhibition of ERK1/2 and cyclin D1. *Molecular Nutrition & Food Research*, *53*(7), 897–903. doi:10.1002/mnfr.200800269

Daniel, E. M., Kfcjpnick, A. S., Heur, Y., Blinzler, J. A., Nims, R. W., & Stoner, G. D. (1989). Extraction , Stability , and Quantitation of Ellagic Acid in Various Fruits and Nuts, *349*, 338–349.

Davis, J. N., Kucuk, O., & Sarkar, F. H. (2002). Expression of prostate-specific antigen is transcriptionally regulated by genistein in prostate cancer cells. *Molecular Carcinogenesis*, *34*(2), 91–101. doi:10.1002/mc.10053

Davis, P. a, Vasu, V. T., Gohil, K., Kim, H., Khan, I. H., Cross, C. E., & Yokoyama, W. (2012). A high-fat diet containing whole walnuts (Juglans regia) reduces tumour size and growth along with plasma insulin-like growth factor 1 in the transgenic adenocarcinoma of the mouse prostate model. *The British Journal of Nutrition*, *108*(10), 1764–72. doi:10.1017/S0007114511007288

DeBusk, R. M., Fogarty, C. P., Ordovas, J. M., & Kornman, K. S. (2005). Nutritional genomics in practice: where do we begin? *Journal of the American Dietetic Association*, *105*(4), 589–98. doi:10.1016/j.jada.2005.01.002

Duthie, S. J., & Dobson, V. L. (1999). Dietary flavonoids protect human colonocyte DNA from oxidative attack in vitro. *European Journal of Nutrition*, *38*(1), 28–34. Retrieved from http://www.ncbi.nlm.nih.gov/pubmed/10338685

Elliot, R., & Ong, T. J. (2002). Nutritional genomics. *BMJ*, *324*, 1438–1432. Retrieved from http://www.annualreviews.org/doi/abs/10.1146/annurev.genom.5.061903.180008

Espín, J. C., González-Barrio, R., Cerdá, B., López-Bote, C., Rey, A. I., & Tomás-Barberán, F. a. (2007). Iberian pig as a model to clarify obscure points in the bioavailability and

metabolism of ellagitannins in humans. *Journal of Agricultural and Food Chemistry*, *55*(25), 10476–85. doi:10.1021/jf0723864

Espín, J. C., Larrosa, M., García-Conesa, M. T., & Tomás-Barberán, F. (2013). Biological significance of urolithins, the gut microbial ellagic Acid-derived metabolites: the evidence so far. *Evidence-Based Complementary and Alternative Medicine : eCAM*, *2013*(Figure 1), 270418. doi:10.1155/2013/270418

Fabiani, R., De Bartolomeo, a, Rosignoli, P., Servili, M., Montedoro, G. F., & Morozzi, G. (2002). Cancer chemoprevention by hydroxytyrosol isolated from virgin olive oil through G1 cell cycle arrest and apoptosis. *European Journal of Cancer Prevention : The Official Journal of the European Cancer Prevention Organisation (ECP)*, *11*(4), 351–8. Retrieved from http://www.ncbi.nlm.nih.gov/pubmed/12195161

Ferguson, L. R. (2009). Nutrigenomics approaches to functional foods. *Journal of the American Dietetic Association*, *109*(3), 452–8. doi:10.1016/j.jada.2008.11.024

Fini, L., Hotchkiss, E., Fogliano, V., Graziani, G., Romano, M., De Vol, E. B., … Ricciardiello, L. (2008). Chemopreventive properties of pinoresinol-rich olive oil involve a selective activation of the ATM-p53 cascade in colon cancer cell lines. *Carcinogenesis*, *29*(1), 139–46. doi:10.1093/carcin/bgm255

Fjaeraa, C., & Nånberg, E. (2009). Effect of ellagic acid on proliferation, cell adhesion and apoptosis in SH-SY5Y human neuroblastoma cells. *Biomedicine & Pharmacotherapy = Biomédecine & Pharmacothérapie*, *63*(4), 254–61. doi:10.1016/j.biopha.2008.07.093

Flamini, R. (2003). Mass spectrometry in grape and wine chemistry. Part I: Polyphenols. *Mass Spectrometry Reviews*, *22*(4), 218–250. doi:10.1002/mas.10052

François, I., Sandra, K., & Sandra, P. (2009). Comprehensive liquid chromatography: fundamental aspects and practical considerations--a review. *Analytica Chimica Acta*, *641*(1-2), 14–31. doi:10.1016/j.aca.2009.03.041

Fukuda, T. (2009). Walnut polyphenols: Structures and functions. *Tree Nuts: Composition, Phytochemicals, and Health …*. Retrieved from http://books.google.com/books?hl=en&lr=&id=Uu4nzKx74noC&oi=fnd&pg=PA305&dq=Walnut+Polyphenols:+Structures+and+Functions&ots=H7i5MPzCS1&sig=oXsI6romL79K9m2PMOXa-cCRWyE

Garcia-Muñoz, C., & Vaillant, F. (2014). Metabolic fate of ellagitannins: implications for health, and research perspectives for innovative functional foods. *Critical Reviews in Food Science and Nutrition*, *54*(12), 1584–98. doi:10.1080/10408398.2011.644643

Garg, A. K., Buchholz, T. A., & Aggarwal, B. B. (2005). Chemosensitization and radiosensitization of tumors by plant polyphenols. *Antioxidants & Redox Signaling*, *7*(55), 1630–1647. Retrieved from http://online.liebertpub.com/doi/abs/10.1089/ars.2005.7.1630

Gillies, P. J. (2003). Nutrigenomics: The Rubicon of molecular nutrition. *Journal of the American Dietetic Association*, *103*(12 SUPPL.), 50–55. doi:10.1016/j.jada.2003.09.037

Gómez-Caravaca, A. M., Verardo, V., Segura-Carretero, A., Caboni, M. F., & Fernández-Gutiérrez, A. (2008). Development of a rapid method to determine phenolic and other polar compounds in walnut by capillary electrophoresis-electrospray ionization time-of-flight mass spectrometry. *Journal of Chromatography. A*, *1209*(1-2), 238–45. doi:10.1016/j.chroma.2008.08.117

González-Sarrías, A., Giménez-Bastida, J. a, García-Conesa, M. T., Gómez-Sánchez, M. B., García-Talavera, N. V, Gil-Izquierdo, A., … Espín, J. C. (2010). Occurrence of urolithins, gut microbiota ellagic acid metabolites and proliferation markers expression response in the human prostate gland upon consumption of walnuts and pomegranate juice. *Molecular Nutrition & Food Research*, *54*(3), 311–22. doi:10.1002/mnfr.200900152

González-Sarrías, A., Giménez-Bastida, J. A., Núñez-Sánchez, M. A., Larrosa, M., García-Conesa, M. T., Tomás-Barberán, F. a, & Espín, J. C. (2013). Phase-II metabolism limits the antiproliferative activity of urolithins in human colon cancer cells. *European Journal of Nutrition*. doi:10.1007/s00394-013-0589-4

Granci, V., Dupertuis, Y. M., & Pichard, C. (2010). Angiogenesis as a potential target of pharmaconutrients in cancer therapy. *Current Opinion in Clinical Nutrition and Metabolic Care*, *13*(4), 417–22. doi:10.1097/MCO.0b013e3283392656

Heber, D. (2008). Multitargeted therapy of cancer by ellagitannins. *Cancer Letters*, *269*(2), 262–8. doi:10.1016/j.canlet.2008.03.043

Hocquette, J. (2005). Where are we in genomics? *Journal of Physiology and Pharmacology*, 37–70. Retrieved from http://www.jpp.krakow.pl/journal/archive/06_05_s3/pdf/37_06_05_s3_article.pdf

Hooft, J. van der, & Vos, R. de. (2012). Structural elucidation and quantification of phenolic conjugates present in human urine after tea intake. *Analytical …*, (i). Retrieved from http://pubs.acs.org/doi/abs/10.1021/ac3017339

Hseu, Y.-C., Chou, C.-W., Senthil Kumar, K. J., Fu, K.-T., Wang, H.-M., Hsu, L.-S., … Yang, H.-L. (2012). Ellagic acid protects human keratinocyte (HaCaT) cells against UVA-induced oxidative stress and apoptosis through the upregulation of the HO-1 and Nrf-2 antioxidant genes. *Food and Chemical Toxicology : An International Journal Published for the British Industrial Biological Research Association*, *50*(5), 1245–55. doi:10.1016/j.fct.2012.02.020

Hussain, S. P., Hofseth, L. J., & Harris, C. C. (2003). Radical causes of cancer. *Nature Reviews. Cancer*, *3*(4), 276–85. doi:10.1038/nrc1046

Ignat, I., Volf, I., & Popa, V. I. (2011). A critical review of methods for characterisation of polyphenolic compounds in fruits and vegetables. *Food Chemistry*, *126*(4), 1821–1835. doi:10.1016/j.foodchem.2010.12.026

Igney, F. H., & Krammer, P. H. (2002). Death and anti-death: tumour resistance to apoptosis. *Nature Reviews. Cancer*, *2*(4), 277–288. doi:10.1038/nrc776

Kang, M. H., & Reynolds, C. P. (2009). Bcl-2 inhibitors: targeting mitochondrial apoptotic pathways in cancer therapy. *Clinical Cancer Research : An Official Journal of the American Association for Cancer Research*, *15*(4), 1126–32. doi:10.1158/1078-0432.CCR-08-0144

Kang, N. J., Shin, S. H., Lee, H. J., & Lee, K. W. (2011). Polyphenols as small molecular inhibitors of signaling cascades in carcinogenesis. *Pharmacology & Therapeutics*, *130*(3), 310–24. doi:10.1016/j.pharmthera.2011.02.004

Karakaya, S. (2004). Bioavailability of phenolic compounds. *Critical Reviews in Food Science and Nutrition*, *44*(6), 453–64. doi:10.1080/10408690490886683

Kasimsetty, S. G., Bialonska, D., Reddy, M. K., Thornton, C., Willett, K. L., & Ferreira, D. (2009). Effects of pomegranate chemical constituents/intestinal microbial metabolites on CYP1B1 in 22Rv1 prostate cancer cells. *Journal of Agricultural and Food Chemistry*, *57*(22), 10636–44. doi:10.1021/jf902716r

Khan, N., Afaq, F., & Mukhtar, H. (2008). Cancer chemoprevention through dietary antioxidants: progress and promise. *Antioxidants & Redox Signaling*, *10*(3), 475–510. doi:10.1089/ars.2007.1740

Khan, N., & Mukhtar, H. (2013). Modulation of signaling pathways in prostate cancer by green tea polyphenols. *Biochemical Pharmacology*, *85*(5), 667–72. doi:10.1016/j.bcp.2012.09.027

Kong, L., Yuan, Q., Zhu, H., Li, Y., Guo, Q., Wang, Q., … Gao, X. (2011). The suppression of prostate LNCaP cancer cells growth by Selenium nanoparticles through Akt/Mdm2/AR controlled apoptosis. *Biomaterials*, *32*(27), 6515–22. doi:10.1016/j.biomaterials.2011.05.032

Koochekpour, S. (2010). Androgen receptor signaling and mutations in prostate cancer. *Asian Journal of Andrology*, *12*(5), 639–57. doi:10.1038/aja.2010.89

Kussmann, M., Raymond, F., & Affolter, M. (2006). OMICS-driven biomarker discovery in nutrition and health. *Journal of Biotechnology*, *124*(4), 758–87. doi:10.1016/j.jbiotec.2006.02.014

Lamuela-Raventos, R. M. (2014). *Chapter. Improved Characterization of Polyphenols Using Liquid Chromatography*. doi:10.1016/B978-0-12-397934-6.00014-0

Landete, J. M. (2011). Ellagitannins, ellagic acid and their derived metabolites: A review about source, metabolism, functions and health. *Food Research International*, *44*(5), 1150–1160. doi:10.1016/j.foodres.2011.04.027

Larrosa, M., González-Sarrías, A., García-Conesa, M. T., Tomás-Barberán, F. a, & Espín, J. C. (2006). Urolithins, ellagic acid-derived metabolites produced by human colonic microflora, exhibit estrogenic and antiestrogenic activities. *Journal of Agricultural and Food Chemistry*, *54*(5), 1611–20. doi:10.1021/jf0527403

Lattouf, J., & Srinivasan, R. (2006). Mechanisms of disease: the role of heat-shock protein 90 in genitourinary malignancy. *Nature Clinical Practice …*, *3*(11), 590–601. doi:10.1038/ncpuro0604

Lin, H.-P., Jiang, S. S., & Chuu, C.-P. (2012). Caffeic acid phenethyl ester causes p21 induction, Akt signaling reduction, and growth inhibition in PC-3 human prostate cancer cells. *PloS One*, *7*(2), e31286. doi:10.1371/journal.pone.0031286

Lin, Y., Lu, Z., Kokontis, J., & Xiang, J. (2013). Androgen receptor primes prostate cancer cells to apoptosis through down-regulation of basal p21 expression. *Biochemical and Biophysical Research Communications*, *430*(1), 289–93. doi:10.1016/j.bbrc.2012.10.135

Magiera, S., Baranowska, I., & Kusa, J. (2012). Development and validation of UHPLC-ESI-MS/MS method for the determination of selected cardiovascular drugs, polyphenols and their metabolites in human urine. *Talanta*, *89*, 47–56. doi:10.1016/j.talanta.2011.11.055

Mantena, S. K., Baliga, M. S., & Katiyar, S. K. (2006). Grape seed proanthocyanidins induce apoptosis and inhibit metastasis of highly metastatic breast carcinoma cells. *Carcinogenesis*, *27*(8), 1682–91. doi:10.1093/carcin/bgl030

Marston, A., & Hostettmann, K. (2009). Natural product analysis over the last decades. *Planta Medica*, *75*(7), 672–82. doi:10.1055/s-0029-1185379

Meda, R. N. T., Vlase, L., Lamien-Meda, a, Lamien, C. E., Muntean, D., Tiperciuc, B., … Nacoulma, O. G. (2011). Identification and quantification of phenolic compounds from Balanites aegyptiaca (L) Del (Balanitaceae) galls and leaves by HPLC-MS. *Natural Product Research*, *25*(2), 93–9. doi:10.1080/14786419.2010.482933

Merken, H. M., & Beecher, G. R. (2000). Measurement of food flavonoids by high-performance liquid chromatography: A review. *Journal of Agricultural and Food Chemistry*, *48*(3), 577–99. Retrieved from http://www.ncbi.nlm.nih.gov/pubmed/10725120

Mertens-Talcott, S. U., Jilma-Stohlawetz, P., Rios, J., Hingorani, L., & Derendorf, H. (2006). Absorption, metabolism, and antioxidant effects of pomegranate (Punica granatum l.) polyphenols after ingestion of a standardized extract in healthy human volunteers. *Journal of Agricultural and Food Chemistry*, *54*(23), 8956–61. doi:10.1021/jf061674h

Mikulic-Petkovsek, M., Slatnar, A., Stampar, F., & Veberic, R. (2012). HPLC-MSn identification and quantification of flavonol glycosides in 28 wild and cultivated berry species. *Food Chemistry*, *135*(4), 2138–46. doi:10.1016/j.foodchem.2012.06.115

Minoggio, M., Bramati, L., Simonetti, P., Gardana, C., Iemoli, L., Santangelo, E., … Pietta, P. G. (2003). Polyphenol pattern and antioxidant activity of different tomato lines and cultivars. *Annals of Nutrition and Metabolism*, *47*(2), 64–69. doi:10.1159/000069277

Mutch, D. M., Wahli, W., & Williamson, G. (2005). Nutrigenomics and nutrigenetics: the emerging faces of nutrition. *FASEB Journal : Official Publication of the Federation of American Societies for Experimental Biology*, *19*(12), 1602–16. doi:10.1096/fj.05-3911rev

Naiki-Ito, A., Chewonarin, T., Tang, M., Pitchakarn, P., Kuno, T., Ogawa, K., … Takahashi, S. (2015). Ellagic acid, a component of pomegranate fruit juice, suppresses androgen-dependent prostate carcinogenesis via induction of apoptosis. *The Prostate*, *75*(2), 151–60. doi:10.1002/pros.22900

Narayanan, B. A., Geoffroy, O., Willingham, M. C., Re, G. G., & Nixon, D. W. (1999). p53/p21(WAF1/CIP1) expression and its possible role in G1 arrest and apoptosis in ellagic acid treated cancer cells. *Cancer Letters*, *136*(2), 215–21. Retrieved from http://www.ncbi.nlm.nih.gov/pubmed/10355751

Niemetz, R., & Gross, G. G. (2005). Enzymology of gallotannin and ellagitannin biosynthesis. *Phytochemistry*, *66*(17), 2001–11. doi:10.1016/j.phytochem.2005.01.009

Niu, Y., Yeh, S., Miyamoto, H., Li, G., Altuwaijri, S., Yuan, J., … Chang, C. (2008). Tissue prostate-specific antigen facilitates refractory prostate tumor progression via enhancing ARA70-regulated androgen receptor transactivation. *Cancer Research*, *68*(17), 7110–9. doi:10.1158/0008-5472.CAN-07-6507

Oh, H. L., & Lee, C.-H. (2011). HY251, a novel decahydrocyclopenta[a]indene analog, from Aralia continentalis induces apoptosis via down-regulation of AR expression in human prostate cancer LNCaP cells. *Bioorganic & Medicinal Chemistry Letters*, *21*(5), 1347–9. doi:10.1016/j.bmcl.2011.01.045

Ommen, B. Van, & Stierum, R. (2002). Nutrigenomics: exploiting systems biology in the nutrition and health arena. *Current Opinion in Biotechnology*, 517–521. Retrieved from http://www.sciencedirect.com/science/article/pii/S095816690200349X

Owen, R. W., Giacosa, A., Hull, W. E., Haubner, R., Spiegelhalder, B., & Bartsch, H. (2000). The antioxidant/anticancer potential of phenolic compounds isolated from olive oil. *European Journal of Cancer*, *36*(10), 1235–47. Retrieved from http://www.ncbi.nlm.nih.gov/pubmed/10882862

Peterman, S. M., Duczak, N., Kalgutkar, A. S., Lame, M. E., & Soglia, J. R. (2006). Application of a linear ion trap/orbitrap mass spectrometer in metabolite characterization studies: examination of the human liver microsomal metabolism of the non-tricyclic anti-depressant nefazodone using data-dependent accurate mass measurements. *Journal of the American Society for Mass Spectrometry*, *17*(3), 363–75. doi:10.1016/j.jasms.2005.11.014

Piccolo, M., & Crispi, S. (2012). The Dual Role Played by p21 May Influence the Apoptotic or Anti-Apoptotic Fate in Cancer. *Journal of Cancer Research Updates*, 189–202. Retrieved from http://lifescienceglobal.com/pms/index.php/jcru/article/view/613

Qiu, Z., Zhou, B., Jin, L., Yu, H., Liu, L., Liu, Y., … Zhu, F. (2013). In vitro antioxidant and antiproliferative effects of ellagic acid and its colonic metabolite, urolithins, on human bladder cancer T24 cells. *Food and Chemical Toxicology : An International Journal Published for the British Industrial Biological Research Association*, *59*, 428–37. doi:10.1016/j.fct.2013.06.025

Quideau, S., & Feldman, K. S. (1996). Ellagitannin Chemistry. *Chemical Reviews*, *96*(1), 475–504. doi:10.1021/cr940716a

Regueiro, J., Sánchez-González, C., Vallverdú-Queralt, A., Simal-Gándara, J., Lamuela-Raventós, R., & Izquierdo-Pulido, M. (2014). Comprehensive identification of walnut polyphenols by liquid chromatography coupled to linear ion trap-Orbitrap mass spectrometry. *Food Chemistry*, *152*, 340–8. doi:10.1016/j.foodchem.2013.11.158

Ren, F., Zhang, S., Mitchell, S. H., Butler, R., & Young, C. Y. (2000). Tea polyphenols down-regulate the expression of the androgen receptor in LNCaP prostate cancer cells. *Oncogene*, *19*(15), 1924–32. doi:10.1038/sj.onc.1203511

Rocha, A., Wang, L., Penichet, M., & Martins-Green, M. (2012). Pomegranate juice and specific components inhibit cell and molecular processes critical for metastasis of breast cancer. *Breast Cancer Research and Treatment*, *136*(3), 647–58. doi:10.1007/s10549-012-2264-5

Rodríguez, L., Villalobos, X., Dakhel, S., Padilla, L., Hervas, R., Hernández, J. L., … Noé, V. (2013). Polypurine reverse Hoogsteen hairpins as a gene therapy tool against survivin in human

prostate cancer PC3 cells in vitro and in vivo. *Biochemical Pharmacology*, *86*(11), 1541–1554. Retrieved from http://www.sciencedirect.com/science/article/pii/S0006295213006035

Sánchez-González, C., Ciudad, C. J., Noé, V., & Izquierdo-Pulido, M. (2014). Walnut polyphenol metabolites, urolithins A and B, inhibit the expression of the prostate-specific antigen and the androgen receptor in prostate cancer cells. *Food & Function*, *5*(11), 2922–30. doi:10.1039/c4fo00542b

Saxena, P., Trerotola, M., Wang, T., Li, J., Sayeed, A., Vanoudenhove, J., … Languino, L. R. (2012). PSA regulates androgen receptor expression in prostate cancer cells. *The Prostate*, *72*(7), 769–76. doi:10.1002/pros.21482

Schoonjans, V., Questier, F., Massart, D. L., & Borosy, a. P. (2000). Use of mass spectrometry for assessing similarity/diversity of natural products with unknown chemical structures. *Journal of Pharmaceutical and Biomedical Analysis*, *21*(6), 1197–1214. doi:10.1016/S0731-7085(99)00236-8

Schrijvers, D. (2007). Androgen-independent prostate cancer. *Prostate Cancer*, *1*(October), 34–45. Retrieved from http://link.springer.com/chapter/10.1007/978-3-540-40901-4_14

Seeram, N. P., Aronson, W. J., Zhang, Y., Henning, S. M., Moro, A., Lee, R.-P., … Heber, D. (2007). Pomegranate ellagitannin-derived metabolites inhibit prostate cancer growth and localize to the mouse prostate gland. *Journal of Agricultural and Food Chemistry*, *55*(19), 7732–7. doi:10.1021/jf071303g

Seeram, N. P., Lee, R., & Heber, D. (2004). Bioavailability of ellagic acid in human plasma after consumption of ellagitannins from pomegranate (Punica granatum L.) juice. *Clinica Chimica Acta; International Journal of Clinical Chemistry*, *348*(1-2), 63–8. doi:10.1016/j.cccn.2004.04.029

Selga, E., Morales, C., Noé, V., Peinado, M. a, & Ciudad, C. J. (2008). Role of caveolin 1, E-cadherin, Enolase 2 and PKCalpha on resistance to methotrexate in human HT29 colon cancer cells. *BMC Medical Genomics*, *1*, 35. doi:10.1186/1755-8794-1-35

Selga, E., Oleaga, C., Ramírez, S., de Almagro, M. C., Noé, V., & Ciudad, C. J. (2009). Networking of differentially expressed genes in human cancer cells resistant to methotrexate. *Genome Medicine*, *1*(9), 83. doi:10.1186/gm83

Signorelli, P., & Ghidoni, R. (2005). Resveratrol as an anticancer nutrient: molecular basis, open questions and promises. *The Journal of Nutritional Biochemistry*, *16*(8), 449–66. doi:10.1016/j.jnutbio.2005.01.017

Stacewicz-Sapuntzakis, M., Borthakur, G., Burns, J. L., & Bowen, P. E. (2008). Correlations of dietary patterns with prostate health. *Molecular Nutrition & Food Research*, *52*(1), 114–30. doi:10.1002/mnfr.200600296

Stanner, S., Hughes, J., Kelly, C., & Buttriss, J. (2007). A review of the epidemiological evidence for the "antioxidant hypothesis." *Public Health Nutrition*, *7*(03), 407–422. doi:10.1079/PHN2003543

Sudheer, A. R., Muthukumaran, S., Devipriya, N., & Menon, V. P. (2007). Ellagic acid, a natural polyphenol protects rat peripheral blood lymphocytes against nicotine-induced cellular and DNA damage in vitro: with the comparison of N-acetylcysteine. *Toxicology*, *230*(1), 11–21. doi:10.1016/j.tox.2006.10.010

Tamburrino, L., Salvianti, F., Marchiani, S., Pinzani, P., Nesi, G., Serni, S., … Baldi, E. (2012). Androgen receptor (AR) expression in prostate cancer and progression of the tumor: Lessons from cell lines, animal models and human specimens. *Steroids*, *77*(10), 996–1001. doi:10.1016/j.steroids.2012.01.008

Tsao, R. (2010). Chemistry and biochemistry of dietary polyphenols. *Nutrients*, *2*(12), 1231–46. doi:10.3390/nu2121231

Tsao, R., & Deng, Z. (2004). Separation procedures for naturally occurring antioxidant phytochemicals. *Journal of Chromatography. B, Analytical Technologies in the Biomedical and Life Sciences*, *812*(1-2), 85–99. doi:10.1016/j.jchromb.2004.09.028

Vallverdú-Queralt, A. (2010). Improved characterization of tomato polyphenols using liquid chromatography/electrospray ionization linear ion trap quadrupole Orbitrap mass spectrometry and. *Rapid Communications in Mass Spectometry*, *24*, 2986–2992. doi:10.1002/rcm

Vauzour, D., Rodriguez-Mateos, A., Corona, G., Oruna-Concha, M. J., & Spencer, J. P. E. (2010). Polyphenols and human health: prevention of disease and mechanisms of action. *Nutrients*, *2*(11), 1106–31. doi:10.3390/nu2111106

Venkateswaran, V., & Klotz, L. H. (2010). Diet and prostate cancer: mechanisms of action and implications for chemoprevention. *Nature Reviews. Urology*, *7*(8), 442–53. doi:10.1038/nrurol.2010.102

Vicinanza, R., Zhang, Y., Henning, S. M., & Heber, D. (2013). Pomegranate Juice Metabolites, Ellagic Acid and Urolithin A, Synergistically Inhibit Androgen-Independent Prostate Cancer Cell Growth via Distinct Effects on Cell Cycle Control and Apoptosis. *Evidence-Based Complementary and Alternative Medicine : eCAM*, *2013*(Figure 1), 247504. doi:10.1155/2013/247504

Vinson, J. A., & Cai, Y. (2012). Nuts, especially walnuts, have both antioxidant quantity and efficacy and exhibit significant potential health benefits. *Food & Function*, *3*(2), 134–40. doi:10.1039/c2fo10152a

Wang, J., & Sporns, P. (2000). MALDI-TOF MS Analysis of Isoflavones in Soy Products. *Journal of Agricultural and Food Chemistry*, *48*(12), 5887–5892. doi:10.1021/jf0008947

Wang, L. G., Ossowski, L., & Ferrari, A. C. (2001). Overexpressed Androgen Receptor Linked to p21 WAF1 Silencing May Be Responsible for Androgen Independence and Resistance to Apoptosis of a Prostate Cancer Cell Line 1. *Cancer Research*, *61*(24), 7544–7551.

Webber, M. M., Waghray, a, & Bello, D. (1995). Prostate-specific antigen, a serine protease, facilitates human prostate cancer cell invasion. *Clinical Cancer Research : An Official Journal of the American Association for Cancer Research*, *1*(10), 1089–94. Retrieved from http://www.ncbi.nlm.nih.gov/pubmed/9815898

Williams, S., Singh, P., Isaacs, J., & Denmeade, S. (2007). Does PSA play a role as a promoting agent during the initiation and/or progression of prostate cancer? *The Prostate*, *329*(December 2006), 312–329. doi:10.1002/pros

Wittwer, J., Rubio-Aliaga, I., Hoeft, B., Bendik, I., Weber, P., & Daniel, H. (2011). Nutrigenomics in human intervention studies: current status, lessons learned and future perspectives. *Molecular Nutrition & Food Research*, *55*(3), 341–58. doi:10.1002/mnfr.201000512

Wolfender, J. (2009). HPLC in natural product analysis: the detection issue. *Planta Medica*, *75*(7), 719–34. doi:10.1055/s-0028-1088393

Zhang, J., Grieger, J. a, Kris-Etherton, P. M., Thompson, J. T., Gillies, P. J., Fleming, J. a, & Vanden Heuvel, J. P. (2011). Walnut oil increases cholesterol efflux through inhibition of stearoyl CoA desaturase 1 in THP-1 macrophage-derived foam cells. *Nutrition & Metabolism*, *8*(1), 61. doi:10.1186/1743-7075-8-61

APPENDIX

View Online / Journal Homepage
Dynamic Article Links

Analyst

Cite this: DOI: 10.1039/c2an35286a

www.rsc.org/analyst

PAPER

Attenuated total reflection infrared microspectroscopy combined with multivariate analysis: a novel tool to study the presence of cocoa polyphenol metabolites in urine samples

Claudia Sánchez-González,†[a] Worku Nigussie,†[b] Ramon Estruch,[cd] Rosa M. Lamuela-Raventós,[ad] Maria Izquierdo-Pulido[a] and Silvia de Lamo-Castellví*[b]

Received 29th February 2012, Accepted 21st May 2012
DOI: 10.1039/c2an35286a

Published on 23 May 2012 on http://pubs.rsc.org | doi:10.1039/C2AN35286A
Downloaded by Universitat de Barcelona on 19 June 2012

The detection and quantification of polyphenols in biological samples is mainly performed by liquid chromatography in tandem with mass spectrometry (HPLC-MS/MS). This technique requires the use of organic solvents and needs control and maintenance of several MS/MS parameters, which makes the method expensive and time consuming. The main objective of this study was to evaluate, for the first time, the potential of using attenuated total reflection infrared microspectroscopy (ATR-IRMS) coupled with multivariate analysis to detect and quantify phenolic compounds excreted in human urine. Samples were collected from 5 healthy volunteers before and 6, 12 and 24 h after ingestion of 40 g cocoa powder with 250 mL of water or whole milk, and stored at −80 °C. Each sample was centrifuged at 5000 rpm for 10 min and at 4 °C and applied onto grids of a hydrophobic membrane. Spectra were collected in the attenuated total reflection (ATR) mode in the mid-infrared region (4000–800 cm^{-1}) and were analyzed by a multivariate analysis technique, soft independent modeling of class analogy (SIMCA). Spectral models showed that IR bands responsible for chemical differences among samples were related to aromatic rings. Therefore, ATR-IRMS could be an interesting and straightforward technique for the detection of phenolic compounds excreted in urine. Moreover, it could be a valuable tool in studies aimed to identify biomarkers of consumption of polyphenol-rich diets.

Introduction

Polyphenols commonly present in the human diet are not necessarily the most active within the body. The reasons for this can include low intrinsic activity, poor intestinal absorption, high metabolism or rapid elimination.[1]The effects of the food matrix on flavonoid bioavailability have not been examined in too much detail.[2] Direct interaction between flavonoids and some components in food, such as proteins, can occur; polyphenols bind to proteins possibly affecting their absorption. The effects of milk as a food matrix on the excretion of cocoa epicatechin metabolites in humans have been studied; Roura *et al.*[3] reported that while the total amount of epicatechin and its metabolites excreted by urine did not change after consumption of cocoa with water or cocoa with milk, the metabolite profile did indeed differ. This indicates a possible influence of other diet components on the conjugation of polyphenol metabolites. Although total urinary excretion is roughly correlated with maximum plasma concentrations, low values of urinary excretion could be indicative of pronounced biliary excretion or extensive metabolism.[4]

The Fourier Transform Infrared Spectrometer (FT-IR) uses an interferometer which is capable of collecting every component of the full electromagnetic spectrum simultaneously.[5] In particular, mid infrared (MIR) spectroscopy provides unique absorption patterns for each constituent of a sample (fingerprint region) and enables direct constituent identification at a molecular level. Combining this technology with multivariate data analysis results in a powerful tool to obtain and interpret chemical data.[6] Specifically, attenuated total reflection (ATR) infrared microspectroscopy (IRMS) has the potential for detecting subtle compositional characteristics and differences between distinct samples. Absorption of radiation in the MIR spectral region provides rich information on the molecular properties of the sample, in particular regarding composition.[7] Hence, ATR infrared microspectroscopy may be used as a diagnostic and monitoring technique in a variety of clinical scenarios such as alcaptonuria, Barret esophagus, esophageal adenocarcinoma

[a]*Department of Nutrition and Food Science- XaRTA- INSA, University of Barcelona, Barcelona, Spain*
[b]*Department of Chemical Engineering, University Rovira i Virgili, Tarragona, Spain. E-mail: silvia.delamo@urv.cat; Fax: +34 977 559 621; Tel: +34 977 559 673*
[c]*Department of Internal Medicine, Hospital Clinic, Institute of Biomedical Investigation August Pi i Sunyer (IDIBAPS), University of Barcelona, Barcelona, Spain*
[d]*CIBER 06/003 Physiopathology of obesity and nutrition (CIBEROBN) and RETICS RD06/0045/0003, Institute of Health Carlos III, Spain*
† Both authors contributed equally to this work.

Published on 23 May 2012 on http://pubs.rsc.org | doi:10.1039/C2AN35286A
Downloaded by Universitat de Barcelona on 19 June 2012

and interstitial cystitis.[8,9] It has also been used for the detection and discrimination of microorganisms at the serovar level.[10–12]

Infrared-based analysis could be advantageous over other methods because of its much easier sample pre-treatment, short time of analysis and its lower costs of purchase and maintenance.[8] The analytical applications of infrared spectroscopy have grown greatly in the past years; this is mainly attributed to the sensitivity of modern spectrometers combined with multivariate analysis.[8] Multivariate data analysis uses mathematical, statistical and computer sciences to efficiently extract useful information from data generated *via* chemical measurements.[6,13]

The detection and quantification of polyphenols and their metabolites in human biological samples is mainly performed by liquid chromatography in tandem with mass spectrometry (HPLC-MS/MS). This technique requires the use of organic solvents and needs control and maintenance of several MS/MS parameters, which makes the method expensive and time consuming. Given the versatility and simplicity of the infrared-based methodologies, the aim of this study was to evaluate, for the first time, the potential of using attenuated total reflection Fourier transform infrared microspectroscopy (ATR-IRMS) coupled with multivariate analysis as a method to detect and quantify phenolic compounds excreted in human urine. For that purpose, urine samples from an intervention study with cocoa polyphenols that were already quantified by our group were analyzed by ATR-IRMS in order to prove the validity of this new methodology. If the IR-based methodology proves its validity, it could be a valuable tool in studies aimed to identify biomarkers of consumption of polyphenol-rich diets.

Experimental methods

Subjects and study design

Urine samples were obtained from 5 healthy volunteers; these samples were obtained in a previous study[14] aimed to investigate the bioavailability of cocoa polyphenols. Samples were stored at −80 °C to maintain their integrity. Briefly, nine samples were obtained from each volunteer after a specific test meal and time frame. Volunteers were submitted to three interventions: milk only (M), cocoa with milk (CM), and cocoa with water (CW) and urine samples were taken at 6, 12 and 24 h post M, CM, and CW intake. The description of how urine samples were obtained and the composition of the test meals used are described in Roura *et al.*[14] The Institutional Review Board of the Hospital Clinic, Barcelona, approved the study protocol and all the volunteers gave written consent before their inclusion in the trial.

Sample preparation

Urine samples were thawed at room temperature and in darkness for preparation. Once at room temperature, 1 mL of each urine sample was placed in an Eppendorf tube and centrifuged at 5000 rpm for 10 min and at 4 °C. After centrifugation, the resulting pellet was removed from the samples. An aliquot of each urine sample (22 μL) was placed by vacuum filtration onto 3 grids of hydrophobic membrane (HGM; ISO-GRID, Neogen Corporation, Lansing, MI). Then, membranes were dried at room temperature in dark conditions and later were stored in a desiccator at 4 °C until being analyzed by ATR-IRMS. In total 45 samples were prepared, 15 for each group, MC (6, 12 and 24 h), LC (6, 12 and 24 h) and M (6, 12 and 24 h).

Attenuated total reflection (ATR) infrared microspectroscopy (IRMS)

Six spectra (two per grid) for each sample were collected using a FT-IR microscope (Illuminate IR, Smiths detection) interfaced with a mercury–cadmium–telluride (MCT) photoconductive detector and equipped with a microscope with a motorized x–y stage, 20× and 50× objectives, and slide-on attenuated total reflection (ATR) diamond objective (Smiths detection). Spectral data were obtained from 128 scans at 4 cm^{-1} resolution. The microscope was software-controlled using Wire 3.2 version software (Renishaw plc, New Mills, Wotton-under-Edge, Gloucestershire, GL12 8JR, United Kingdom). Spectra were collected over the wave-number range 4000–800 cm^{-1}. Spectra were displayed in terms of absorbance obtained by rationing the single beam spectrum against that of the air background. The time required to obtain one spectrum was about 40 seconds.

Multivariate analysis

Spectra were exported to the Pirouette® multivariate analysis software (version 3.1, InfoMetrix, Inc., Woodville, WA) as ".spc" files. The FT-IR spectral data were mean-centered, transformed to their second derivative using a 15-point Savitzky–Golay polynomial filter, and vector-length normalized; sample residuals and Mahalanobis distance were used to determine outliers.[15–17] Soft independent modeling of class analogy (SIMCA) was used to build a predictive model based on the construction of separate PCA models for each class to describe and model the variation.[16] SIMCA class models were interpreted based on class projections, class discriminating power and interclass distances. Variable importance, also known as discriminating power, was used to define the variables (wave-numbers) that are different between samples.[18] SIMCA is used for classifying and discriminating between samples, and to identify the component that is most responsible for the changes between samples without using standards.

Results and discussion

Discrimination of cocoa-water polyphenol metabolites in urine samples placed onto grids of HGM by ATR-IRMS

Typical spectra of cocoa-water polyphenol metabolites in urine samples taken 6, 12 and 24 h after CW consumption are shown in Fig. 1. The bands of highest proportion in the raw spectra at approximately 1600, 1580 and 1100 cm^{-1} were associated to –C=C– stretching in aromatic rings[19] and C–O stretching from esters/ethers. These functional groups are common groups of cocoa polyphenols.

Infrared spectra analysis (1800–900 cm^{-1}) using SIMCA classification models of CW samples (data not shown) permitted tight clustering and clear differentiation among samples. Interclass distances (ICDs) are Euclidian distances between centers of clusters, and above 3.0 are considered to be significant enough to identify 2 groups of samples as different classes.[18] Values ranged from 2.0 to 4.4 (Table 1) showing differences between their

This journal is © The Royal Society of Chemistry 2012

Downloaded by Universitat de Barcelona on 19 June 2012
Published on 23 May 2012 on http://pubs.rsc.org | doi:10.1039/C2AN35286A

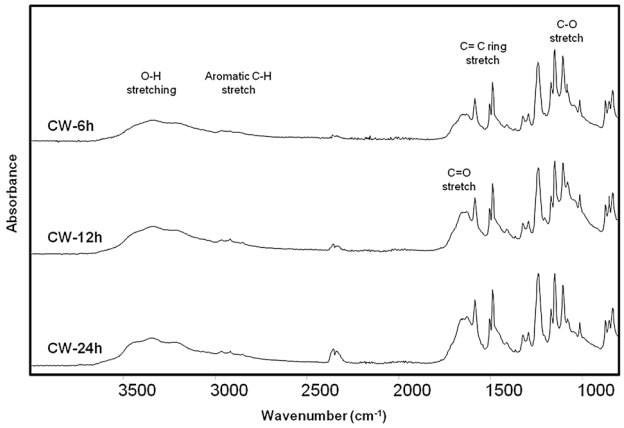

Fig. 1 Typical attenuated total-reflection infrared spectrum of urine samples 6, 12 and 24 h after CW consumption, using a diamond crystal accessory in reflection mode.

Table 1 Soft independent modeling of class analogy interclass distances of urine samples taken 6, 12 and 24 h after CW consumption. These distances were obtained using transformed (second derivative) attenuated total reflection microspectroscopy spectra using a diamond crystal accessory in reflection mode and collected in the 1800–800 cm^{-1} region

Sample	CW 24 h	CW 12 h	CW 06 h
CW 24 h	0.0		
CW 12 h	2.0	0.0	
CW 06 h	4.4	3.0	0.0

biochemical patterns in all classes, except between CW-12 h and CW-24 h. These results are in agreement with Roura *et al.*[20] These authors analyzed the content of the epicatechin metabolites epicatechin-sulphate (Ec-S) and epicatechin-glucuronide (Ec-G) in the same samples by LC-MS/MS and found that the metabolite excretion peak occurred at the 6–12 h period, with the lowest being at 12–24 h after consumption.

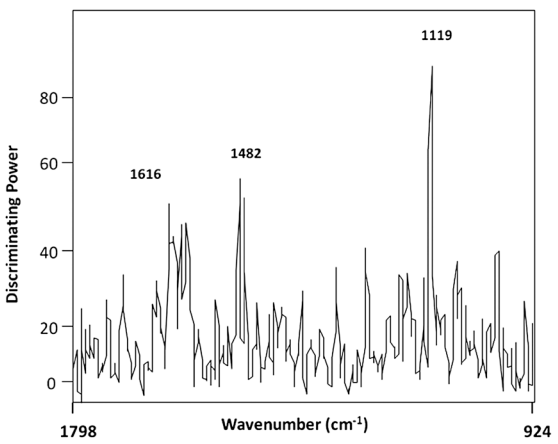

Fig. 2 Soft independent modeling class analogy (SIMCA) discriminating power of transformed (second derivative, 15-point window) attenuated total reflection infrared spectra (1800–800 cm^{-1}) using a diamond crystal accessory in reflection mode of urine samples taken 6, 12 and 24 h after CW consumption. The experiments were repeated six times.

The discriminating power of SIMCA, which is a measure of variable importance in infrared frequency,[18] mainly showed 3 strong spectral bands at 1119, 1482 and 1616 cm^{-1} (Fig. 2). The IR band at 1119 cm^{-1} was associated to C–O stretching of ester groups as well as O–H vibrations of phenolic groups, and the bands at 1482 and 1616 cm^{-1} were linked to C–C and C=C–C stretching of benzene ring modes and C=C vibrations of aromatic systems, respectively.[19] These results are also in agreement with Roura *et al.*,[20] since the authors reported a maximum epicatechin metabolite excretion at the 6–12 h period and a difference in the type of epicatechin metabolite excreted. For example, Ec-S[1] had the highest excretion at 0–6 h and the lowest at 12–24 h. Hence, the differences among samples could be associated with different concentrations and/or compositions of the phenolic metabolites excreted in urine depending on the time elapsed after consumption of CW.

Discrimination of cocoa-milk polyphenol metabolites in urine samples placed onto grids of HGM by ATR-IRMS

Typical spectra of cocoa-milk (CM) polyphenol metabolites after 6, 12 and 24 h of CM consumption are shown in Fig. 3. In this case, another IR band at 1650 cm^{-1} linked to amide I of protein breakdown in milk metabolism appeared in each CM raw spectrum. ICDs were calculated between samples taking into account the time passed after CM consumption, CM-06 h, CM-12 h, CM-24 h. ICD values of CM indicated differences between the CM urine samples according to the elapsed time after CM consumption. ICD were in the range between 2.2 and 8.9 (Table 2) showing differences among all classes, except between CM-06 h and CM-12 h. These differences could be related to differences in polyphenol concentrations; these results are also in agreement with Roura *et al.*[3] which stated that the peak metabolite excretion was at the 6–12 h period, with the lowest being at 24 h after consumption. In this case, the IR bands at 1104, 1344 and 1581 cm^{-1} were found to be very influential in the discrimination power of this model. These IR bands were related to C–O stretching of ester groups as well as O–H vibrations of phenolic groups, C–O stretching of carboxylic acids and C–C and C=C–C stretching of benzene ring modes[19] (Fig. 4).

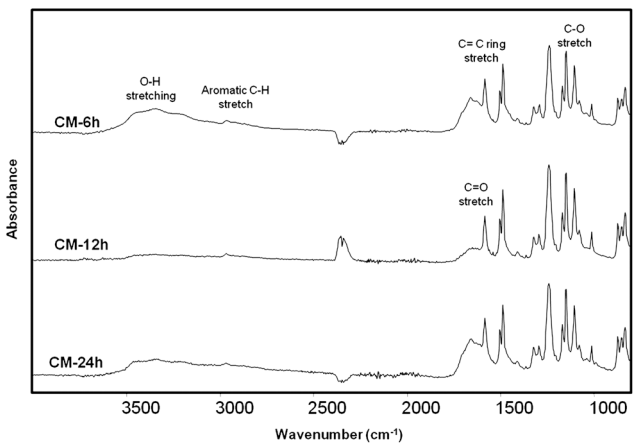

Fig. 3 Typical attenuated total-reflection infrared spectrum of urine samples 6, 12 and 24 h after CM consumption using a diamond crystal accessory in reflection mode.

Downloaded by Universitat de Barcelona on 19 June 2012
Published on 23 May 2012 on http://pubs.rsc.org | doi:10.1039/C2AN35286A

Table 2 Soft independent modeling of class analogy interclass distances of urine samples taken 6, 12 and 24 h after CM consumption. These distances were obtained using transformed (second derivative) attenuated total reflection spectra using a diamond crystal accessory in reflection mode and collected in the 1800–800 cm^{-1} region

Sample	CM 24 h	CM 12 h	CM 06 h
CM 24 h	0.0		
CM 12 h	7.5	0.0	
CM 06 h	8.9	2.2	0.0

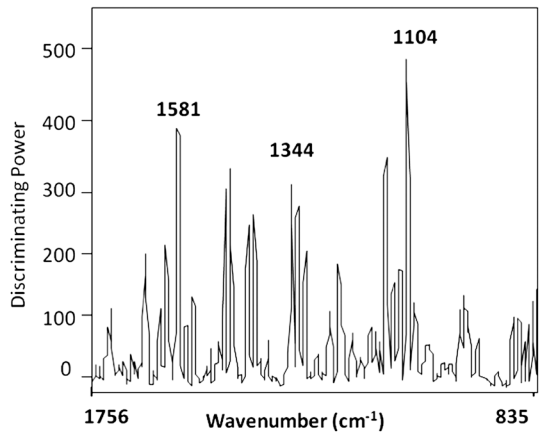

Fig. 4 Soft independent modeling class analogy (SIMCA) discriminating power of transformed (second derivative, 15-point window) attenuated total reflection infrared spectra (1800–800 cm^{-1}) using a diamond crystal accessory in reflection mode of urine samples 6, 12 and 24 h after CM consumption.

Discrimination of cocoa-milk and cocoa-water polyphenol metabolites in urine samples placed onto grids of HGM by ATR-IRMS

The ICDs ranged from 1.8 to 10.5 (Table 3) indicating considerable variability between samples. There are significant differences in total phenolic excretion between CM and CW which could be attributed to a variation in the concentration and composition of polyphenols excreted. The lowest ICD was found between CW-6 h (0–6 h) and CW-12 h (6–12 h) which, according to Roura *et al.*,[20] are the time frames with the highest epicatechin metabolite excretion. The lowest ICD among CM samples was found among the 6 and 12 h samples, consistent with the results found by Roura *et al.*[3] The highest ICDs were found between CM-24 h and the rest of the samples, which could be due to the effect of milk as a food matrix on the excretion profile. The CM-06 h was the CM sample that presented the least differences when compared to the CW samples. According to several authors[3,21,22] the total polyphenol excretion is not affected by food matrix, though milk does affect flavonoid metabolism pathways, increasing sulfation compared with glucuronidation in the first 6 h excretion period. Discrimination power of SIMCA showed three strong spectral bands at 1605, 1331 and 1104 cm^{-1} (Fig. 5) for CM (6, 12 and 24 h) and CW (6, 12 and 24 h) that were very influential in their discrimination. The IR band at 1605 cm^{-1} was associated to C=C vibrations of aromatic systems, and C=O stretching of conjugated ketone and quinones; the IR band at 1331 cm^{-1} was linked to C–O stretching from carboxylic acids; and the band at 1104 cm^{-1} was related to C–O stretching of ester groups as well as O–H vibrations of phenolic groups.[19]

Table 3 Soft independent modeling of class analogy interclass distances of urine samples taken 6, 12 and 24 h after CM and CW consumption. These distances were obtained using transformed (second derivative) attenuated total reflection spectra using a diamond crystal accessory in reflection mode and collected in the 1800–800 cm^{-1} region

Sample	CM 24 h	CM 12 h	CM 06 h	CW 24 h	CW 12 h	CW 06 h
CM 24 h	0.0					
CM 12 h	9.5	0.0				
CM 06 h	8.5	4.2	0.0			
CW 24 h	9.3	5.8	2.6	0.0		
CW 12 h	10.5	5.4	2.3	2.1	0.0	
CW 06 h	9.9	5.4	2.4	3.4	1.8	0.0

Discrimination of milk only and cocoa-milk polyphenol metabolites in urine samples placed onto grids of HGM by ATR-IRMS

The ICD showed significant differences between CM and M samples (Table 4) due to the absence of phenolic groups in the M samples. Some of the class distances obtained in the experiment were lower than 3.

In the discrimination power of the model comparing M and CM samples, two bands were found to be very influential, 1104 and 1581 cm^{-1} (Fig. 6) from the phenolic components present in CM.

The major discriminating bands found in all samples are indicative of phenolic compounds; therefore ATR-IRMS could be an effective method to identify polyphenols in urine. This technique could represent a rapid and effective method to detect biomarkers in human fluids.[23,24]

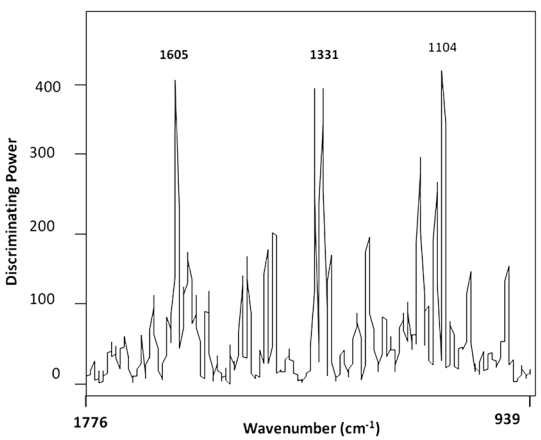

Fig. 5 Soft independent modeling class analogy (SIMCA) discriminating power of transformed (second derivative, 15-point window) attenuated total reflection infrared (ATR-IR) spectra (1800–800 cm^{-1}) using a diamond crystal accessory in reflection mode, for urine samples taken 6, 12 and 24 h after CW and CM consumption.

This journal is © The Royal Society of Chemistry 2012

Table 4 Soft independent modeling of class analogy interclass distances of urine samples taken 6, 12 and 24 h after CM and M consumption. These distances were obtained using transformed (second derivative) attenuated total reflection spectra using a diamond crystal accessory in reflection mode and collected in the 1900–800 cm^{-1} region

Sample	CM 24 h	CM 12 h	CM 06 h	M 24 h	M 12 h	M 06 h
CM 24 h	0.0					
CM 12 h	7.1	0.0				
CM 06 h	8.3	2.3	0.0			
M 24 h	5.7	10.3	12.6	0.0		
M 12 h	7.9	3.2	2.3	11.9	0.0	
M 06 h	8.2	2.9	2.2	11.6	2.3	0.0

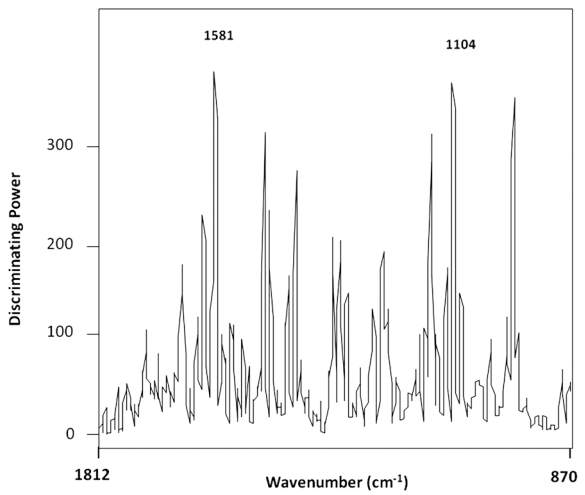

Fig. 6 Soft independent modeling class analogy (SIMCA) discriminating power of transformed (second derivative, 15-point window) attenuated total reflection infrared (ATR-IR) spectra (1900–800 cm^{-1}) using a diamond crystal accessory in reflection mode, for urine samples taken 6, 12 and 24 h after M and CM consumption.

Conclusions

The combination of ATR-IRMS and multivariate analysis could be a rapid, simple and available technique to detect polyphenol metabolites in human urine after cocoa beverage (CM and CW) consumption. FT-IR has been extensively used for food analysis and biomedical applications, it is believed that this work broadens its application and offers a new tool for identifying and quantifying metabolites after the ingestion of foods with functional components. The current applications of ATR-IRMS in the food industry lay mainly in the identification of food pathogens, authentication of products and quality control. This is a preliminary study to evaluate the potential of using ATR-IRMS to identify functional components in foods, as well as their absorption, metabolism and excretion by detecting and quantifying the composition of its metabolites. Further research is undergoing to quantify the polyphenols present in urine samples by ATR-IRMS.

Acknowledgements

The authors would like to thank all volunteers involved in the study, without their collaboration this project would not have been possible. This research was supported by grants from the Ministry of Science and Innovation (CDTI P-02-0277, PROFIT, FIT-06000-2002-99), Generalitat de Catalunya (2009SGR724), Nutrexpa Group (FBG-302218) and Departament Quimica of Universitat Rovira i Virgili. CSG is supported by a CONACYT scholarship and WN by a Universitat Rovira i Virgili scholarship.

Notes and references

1 C. S. Yang, S. Sang, J. D. Lambert and M.-J. Lee, Bioavailability issues in studying the health effects of plant polyphenolic compounds, *Mol. Nutr. Food Res.*, 2008, **52**, S139–S151.
2 S. Tulipani, M. Martinez Huelamo, M. Rotches Ribalta, R. Estruch, E. Escribano Ferrer, C. Andres-Lacueva, M. Illan and R. M. Lamuela-Raventós, Oil matrix effects on plasma exposure and urinary excretion of phenolic compounds from tomato sauces: evidence from a human pilot study, *Food Chem.*, 2012, **130**, 581–590.
3 E. Roura, C. Andres-Lacueva, R. Estruch, M. L. Mata, M. Izquierdo-Pulido and R. M. Lamuela-Raventos, The effects of milk as a food matrix for polyphenols on the excretion profile of cocoa (2)-epicatechin metabolites in healthy human subjects, *Br. J. Nutr.*, 2008, **100**, 846–851.
4 C. Manach, A. Scalbert, C. Morand, C. Remesy and L. Jimenez, Polyphenols: food sources and bioavailability, *Am. J. Clin. Nutr.*, 2004, **79**, 727–747.
5 *Principles of instrumental analysis*, ed. D. A. Skoog, F. J. Holler and T. A. Nieman, Harcourt Brace College Publishers, USA, 5th edn, 1998, pp. 380–403.
6 L. Wang and B. Mizaikoff, Application of multivariate data-analysis techniques to biomedical diagnostics based on mid-infrared spectroscopy, *Anal. Bioanal. Chem.*, 2008, **391**, 1641–1654.
7 L. Quaroni and A. Casson, Characterization of barret esophagus and esophageal adenocarcinoma by fourier-transform infrared microscopy, *Analyst*, 2009, **134**, 1240–1246.
8 A. Patrick, J. A. Markus, D. W. Swinkels, B. S. Jakobs, R. A. Wevers and J. M. Frans Trijebls, *et al.* New technique for diagnosis and monitoring of alcaptonuria: quantification of homogentistic acid in urine with mid- infrared spectroscopy, *Anal. Chim. Acta*, 2001, **429**, 287–292.
9 D. E. Rubio-Diaz, M. E. Pozza, J. Dimitrakov, J. P. Gilleran, M. Giusti and J. L. Stella, *et al.* A candidate serum biomarker for bladder pain syndrome/interstitial cystitis, *Analyst*, 2009, **134**, 1133–1137.
10 N. A. Baldauf, L. A. Rodriguez-Romo, A. E. Yousef and L. E. Rodriguez-Saona, Differentiation of selected Salmonella enterica serovars by fourier-transform mid-infrared spectroscopy, *Appl. Spectrosc.*, 2006, **60**, 592–598.
11 E. M. Grasso, A. E. Yousef, S. De Lamo Castellvi and L. E. Rodriguez-Saona, Rapid detection and differentiation of Alicyclobacillus species in fruit juice using hydrophobic grid membranes and attenuated total reflection infrared microspectroscopy, *J. Agric. Food Chem.*, 2009, **57**, 10670–10674.
12 S. De Lamo-Castellví, A. Männing and L. E. Rodriguez-Saona, Fourier-transform infrared spectroscopy combined with immunomagnetic separation as a tool to discriminate Salmonella serovars, *Analyst*, 2010, **135**, 2987–2992.
13 D. Naumann, FT-infrared and FR-Raman spectroscopy in biomedical research, in *Infrared and Raman Spectroscopy of Biological Materials*, ed. H. U. Gremlich and B. Yan, Marcel Dekker, USA, 2001, p. 323.
14 E. Roura, C. Andres-Lacueva, R. Estruch, M. L. Mata, M. Izquierdo-Pulido and A. L. Waterhouse, Milk does not affect the bioavailability of cocoa powder flavonoid in healthy human, *Ann. Nutr. Metab.*, 2007, **51**, 493–498.
15 P. Hourant, V. Baeten, M. T. Morales, M. Meurens and R. Aparicio, Oil and fat classification by selected bands of near-infrared spectroscopy, *Appl. Spectrosc.*, 2000, **54**(8), 1168–1174.
16 M. Kansiz, P. Heraud, B. Wood, F. Burden, J. Beardall and D. Mcnaughton, FTIR spectroscopy as a tool to discriminate between cyanobacterial strains, *Phytochemistry*, 1999, **52**, 407–417.

Published on 23 May 2012 on http://pubs.rsc.org | doi:10.1039/C2AN35286A
Downloaded by Universitat de Barcelona on 19 June 2012

17 W. R. Hruschka, Data analysis: wavelength selection methods, in *Near-Infrared Technology in the Agricultural and Food Industries*, ed. P. Williams and K. Norris, EUA: AACC Inc, 2001, pp. 39–58.
18 W. J. Dunn and S. Wold, SIMCA pattern recognition and classification, in Chemometric Methods in Molecular Design, ed. H. van de Waterbeemd, EUA: VCH Publishers, 1995, pp. 179–193.
19 C. Shiroma-Kian, D. Tay, I. Manrique, M. Giusti and L. E. Rodriguez-Saona, Improving the screening process for the selection of potato breeding lines with enhanced polyphenolics content, *J. Agric. Food Chem.*, 2008, **56**, 9835–9842.
20 E. Roura, M. P. Almajano, C. Andres-Lacueva, R. Estruch, M. L. Mata and R. M. Lamuela-Raventos, Human urine: epicatechin metabolites and antioxidant activity after cocoa beverage intake, *Free Radical Res.*, 2007, **41**(8), 943–949.
21 P. C. H. Hollman, K. H. van het Hof, L. B. M. Tijburg and M. B. Katan, Addition of milk does not affect the absorption of flavonols from tea in man, *Free Radical Res.*, 2001, **34**, 297–300.
22 K. H. van het Hof, G. A. A. Kivits, J. A. Westrate and L. B. M. Tijburg, Bioavailability of catechins from tea: the effect of milk, *Eur. J. Clin. Nutr.*, 1998, **52**, 356–359.
23 C. P. Schultz, K.-Z. Liu, J. B. Johnson and H. H. Mantsch, Study of chronic lymphatic leukemia from infrared spectra of lymphocytes by FT-IR spectroscopy and cluster analysis, *Leuk. Res.*, 1998, **20**, 649–655.
24 K. Z. Liu, M. H. Shi and H. H. Mantsch, Molecular and chemical characterization of blood cells by infrared spectroscopy: a new optical tool in hematology, *Blood Cells, Mol., Dis.*, 2005, **35**, 404–412.

Published on 23 May 2012 on http://pubs.rsc.org | doi:10.1039/C2AN35286A
Downloaded by Universitat de Barcelona on 19 June 2012